HEAT DISSIPATION FROM ELECTRONIC PACKAGES WITH THE HELP OF HEAT PIPE NETWORK AND ITS APPLICATION TO ROTARY PLATFORMS

A THESIS SUBMITTED TO
THE GRADUATE SCHOOL OF NATURAL AND APPLIED SCIENCES
OF
MIDDLE EAST TECHNICAL UNIVERSITY

BY

ANIL ÇALIŞKAN

IN PARTIAL FULFILLMENT OF THE REQUIREMENTS
FOR
THE DEGREE OF MASTER OF SCIENCE
IN
MECHANICAL ENGINEERING

SEPTEMBER 2015

Approval of the thesis:

HEAT DISSIPATION FROM ELECTRONIC PACKAGES WITH THE HELP OF HEAT PIPE NETWORK AND ITS APPLICATION TO ROTARY PLATFORMS

submitted by **ANIL ÇALIŞKAN** in partial fulfillment of the requirements for the degree of **Master of Science in Mechanical Engineering Department, Middle East Technical University** by,

Prof. Dr. Gülbin Dural Ünver
Dean, Graduate School of **Natural and Applied Sciences** _____

Prof. Dr. R.Tuna Balkan
Head of Department, **Mechanical Engineering Dept.** _____

Assoc. Prof. Dr. İlker Tarı
Supervisor, **Mechanical Engineering Dept., METU** _____

Examining Committee Members:

Assoc. Prof. Dr. Cemil Yamalı
Mechanical Eng. Dept., METU _____

Assoc. Prof. Dr. İlker Tarı
Mechanical Eng. Dept., METU _____

Assoc. Prof. Dr. Derek K. Baker
Mechanical Eng. Dept., METU _____

Assoc. Prof. Dr. Tuba Okutucu Özyurt
Mechanical Eng. Dept., METU _____

Assoc. Prof. Dr. Cemil Koçar
Nuclear Eng. Dept., Hacettepe University _____

Date: 11.09.2015

I hereby declare that all information in this document has been obtained and presented in accordance with academic rules and ethical conduct. I also declare that, as required by these rules and conduct, I have fully cited and referenced all material and results that are not original to this work.

Name, Last name: Anıl ÇALIŞKAN

Signature:

ABSTRACT

HEAT DISSIPATION FROM ELECTRONIC PACKAGES ON ROTARY PLATFORMS WITH THE HELP OF HEAT PIPE NETWORKS

Çalışkan, Anıl
M.S., Department of Mechanical Engineering
Supervisor: Assoc. Prof. Dr. İlker Tarı

September 2015, 144 pages

An electronics package on a rotary platform including two components with 600 W, one component with 350 W and one small component with 70 W heat dissipation rates (1620 W total heat load) is numerically and experimentally investigated under steady state conditions. In order to avoid rotary joints and to reduce the costs of design, maintenance and production, the thermal management solution for the heat dissipation is entirely placed on the rotary platform. The thermal management solution includes heat sinks attached to the vertical side surfaces of the platform and heat pipes connected to heat sinks. The heat dissipating components are connected to the heat sinks with heat pipes. The heat sinks are cooled by forced convection with high power fan assemblies. Two different fin configurations are considered. One of them is a pin fin design and the other one is a plate fin covered with duct design. The thermal management systems are numerically modeled and then one of the numerical models is validated with a set of experiments. The validated model is used for the optimization of the system and as a demonstration of feasibility of the heat pipes. The optimization parameters are the heat pipe locations, their connections to the heat sinks and geometrical properties of the heat sinks. The optimization criteria are to maintain nearly uniform temperature distributions on the heat sinks and to keep critical

components below their thermal shut-down points. The constraints are the lengths of the standard heat pipes and the limited options to bend the heat pipes due to their fragile structures. The success of the system is that it can keep the hot spot temperatures below the allowed maximum temperature of 120 ^{o}C even for the case of 50 °C ambient air temperature. The limitation of 120 ^{o}C working temperature comes from the thermal shut-down limits of the components in the electronics package.

Keywords: Electronics cooling, Forced convection, Rotary platforms, Heat sinks, Heat pipes, CFD

ÖZ

ISI BORUSU AĞLARI YARDIMIYLA ELEKTRONİK PAKETLERDEN ISI ATIMI VE BUNUN DÖNER TABLALARA UYGULANMASI

Çalışkan, Anıl
Yüksek Lisans, Makina Mühendisliği Bölümü
Tez Yöneticisi: Doç. Dr. İlker Tarı

Eylül 2015, 144 sayfa

Döner platform üzerinde bulunan, 600 W'lık 2 adet, 350 W'lık 1 adet ve küçük bir 70 W'lık ısı atım kapasitesine sahip olan bileşenlerden oluşan (toplamda 1620 W'lık ısı atımı) bir elektronik paket sabit koşullar altında sayısal ve deneysel olarak incelenmiştir. Döner (hareketli) bağlantılardan kaçınmak ve tasarım, bakım, üretim maliyetini azaltmak için, ısı atımı için kullanılan termal yönetim çözümü tamamen döner platform üzerine yerleştirilmiştir. Termal yönetim çözümü platformun yanal yüzeyine tutturulmuş soğutucuları ve bunlara bağlı ısıl boruları içerir. Elektronik paket içerisindeki ısı atımı yapan bileşenler soğutuculara ısıl borularla bağlıdır. Soğutucular yüksek güçlü fanlar yardımıyla zorlamalı ısı taşınımı ile soğutulmuştur. Bu kapsamda iki farklı soğutucu tasarımı üzerinde durulmuştur. Bunlardan biri pin soğutucu tipi, diğeri ise düz plaka soğutucu tipi tasarımıdır. Oluşturulan bu termal yönetim sistemleri sayısal olarak modellenmiş ve seçilen örnek sayısal model deney çalışması ile doğrulanmıştır. Doğrulanmış model, ısıl boruların güvenilirliğinin ispatlanmasında ve sistemin en uygun duruma getirilmesinde kullanılmıştır. En uygun duruma getirme değişkenleri ise ısıl boruların yerleri, boruların soğutuculara olan bağlantıları ve soğutucu blokların geometrik yapılarıdır. En uygun durum ölçütü ise soğutucular üzerinde eş ısıl dağılımlarının oluşturulması ve önemli yüzeylerin ısıl-kapanma sınırı

altında kalmasıdır. Standart ısıl boruların uzunluğu ve kırılgan yapıları nedeniyle boruları bükmede sınırlı seçenek olması kısıtlamalara neden olmuştur. Sistem başarısı ise 50 ^{o}C çevresel sıcaklıkta, sıcak bölge sıcaklığını izin verilen azami 120 ^{o}C altında tutabilmesidir. 120 ^{o}C sınırı elektronik paket içerisinde bulunan bileşenlerin, ısıl-kapanma sınırından gelmektedir.

Anahtar Kelimeler: Elektronik soğutma, Zorlamalı ısı taşınımı, Döner platformlar, Soğutucular, Isı boruları, CFD, Bilgisayar Destekli Akışkanlar Mekaniği

To my family

ACKNOWLEDGEMENTS

The author would like to express his sincere appreciation to his supervisor Assoc. Prof. Dr. İlker TARI for his continuous guidance, support, encouragement, inspiration and patience throughout the progress of this study. Besides, the author is very grateful to find a chance of being a master student of his supervisor. The committee members of thesis are appreciated for their valuable comments and suggestions on the contents of this study.

This study is a project, which is supported by ASELSAN Inc. and Republic of Turkey Ministry of Science, Industry and Technology as SAN-TEZ project 0233.STZ.2013. The author would like to thank both ASELSAN Inc. and Republic of Turkey Ministry of Science, Industry and Technology for financial support. In addition to this, ASELSAN Inc. is thanked due to providing manufacturing and testing background.

The author is thankful to his colleagues Mehmet YENER, Hakan BORAN, Murat PARLAK and Çağrı BALIKÇI for valuable contribution about applications of electronic cooling and heat pipe. Apart from appreciations to all, the author is grateful to find working together with Çağrı BALIKÇI in SANTEZ project and this study.

The author would to declare his graces about Suna KIYAK, who always supports during the study and helps during writing period of the thesis.

Finally, for their understanding, endless patience and encouragement throughout his study, his sincere thanks go to his parents, Recai ÇALIŞKAN and Aysel ÇALIŞKAN, and his sister, Sırma ÇALIŞKAN.

TABLE OF CONTENTS

LIST OF TABLES

TABLES

LIST OF FIGURES

FIGURES

LIST OF ABBREVIATIONS

Abbreviations

APG	Annealed Pyrolytic Carbon
CAD	Computer Aided Drawing
CFD	Computational Fluid Dynamics
FVM	Finite Volume Method
HVAC	Heating, Venting and Cooling
LRU	Line Replaceable Unit
LTCC	Low Temperature Co-firing Ceramic
TEC	Thermo-Electronic Cooling
TWT	Travelling Wave Tube
PA	Power Amplifier
PCB	Printed Circuit Board
RF	Radio Frequency
SIMPLE	Semi-Implement Method for Pressure-Linked Equations

Nomenclature

A	Area (mm^2 or m^2)
A_{block}	Heat Input Area of Evaporator Block (mm^2 or m^2)
A_{fin}	Total Surface Area of Fin(mm^2 or m^2)
A_s	Surface Area (mm^2 or m^2)
A_v	Surface Area of Vapor Section (mm^2 or m^2)

C_p	Specific Heat of Air (kJ/(kg.K))
D_h	Hydraulic Diameter (mm)
D_{HP}	Diameter of Heat Pipe (mm)
D_{VS}	Diameter of Heat Pipe Vapor Space (mm)
δ	Enthalpy of Vaporization (J)
ε	Turbulent Dissipations
ΔP_{cap}	Pressure Drop due to Capillary Limit
ΔP_g	Pressure Drop due to Gravitational Effect
ΔT_{air}	Temperature Difference of Cooling Air Flow
ΔT_{block}	Temperature Difference of Evaporator Block
ΔT_{conv}	Temperature Difference due to Convection
ΔT_{fin}	Temperature Difference of Fin
ΔT_{HP}	Temperature Difference of Heat Pipe
ΔT_{inter}	Temperature Difference of Evaporator Block / Heat Pipe Interface
ΔT_{total}	Total Temperature Changes
g	Acceleration of Gravity (m/s^2)
Gr	Groshof Number
h	Convection Coefficient ($W/(m^2.K)$)
h_f	Convection Coefficient of Fluid ($W/(m^2.K)$)
I	Turbulence Intensity (%)
η_{fin}	Fin Efficiency
k	Turbulent Kinetic Energy
k	Thermal Conductivity (W/(m.K))
k_{block}	Thermal Conductivity of Evaporator Block (W/(m.K))
k_{fin}	Thermal Conductivity of Fin (W/(m.K))

L	Length (mm or m)
L_{Cond}	Length of Condenser Section (mm)
L_{Eff}	Effective Length of Heat Pipe (mm)
L_{fineff}	Effective Fin Length (mm)
L_{evap}	Length of Evaporator Section (mm)
l_s	Turbulent Length (mm)
m_{fin}	Fin Factor for Uniform Cross-sectional Area
μ_v	Dynamic Viscosity of Vapor Phase (Pa.s)
Q	Heat Load to be Dissipated (W)
θ	Angle Between a Heat Pipe and Horizontal Plane
q_{ent}	Heat Transfer Rate for Avoiding Entrainment Limit
q_{sonic}	Heat Transfer Rate for Avoiding Sonic Limit
q_{vis}	Maximum Axial Heat Transfer Rate Reaching Viscous Limit
Pr	Prandtl Number
P_v	Vapor Pressure (Pa)
R_{air}	Thermal Resistance of Cooling Air Flow ($^oC/W$ or K/W)
R_{axial}	Thermal Resistance Along Heat Pipe ($^oC/W$ or K/W)
R_{block}	Thermal Resistance of Evaporator Block ($^oC/W$ or K/W)
R_{cond}	Thermal Resistance of Conduction Heat Pipe and Its Contact ($^oC/W$ or K/W)
$R_{condenser}$	Thermal Resistance of Heat Pipe Condenser ($^oC/W$ or K/W)
$R_{evaporator}$	Thermal Resistance of Heat Pipe Evaporator ($^oC/W$ or K/W)
R_{fin}	Thermal Resistance of fin ($^oC/W$ or K/W)
R_{HP}	Thermal Resistance of Heat Pipe ($^oC/W$ or K/W)
R_{inter}	Thermal Resistance of Evaporator Block / Heat Pipe Interface ($^oC/W$ or K/W)
R_{s-a}	Thermal Resistance of Heat Sink to Ambient ($^oC/W$ or K/W)

R_{wall}	Thermal Resistance of Heat Pipe's Wall ($^oC/W$ or K/W)
Re	Reynold Number
r_σ	Effective Radius of Wick (mm)
ρ	Density (g/cm^3)
ρ_v	Density of Vapor Phase (g/cm^3)
σ	Surface Tension for Working Liquid (N/mm)
t	Thickness (mm)
t_{block}	Thickness of Evaporator Block (mm)
t_{fin}	Thickness of Fin (mm)
T_∞	Ambient Temperature (^oC or K)
v	Velocity (m/s)
x	Characteristic Dimension of Wick Structure

Subscripts

a	Air
cap	Capillary Limit
cond	Conduction
conv	Convection
eff	Effective
ent	Entrainment Limit
evap	Evaporator
fluid	Fluid
g	Gravitational
HP	Heat Pipe
inter	Interface

liq	Liquid
surr	Surrounding
surf	Surface
v	Vapor
vis	Viscous Limit
VS	Vapor Space

CHAPTER 1

INTRODUCTION

The main topic of this thesis is the application of forced convection cooling to electronics on rotary platforms which is a very common application for the defense electronics industry. In this chapter, a general overview of the topic will be covered together with the motivation and the objectives of the study.

1.1 Motivation of the Study

The defense electronics industry has been continuously developing following the trends in other high technology areas. One of the biggest trends is miniaturization. This trend can be traced back to the introduction of electronics and computers to our lives.

Computers are probably the best illustration of how fast the technology has been evolving. At the beginning of the information age, conceptual design of the first computer created by Charles Babbage in 1822 (see Fig. 1.1a), was totally mechanical, and it might have only mechanical problems, which means there were no other complicated problems. In 1936, Konrad Zuse made the first electro-mechanical computer, and it was the first step where the complicated problems started. In 1946, ENIAC (see Fig. 1.1b) was the first digital computer, which occupied about 1,800 square feet area (approximately 167 m^2) and used about 18,000 vacuum tubes, weighing almost 50 tons, which means a very large room was required for that computer that can make only thousands of calculations in a second [1]. In the middle of 1950s, the first personal computers (see Fig. 1.1c) were introduced with more compact designs after a significant decrease in their dimensions. The reduction in size requires smaller components and the improvements in computing capability requires more power, combination of both leading to more heat dissipation per unit area.

Recently, as a consequence of the mobility trend in electronic devices, there are many small and micro devices produced with high power consumptions requiring dissipation of very high heat fluxes (e.g. Fig. 1.1d).

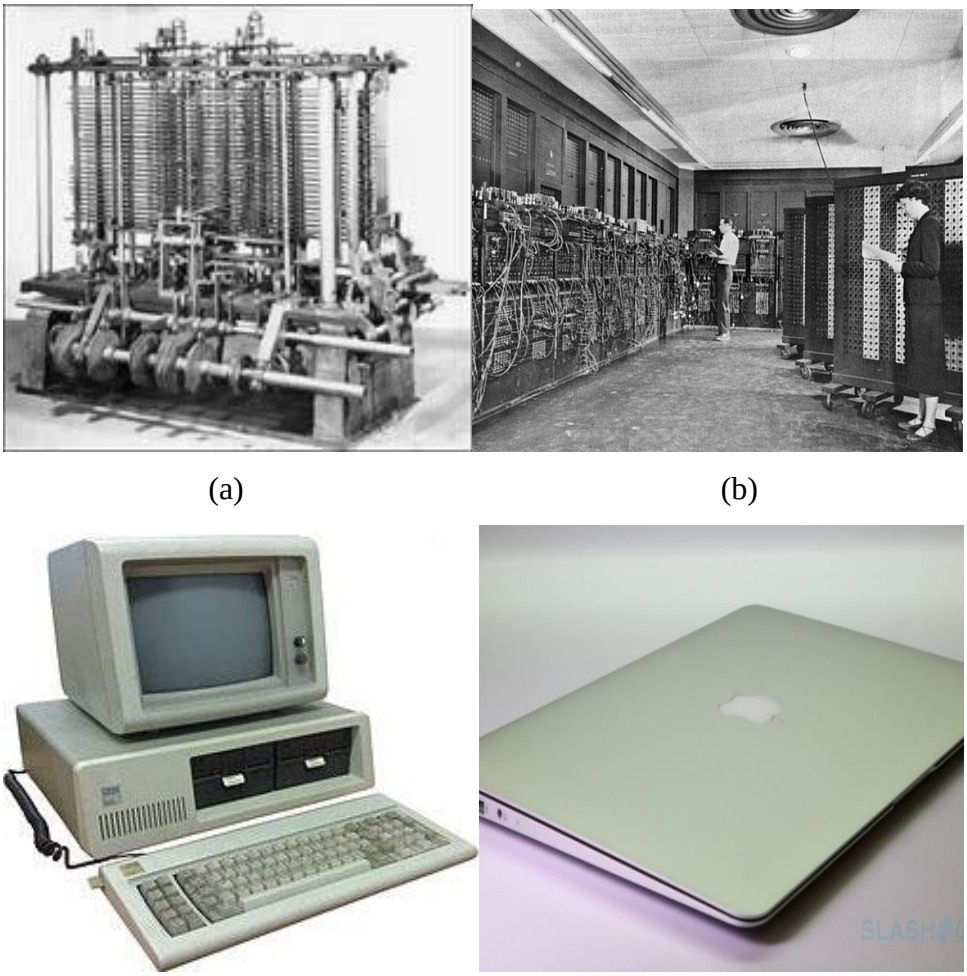

(a) (b)

(c) (d)

Figure 1.1 (a) Babbage's mechanical computer [1] (b) ENIAC, first fully functional digital computer [1] (c) IBM ACORN, first personal computer [1] (d) APPLE MacBook Air, one of the thinnest ultra-books [2]

Miniaturization of electronics is achieved with the miniaturization of the microchips made out of semiconductor materials. These materials are very sensitive to working temperatures. If they are not properly cooled, they may malfunction or may get permanently damaged due to high heat fluxes. If 'Moore's Law', which was suggested by Gordon Moore of INTEL Corporation in 1965 [3], continues to hold, more powerful semiconductor devices will continue to be placed in smaller and smaller areas, year

after year, causing the heat transfer problems we encounter with to get more and more challenging in the future.

Dissipation of waste heat is a problem in every area such as electronic devices, an engine of a car, air-conditioner system. In electronic devices, it is even a bigger problem due to miniaturization and the temperature sensitivity of the semiconductors. Semiconductor microcircuits should be maintained below their maximum allowable temperature limit during their operation. At steady state, waste heat should be continuously dissipated to keep the device at a certain temperature. In military electronics, ambient temperatures may be much higher than the ones dealt with in consumer electronics making heat dissipation more difficult due to lower temperature differences through which high heat fluxes should be dissipated. In our case, since we dissipate the heat from military electronics on a rotary platform, heat transfer problem gets more difficult and more complicated, further. Creating a solution for this challenging problem is the motivation of this study.

1.2 Electronic Cooling Techniques

Heat transfer can be defined as thermal energy transfer from a hot reservoir (source) to a cold reservoir (sink). Heat transfer occurs in three different modes, namely conduction, convection and radiation. Generally, in electronic system design, conduction is used for basic design and for spreading heat on the base material; convection and radiation are used for eliminating or removing dissipated heat from the system to the surroundings. The thermal resistance in convection mechanism is higher than conduction and radiation resistances thus cooling behavior of the packaged system is mostly determined by convection [4].

High power military electronic devices mostly use forced convection with air or liquid flow. However less power dissipating military products use natural convection which is simpler and more reliable. In military device design, conduction performance is improved by using proper materials such as aluminum and copper due to their high thermal conductivity. Radiation is only considered in harsh environmental conditions e.g. in oceans and deserts. In a suitable environment, radiation can support the system

by cooling it. On the other hand, solar load is a big problem in ocean and desert environments, which may make the system a heat sink for the high temperature surroundings. The radiation mechanism may start to heat up the system.

Figure 1.2 shows a comparison of various cooling techniques as a function of the attainable heat transfer in terms of the heat transfer coefficient. To accommodate a heat flux of 100 W/cm^2 at a temperature difference of 50 K requires an effective heat transfer coefficient (including a possible area enlargement factor) of 20,000 W/m^{2}K [5].

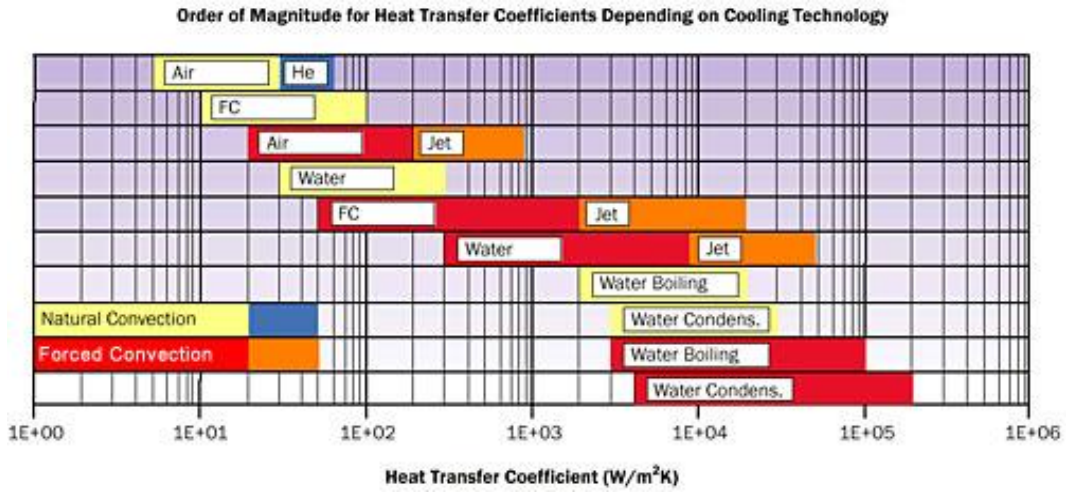

Figure 1.2 Heat transfer coefficient attainable with natural convection, single-phase liquid forced convection and boiling for different coolants [5]

Although liquid forced convection may lead to better cooling performance, designers cannot use it easily due to design limitations such as size, cost and reliability. In contrast, all standard cooling techniques have physical limitations in terms of heat transfer capacity. These techniques are limited by the thermal conductivity of air for convection and the thermal conductivity of copper (the best pure material with the highest thermal conductivity) for conduction. To eliminate or to reduce the effects of these limitations, engineers developed many techniques. Some of these techniques are summarized below.

1.2.1 Conduction and Thermal Interface Materials

Conduction is generally used in point of contact and as a heat spreading operation. Especially pure metals which have higher conductivity should be preferred. Thermal conductivities of some of the common materials are listed in Table 1.1. In electronics cooling, copper and aluminum are the materials of choice when high thermal conductivies are needed.

Table 1.1 Thermal Conductivities of Some Common Materials

Thermal Conductivity of Some Common Materials

Material	*Thermal Conductivity (W/m^{o}C)*
Diamond	2000 – 2300
Copper	380 – 403
Gold	319
Aluminum	210 – 237
Silicon	124 – 148
Germanium	64
Aluminum Oxide	15 – 33
Aluminum Nitride	82 - 320
Silicon Carbide	120 - 270
Solder (95Pb5Sn)	35.5
Solder (37Pb63Sn)	50.6
Polyimide	0.18
Saturated Water (@ 25^{0}C)	0.613
Air (@ 25^{0}C)	0.0261

As it is seen in Table 1.1 Diamond which has a crystal structure has very high conductivity. The reason for that is the Carbon structures which have anisotropic thermal conductivity. Pure crystalline structure has a different thermal conductivity in different crystalline axis, and this phenomena is known as thermal anisotropy, which makes carbon atoms function as insulators, but in certain atomic direction, they act like high conductive materials. It can reach up to 2300 W/mK, which is 10 times higher than aluminum which is one of the most commonly used engineering materials. High

thermal conductivity leads to low temperature gradient in high power applications while making heat sinks more efficient [6]. This feature of carbon is often used by designers. The company ‘Thermacore’, located in USA, produces a special product by using anisotropy of materials. They make a composite material with aluminum and annealed pyrolytic carbon (APG). It is called ‘k-core material’ and is three times more conductive than copper and two times lighter than aluminum. Basically, this product acts like heat spreader and prevents hot-spots (Figure 1.3). This technology is used in aerospace satellites, avionics and military aircraft such as the F-35, F-22 and F-16 fighter planes.

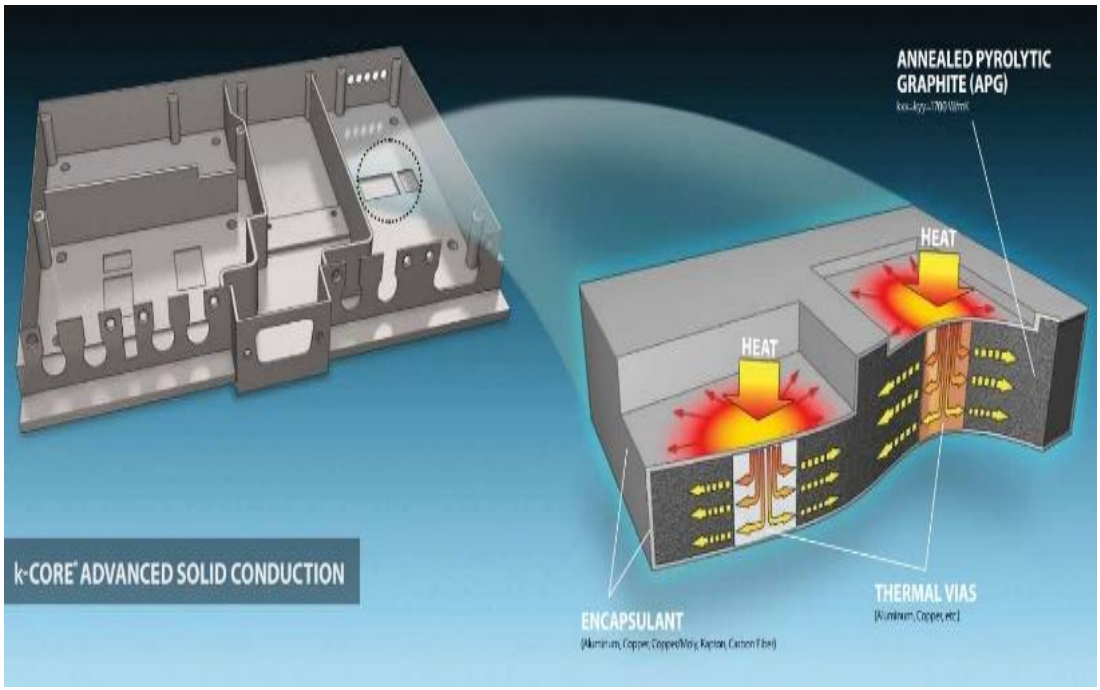

Figure 1.3 The Section of Thermacore’s K-Core [7]

The thermal interface materials are also commonly used in electronics cooling for improving conduction heat transfer performance. If there is a gap between two contact surfaces, the thermal resistance is high at these sections. Due to the manufacturing process, the machined surfaces have some roughness creating small voids at the interface. Gas molecules fill up the voids as it is illustrated in Figure 1.4, which reduces solid-solid conduction at the contact points and generates a thermal resistance due to the low thermal conductivity of gases. To fill up these voids, conductive sheets, grease and adhesive materials are used as interface materials.

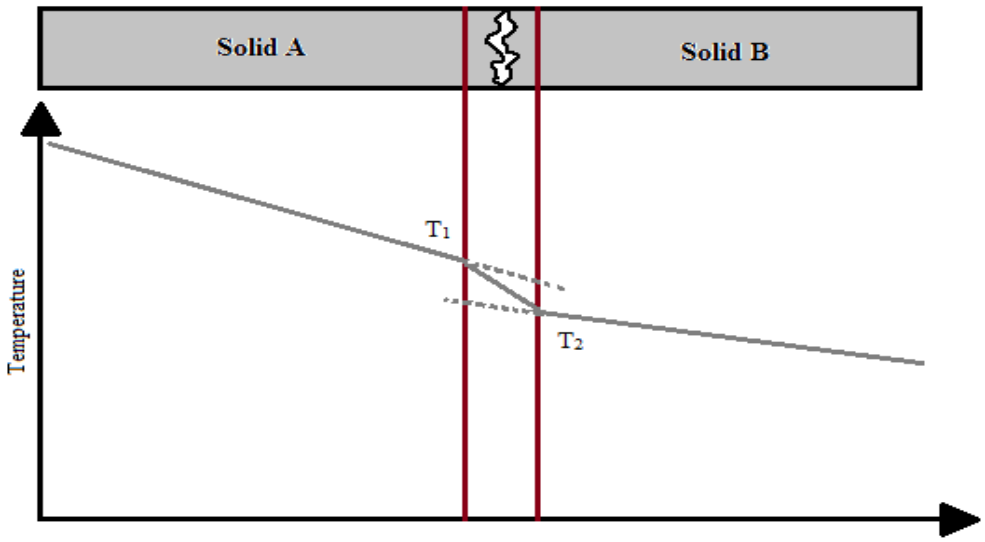

Figure 1.4 The illustration of gap between two solid and temperature drop due to imperfect contact

1.2.2 Convection Cooling

Heat transfer between a solid and an adjacent moving fluid such as liquid or gas is known as convection heat transfer. The main requirement is the fluid, and there must also be a temperature gradient as the driving force. Increase in the temperature gradient results in an increase in the performance of the heat transfer.

$$Q_{conv} = h_f A_{surf} \Delta T \tag{1.2}$$

$$\Delta T = T_{surf} - T_{\infty} \tag{1.3}$$

The governing equation for convective heat transfer is given in Equation 1.2, which is known as Newton's law of cooling. Convection heat transfer depends on the type of fluid (Prandtl number of the fluid), flow conditions (Reynolds number of the flow), fluid interaction area and the temperature difference between the surface and the ambient (Eq. 1.3). Engineers design the cooling system according to these parameters. They can increase the interaction areas by using specific geometries and increase the heat transfer coefficient by choosing the proper fluid or conditioning the fluid. Two main types of cooling relying on convection are explained below.

1.2.2.1 Air Cooling

There are two different air cooling methods: by natural convection and by forced convection. In military electronics, less power consuming devices use natural convection for its low cost and high reliability. For high power consuming devices, forced convection is often used.

Natural convection system guarantees the long term reliability and reduction in cost; however, it is restricted to low heat dissipation values. It is also a type of passive cooling because there is no need for any external power. In the military products with low heat dissipating units such as walkie-talkies, low power control computers, rugged ATR chassis etc. and in the commercial marketing products such as radios, TVs, smartphones etc., natural convection is used. The main goal in natural convection design is to maximize the convection area. This is done by using properly designed fin structures because other parameters of air cannot be controlled in natural convection. The heat transfer coefficient for natural convection is given with;

$$h_{conv} \propto \frac{k_{fluid}}{L} (\mathrm{Pr}\, Gr)^n \qquad (1.4)$$

Where k_{fluid} is the thermal conductivity of fluid, L is the length of the surface which is controlled by design engineers, Pr is the Prandtl Number and Gr is the Grashof Number. Pr and k_{fluid} are the material properties. Gr is the ratio of buoyant and viscous forces and depends on the surface geometry, fluid properties and the temperature difference between the surface and the fluid. The chosen geometry, fin structure, must support the buoyancy effect of the air. (Figure 1.5). Geometry plays an important role in natural convection systems.

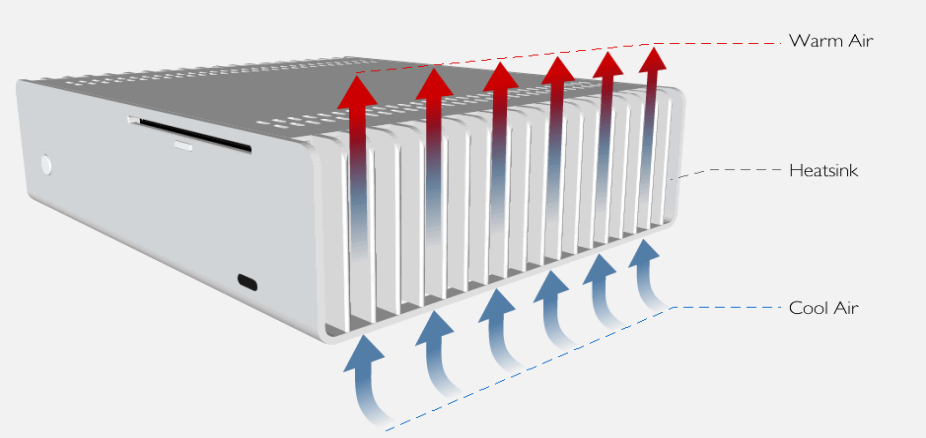

Figure 1.5 Example of a product cooled by natural convection [8]

The biggest obstacle in natural convection is localized hot spots because natural convection has limited heat carrying capacity. Maximum heat flux obtained with natural convection in electronic devices is just 0.05 W/cm^2 [9]. This result demonstrates that the thermal resistance for natural convection is too high due to the low conductivity of air (the fluid).

In forced convection, fluid motion is facilitated by an external power source, which makes forced convection an active method. There is need for an external power to drive fans or pumps. Unlike air natural cooling systems, air is driven through the heat transfer section by using fans. Engineers generally choose air as cooling fluid because air is available everywhere and has no additional cost. Using standard fans, the maximum heat transfer coefficient can be reached to 150 W/m^{2}K with acceptable noise levels, which refers to 1 W/cm^2 for a 60 K temperature difference. Special fans with heat sink assemblies can reach to the maximum flux of 50 W/cm^2, which is a factor of 10 times higher than the values expected 15 years ago [5]. Being an active component, fans can reduce reliability slightly. The weakness of forced convention air cooled systems is the decrease in reliability and the increase in noise levels due to fans.

Instead of common fans, piezo fans are used as a new trend, nowadays. Piezoelectric fans are low power, small, relatively low noise, solid-state devices that recently emerged as viable thermal management solutions for a variety of portable electronics applications including laptop computers and cellular phones. Piezoelectric fans utilize piezo-ceramic patches bonded onto thin, low frequency flexible blades to drive the fan at its resonance frequency. The resonating low frequency blade creates a streaming

airflow directed at electronic components [5]. A group at Purdue reports that piezo-electric fans are more efficient than natural convection heat transfer up to a 100% [10].

1.2.2.2 Liquid Cooling

Liquid cooling is a successful technique in electronics cooling, but it has some disadvantages such as high cost and significant decrease in reliability. Engineers may prefer a liquid as the cooling fluid instead of air or a gas because heat transfer coefficients for liquids are higher than that for gases. In liquid cooling, engineers must identify the hot-spots and create a liquid interface between cooling liquid and the hot-spot region. Water is the most commonly used coolant for cooling high power electronics.

The design stage of a liquid cooling system is complicated. The type of cooling, coolant fluid, power requirement, interface between environment and other additional requirements such as chiller, reservoir, and drainage are the main parameters that define the size of the system. Due to the complexity and the existence of many connected parts, the system setup cost drastically increases, and system reliability decreases because of leakages and power losses of the supporting system.

In a liquid cooling system (see Figure 1.6), heat is added to the system from the hot-spots, and it is eliminated from the system at the heat exchanger. Liquid cooling system requires a heat exchanger and fans, pumps for moving the liquid, a filter to prevent clogging, a reservoir tank to collect the coolant liquid and a cold plate to create an interface between the hot spot and the working fluid.

There are two main types of liquid cooling: direct and indirect liquid cooling. In the direct cooling method, coolant is in direct contact with the electronics, which reduces the thermal resistance. In the indirect cooling method, liquid does not have any contact with the electronics; under such condition, liquid moves inside a special path (e.g. a serpentine) and some section of it contacts the heat affected region, which leads to an increase in thermal resistance.

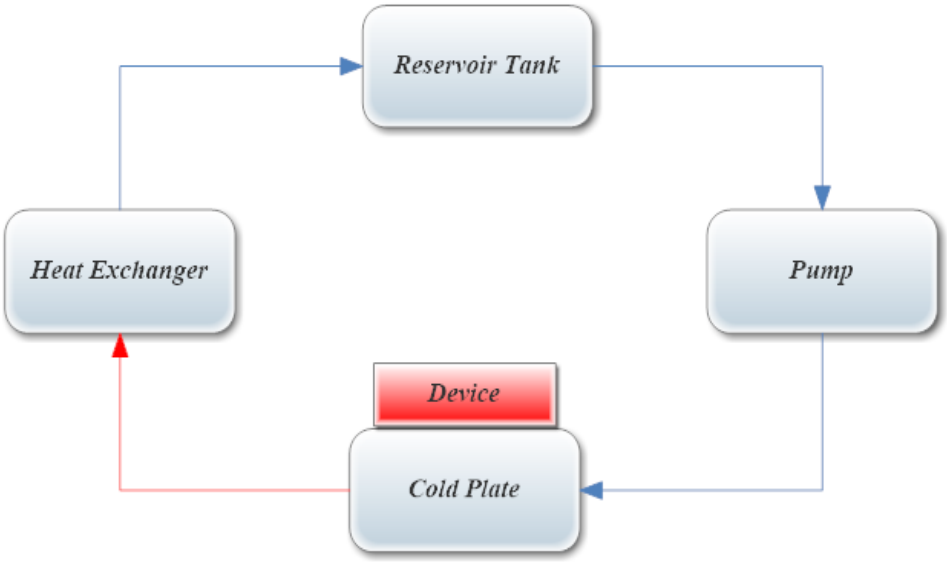

Figure 1.6 Schematic of liquid cooling system

The type of liquid and the selection of it are the most important steps of liquid cooling. Existence of liquid can create leakage risk. If there is a leakage, contact with electronics may cause short circuits and unrepairable damages that may occur if an electrically conductive liquid is used. The most frequently used liquids such as water, alcohol, glycol etc. are electrically conductive, but they have high heat cooling capacity. Because of all these, in order to provide adequate reliability for military products, engineers need to pay much more attention. The typical operating temperature under 0 ^{o}C for military devices is between -20 ^{o}C and -40 ^{o}C according to military quality control test procedures. At that point, water cannot be used anymore due to the fact that freezing point of water is 0 ^{o}C. To overcome this situation, a liquid mixture such as glycol and water is used. On the other hand, pumping power need considerably increases for glycol based liquids due to high viscosity values at low temperatures [11].

Liquid cooling can be named differently according to applications. There are several liquid cooling techniques some of which will be explained below. Main idea of the whole technique is using the advantage of liquid's high heat carrying capacity.

1.2.2.2.1 Single Phase Liquid Cooling

In single phase liquid cooling, coolant always remains in liquid phase, which means there is no phase change. First, the coolant contacts with the heat affected zone, and the temperature of the coolant is changed without phase change. Then, heated liquid is cooled by the heat exchanger. This cycle goes on in the same way. The weakness of this system is requirement of the design space that is the dimension of the system. The heat exchanger may be larger than expected.

1.2.2.2.2 Liquid Cooling with Micro-channels and Mini-channels

The term ‘micro channel’ is applied to channels having hydraulic diameters of ten to several hundred micrometers while ‘mini channel’ refers to diameters on the order of one to few millimeters. In many practical cases, the low flow rate within micro-channels produces laminar flow resulting in a heat transfer coefficient inversely proportional to the hydraulic diameter. In other words, the smaller the channel, the higher the heat transfer coefficient. Unfortunately, the pressure drop increases with the inverse of the second power of the channel size, keeping the mass flow constant and limiting ongoing miniaturization in practice [5].

Liquid cooling with mini and micro –channels is a very effective technique, but the production of these channels is another problem for cooling systems. The production cost is high, and it needs special manufacturing techniques. Engineers should take into consideration whether it is worth spending time and money or not. In Mudawar [11], a high heat flux thermal management scheme was demonstrated with heat fluxes ranging between 1000 W/cm^2 and 100000 W/cm^2. Besides, in 2005, Georgia Tech also announced a novel fabricating technique for liquid channel cooling onto the back of high performance integrated circuits, which was done by embedded fluidic channels into PCB [12]. The German company, IMST, has been working on producing an LTCC with micro-channels to upgrade a compact phased array radar. This trend is still being investigated by other researchers and institutions. This technology will be used in the future for super computers and military detecting systems for weapons.

1.2.2.2.3 Two Phase Liquid Cooling

Two phase refers to phase change. In two phase liquid cooling, coolant contacts with the heated zone, then liquid turns into saturated or supersaturated vapor phase. The main idea behind this technique is high latent heat absorbing capacity during the phase change. During the phase change, there is no change in temperature, hence engineers accept that the temperature distribution on the heated surface is uniform. The performance of this application can easily be affected by gravity and acceleration.

At the heated section, coolant turns into vapor and liquid mixture, and it returns to the liquid phase again in the heat exchanger system. Figure 1.7 demonstrates the stages of two phase liquid cooling. The configuration of the system is similar to single phase liquid cooling, and the only difference is the phase change.

This type of cooling should not be used unless it is really necessary due to its low reliability and high cost. The system may dramatically cause the leakage problem because the vapor form can leak more easily from small gaps than the liquid form and change in specific volume may create leakages. Another problem is in controlling the mechanism. If there is any breakdown at the heat exchanger stage, the heat exchanger can start to behave as heater, and whole system temperature distribution can reach or exceed the critical limits. On the other hand, heat pipes are safe forms of two phase cooling method. There is no need for special safety applications, and they have infinite life-cycles. Heat pipes will be explained in detail in Section 1.2.4.

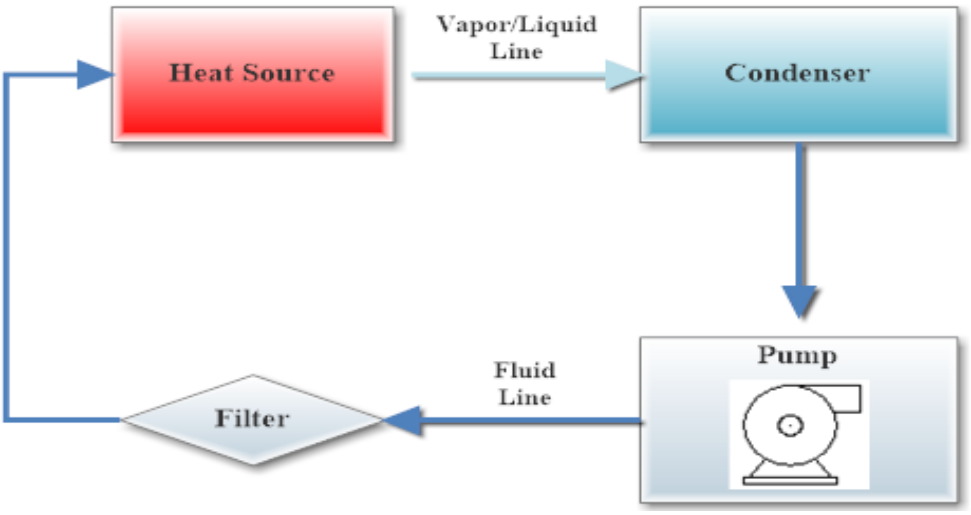

Figure 1.7 Scheme of two phase liquid cooling system design [13]

1.2.2.2.4 Spray Cooling

Spray cooling method is a new trend. Coolant liquid is directly sprayed to hot electronic component such as chips or ICs. It is a direct cooling method because the coolant directly contacts with heated zone. It can be single and two phase type. Spray cooling with two phase condition is more applicable for high heat fluxes. The coolant is sprayed by a nozzle which is also known as atomizer. The nozzle creates fine liquid droplets. When these droplets hit the heated surface, they suddenly vaporize and this absorbs excessive amount of heat.

The coolant here is generally different from the liquids used in other liquid cooling applications. Due to risk of short circuits, these liquids are generally dielectric (electrically non-conductive) type such as FC-72, FC-84 etc.

Important components of spray cooling are nozzle and pump because of the requirement of high pressure for producing droplets. The nozzle design and its position are very important factors affecting the performance. Balıkçı, (2013), studied the types of coolants and positions of the nozzle [14]. In a related study, Öksüz [15] made an investigation about characterization of the spray cooling for electronic devices. They tried to solve the problems on a prototype of an ASELSAN Inc. product which was a rugged chassis design using spray cooling.

1.2.2.2.5 Jet Impingement

The idea behind jet impingement is similar to spray cooling. The main difference between spray cooling and jet impingement is the velocity of sprayed liquid. In jet impingement, heated zone is directly cooled by high velocity liquid from a nozzle whose position is normal to the surface. Due to high speed fluid contact, there can be metal abrasion and corrosion on the cold surface. Hence, this method is not used for long-life electronic devices.

1.2.3 Thermo-electric Cooling (TEC)

Thermoelectric cooling uses Peltier effect to create a heat flux between two different types of materials. A thermoelectric is a small electronic heat pump without any moving parts. It can cool the application surface up to sub-ambient temperature. The cooler operates with direct current. According to the direction of current, it can be used as a cooler or a heater. Such an instrument is also called a Peltier device, Peltier heat pump, solid state refrigerator, or thermoelectric cooler (TEC). The advantage of it is that there are no moving parts, so it operates silently. The disadvantage of the system is that efficiency of TECs is less than that of other techniques, and TECs can resist low heat fluxes. The structural layers of a TEC are illustrated in Figure 1.8.

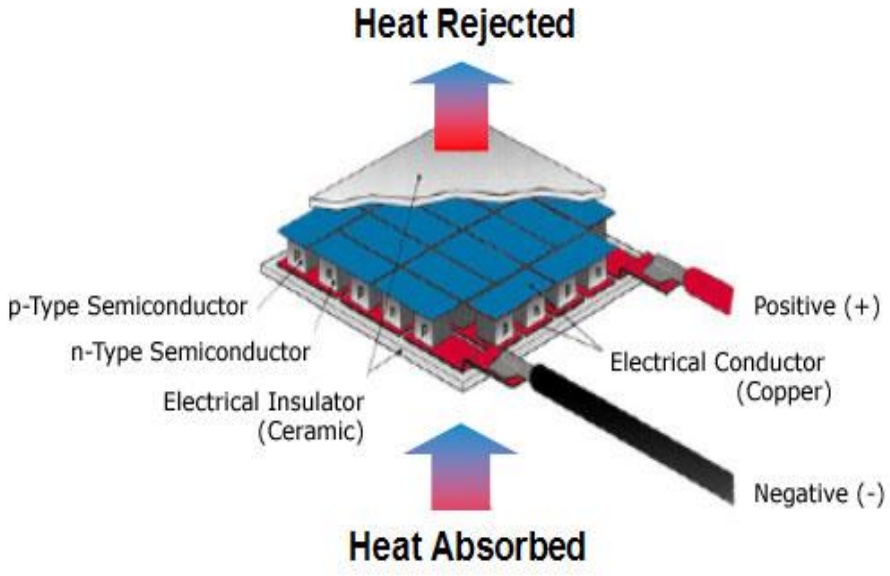

Figure 1.8 Layers of TECs (Peltier Cooler) [16]

1.2.4 Heat Pipe

Heat pipes provide passive and indirect cooling. For this reason, their reliability is very high, and their product life is infinite. Heat pipes cannot be used as coolers by themselves, but they can enrich the performance of conduction and convection. Working principle of heat pipes comes from two phase cooling mechanism. Heat pipes are sealed and vacuum pumped vessels that are partially filled with a liquid. The internal walls of heat pipes are lined with a porous medium (the wick) that acts as a

passive capillary pump. When heat is applied to one side of a heat pipe, the liquid starts evaporating. A pressure gradient exists causing the vapor to flow to the cooler regions. The vapor condenses at the cooler regions, and the condensate is transported back by the wick structure, thereby closing the loop [5].

Heat pipes are also known as super conductive materials. Their directional thermal conductivity is almost 200 times higher than pure copper [17]. The effective thermal conductivity of a heat pipe can reach to values from 50000 W/mK to 200000 W/mK [18]. Heat pipes are used in specific areas such as cooling of a computer CPU, nuclear plants, special studies in aerospace applications, petroleum piping structures and waste heat recovery.

Chapter 2 includes a section with some specific information about heat pipes, their limitations and their applications.

1.3 Summary of Cooling Techniques

In Section 1.2, different types of electronics cooling methods are covered in general, emphasizing the advantages and disadvantages of the cooling system. In addition to summarized techniques, there are several novel and recent methods for cooling. For example, phase change materials, thermionic and thermotunneling cooling, electrohydrodynamic and electrowetting cooling, immersion cooling and magnetic cooling are the popular research topics in the 21st century. Yan et al. [19] made a review comparing the performance of different cooling techniques, and they tabulated the results given in Table 1.2.

Table1.2 Cooling Techniques and Respective Heat Fluxes and Heat Transfer Coefficients (Glassman, 2005) [20]

Mechanism	*Cooling Method*	*Convection Coefficient (W/cm^2K)*	*Heat Flux (W/cm^2)*	*Reference*
Single Phase	Air Natural Convection	0.0005 – 0.0025	15	(Mudawar,2001) [11] (Azar, 2002) [21]
Single Phase	Forced Air Convection	0.001 – 0.025	35	(Mudawar,2001) [11]
Single Phase	FC Natural Convection	0.1	0.1 – 3	(Anderson et al.,1989) [22]
Single Phase	Water Natural Convection	0.08 - 0.2	5 – 90	(Mudawar,2001) [11]
Two Phase	Heat Pipe	N.A.	250	(Zuo et al.,2001) [23]
Single Phase	Micro-channel	N.A.	790	(Tukerman et al.,1981) [24]
Electrical	TECs	N.A.	125	(Riffat et al.,2004) [25]
Two Phase	Pool Boiling (Water)	3.7	140	(Rainey et al.,2003) [26]
Two Phase	Subcooled Flow Boiling (Water)	2	129	(Sturgis and Mudawar, 1999) [27]
Two Phase	Micro-channel Boiling (Water)	10 - 20	275	(Faulkner et al.,2003) [28]
Two Phase	Spray Cooling (Water)	20 - 40	1200	(Pais et al.,1992) [29]
Two Phase	Jet Impingement (Water)	28	1820	(Overholt et al.,2005) [30]

1.4 Objective of Study

Achieving the best heat transfer solution for an electronic package is not only about using or choosing a technique, but also about applying it. Many engineering parameters must be considered while designing cooling systems for products. Performance, cost, sustainability, reliability, feasibility, simplicity etc. are the main engineering parameters, which must be considered at the design stage by design engineers.

As indicated in Section 1.2, there are many techniques with many parameters and some limitations to select as an appropriate cooling for a designed system. Combination of these techniques generally gives the best results.

Aim of this study is to design a combined cooling system for the military electronic devices on rotary platforms. The major concerns for the design are performance, simplicity and cost. To achieve in all of these, heat pipes and forced convection techniques are combined.

Rotary platforms in land and naval military systems can carry weapons, active and passive antennas, radar system and telecommunication system as illustrated in Figure 1.9. These platforms rotate 360 degree around the z-axis. Due to rotation, there must be special components which must provide electrical, mechanical and fluidic connections. This part is called 'slip ring'. Slip ring is an electromechanical device that allows transmission of power, electrical signals and mechanical interface from the stationary part of the system to the rotating structure.

(a) **(b)**

Figure 1.9 Examples of Rotary Platforms (a) ASELSAN Naval System [31] and (b) ASELSAN Automatic Weapons System [32]

A slip ring with only an electrical interface has a price between 10,000 and 60,000 dollars. A slip ring with both electrical and fluidic connections cost more than hundred thousand dollars. Besides being expensive, these parts also reduce the reliability of the whole system. Slip ring can carry control signals, power connection, RF (radio frequency) for radar applications and fluidic connections for liquid cooling. For the

high speed rotation ranges, there might be leakage problems, which may cause whole system failure.

In order to overcome the difficulties associated with slip-rings, in this study, long bended heat pipes are used together with forced convection. Heat pipes are connected to heat sinks with different shapes and sizes of fins. At the first stage of the study, a preliminary design and numerical analyses of the preliminary design are done. Then, these results are validated with experiments. Finally, there is a design optimization in light of the information coming from the numerical analyses.

CHAPTER 2

THEORY AND LITERATURE SURVEY

In this chapter, the theories of heat pipes and forced convection are presented. First, the heat pipe is explained in detail. Then, the theory section continues with forced convection and its parameters. Finally, there is a review of the related literature.

2.1 Historical Development of Heat Pipe

The heat pipe is a simple passive cooling device, operating principle of which combines the theories of thermal conductivity and two-phase heat transfer between two solid interfaces. This combination makes the heat transfer problem in heat pipes complex. It is a passive device because there is no need to provide any power from outside. There is one driving force that is the temperature gradient between solid interfaces at its ends.

The initial appearance of heat pipes was in 1800s with Perkins tube which is a heat transfer device operating like a two-phase thermosyphon. A.M. Perkins and J. Perkins focused on single or two phase heat transfer phenomena from a furnace to a boiler. This device was produced in order to make rapid superheated steam [33].

The first occurrence of a heat pipe product was in 1942 by Richard S. Gaugler. It was patented by General Motors Corp (Patent no: US 2350348 A). It was the first passive device which was based on two phase heat transfer with capability of transfer of large heat loads with minimum temperature drop [33] [34]. It was the proof of the adiabatic assumption of heat pipes.

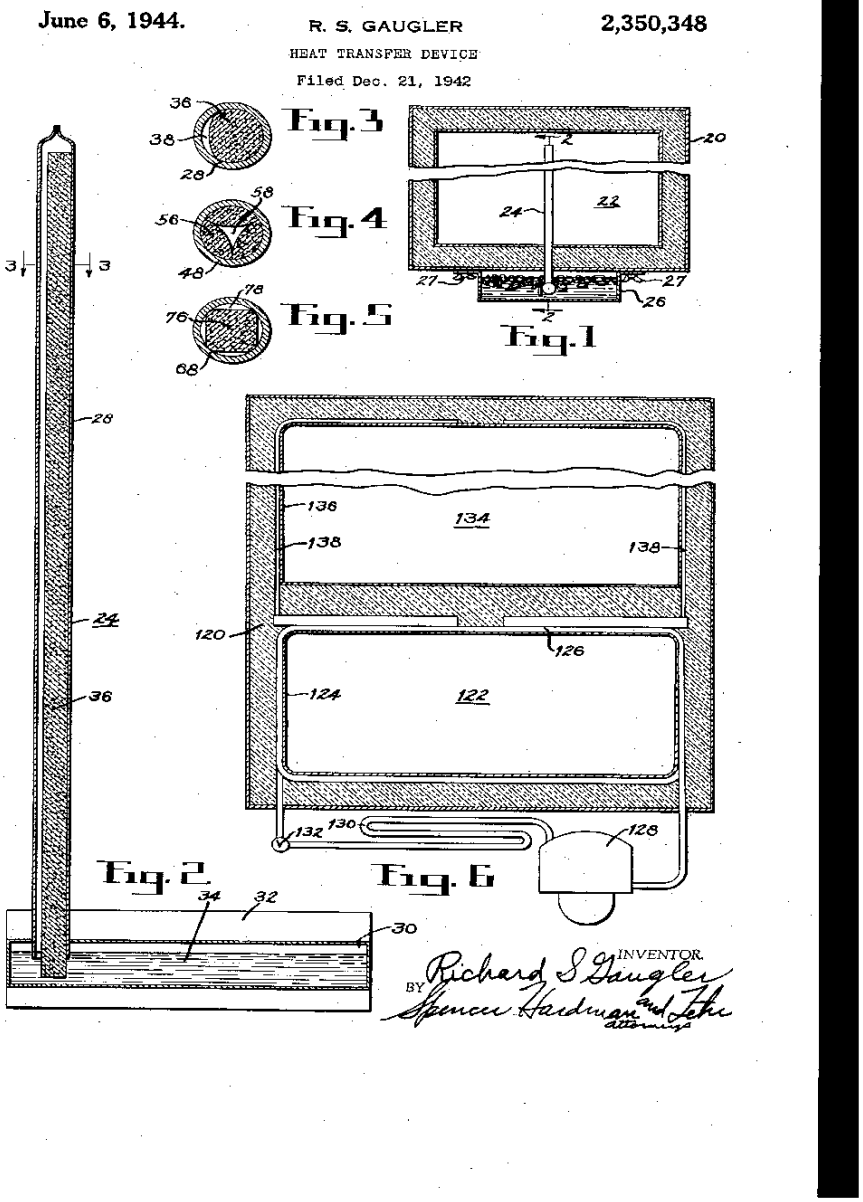

Figure 2.1 Gaugler's patent drawing [34]

Figure 2.1 illustrates the thermal device of Richard Gaugler which was a non-compact form of heat pipe. The part of the drawing marked as "Fig.2" in Figure 2.1 shows the setup of the product. The product was made up of a thin sealed vessel filled up with a volatile liquid which evaporates easily. In the inner section of the product, Gaugler tried wick structures with three different cross-sections that are illustrated as "Fig.3", "Fig.4" and "Fig.5" in Figure 2.1. In his patent, he did not use the word, '*heat pipe'*;

the product was called *'heat transfer device';* and it was declared as a refrigeration unit [34].

In 1960s, space applications became popular, and NASA started to finance thermal management applications for space. In 1964, Grovers et al. [35] from Los Alamos National Laboratory announced a study about a heat transfer device, and this device was named *'heat pipe'*. In addition, this study was patented, which was filed on behalf of the United States Atomic Energy Commission. The word of *'heat pipe'* was new, but the idea behind it was the same as Gaugler's idea. The difference from Gaugler's is that they studied the temperature ranges (operational conditions) and upgraded the mathematical modelling.

After appearance of heat pipes, scientists and researchers began to investigate working conditions and heat pipe behavior in space. In 1967, an experiment which was the first flight of a heat pipe to space was done. The experimental setup consisted of an electrical heater at one side of the heat pipe, a compact heat pipe which was a water / stainless steel heat pipe and a telemetric data collector. It was launched into earth orbit from Cape Kennedy on an Atlas-Agena Vehicle [36]. After the success in 1967, the first use of heat pipes in a space thermal control application was on GEOS-B satellite, launched from Vandenburg Air Force Base. The heat pipe in the satellite was manufactured from aluminum 6061-T6 as a vessel material and freon-11 was used as the working fluid [37]. The main goal of using the heat pipe was obtaining isothermal surfaces on satellite's panels.

The first commercial company producing heat pipes was RCA which was supported by U.S. Government. They used glass, copper, nickel, stainless steel, molybdenum and TZM molybdenum as vessel materials in their heat pipes. In addition to these, they used water, cesium, sodium, lithium and bismuth as working fluids. Maximum operating temperature of 1650 ^{o}C was achieved [38] [39] [40].

Apart from the developments in USA, there were also several investigations about heat pipes, elsewhere. In mid 1960s, The Harwell Comp. made an investigation about using heat pipes in a nuclear application in Ispra, Italy [41]. In Japan, (1968), Kisha Seizo Kaisha Company started a program about using heat pipes in refrigeration engines and

air conditioners [42]. During 1969, the companies from Europe, British Aircraft Corp. (BAC) and Royal Aircraft Establishment, made investigations in using heat pipes in aviation systems [43]. The avionic researches proved how heat pipe was used in electronic cooling. The first electronic cooling application was done by Calimbas and Hultt of the Philco-Ford Corp., which was mainly about high-power airborne travelling wave tube (TWT) [44].

Today's technologies are more complex than the ones in 1960s or 1970s due to increased power consumption and decreased dimensions. Engineers do not want to consume extra power for thermal management, hence the trend of using passive techniques is increasing rapidly. That is, heat pipe is becoming a new trend in the area of cooling.

2.2 Applications and Advantages of Heat Pipes

Applications of heat pipes are very widespread. Heat pipes can be seen in military devices, in household appliances, in computers especially in tablets and laptops, in air conditioning systems and in molding industry etc. The reasons behind why heat pipes are commonly preferred are that heat pipes are compact in size, and their use in electronics cooling increases system reliability and reduces the initial cost. Another reason may be their long life-cycle. Many producers give infinite life for their products. This is an advantage for satellite and military device applications because maintenance risk must be minimum in these areas. However, for a long service life it is important to choose the proper vessel material and to identify the working fluid which is compatible with that vessel material.

As it is emphasized above, for heat pipe use in electronics cooling, the initial cost is low, and the reliability is high because there is no excessive use of forced convection products. For high power dissipating electronic systems generally liquid cooling is used. Liquid can be selected as oil, water or special chemical mixtures according to working conditions. In addition to this, these systems require liquid guide channels in the product and large heat exchangers, which all increase the initial cost. Designers try to eliminate these obstacles by applying passive cooling techniques. To employ heat

pipes for industrial applications, it is desirable to know thermal performance of the heat pipe under various operating conditions, a priori. Thermal performance of a heat pipe depends on various radial and axial thermal resistances at the evaporator, condenser and inner sections of the heat pipe [45]. Hence, for the heat pipe applications, design engineers must focus on the evaporator and condenser designs. Consequently, use of heat pipes requires detailed focus on the design.

An important point about heat pipe use is that it is not a complete solution to the thermal management problem by itself. It is merely a part of heat transfer enhancement. This enhancement comes from the properties of heat pipes. Heat pipes can be used for spatial separation of the heat source and the heat sink. They are also utilized in temperature flattening, heat flux transformation, and temperature control. In electronics applications, some components generate a hot spot and cause high heat dissipations. However, in some cases these components are surrounded by other components which have different temperature sensitivity levels. As it is shown in above scenario, if the designer cannot remove heat from the hot spot region, a heat pipe can be used as a separator of heat source and heat sink. Heat is captured rapidly and transferred to the remote heat sink through high effective thermal conductivity of the heat pipe. Another application is temperature flatting in which the heat pipe function as a heat spreader. The main aim of thermal design is to generate an iso-thermal base which requires to minimize the temperature gradients. In addition to this, temperature flatting is the idea behind the use of heat pipes in space applications. The third application is flux transformation which is generally used for reactor technology and casting applications. The last one is temperature control which is more complicated than other applications. It requires a variable conductivity heat pipe and used in spacecraft design [46].

In 1960s, NASA started to investigate use of heat pipes in space applications. Today, NASA uses heat pipes as heat spreaders in satellite design. The outer surface of a satellite, facing the sun, has very high temperature values, however inner surface, in the shadow, has an extremely low temperature. Hence, there is a large temperature gradient between the surfaces. These two surfaces are connected with heat pipes, which makes hot section function as a source and cold section as a sink. When the

system reaches to the steady condition, the temperature gradient is minimized. Dornier Company [47] demonstrated the difference between with /without heat pipe designs for a satellite as given in Figure 2.2. As it is seen, heat pipes can eliminate $\Delta T = \sim 100$ ^{o}C.

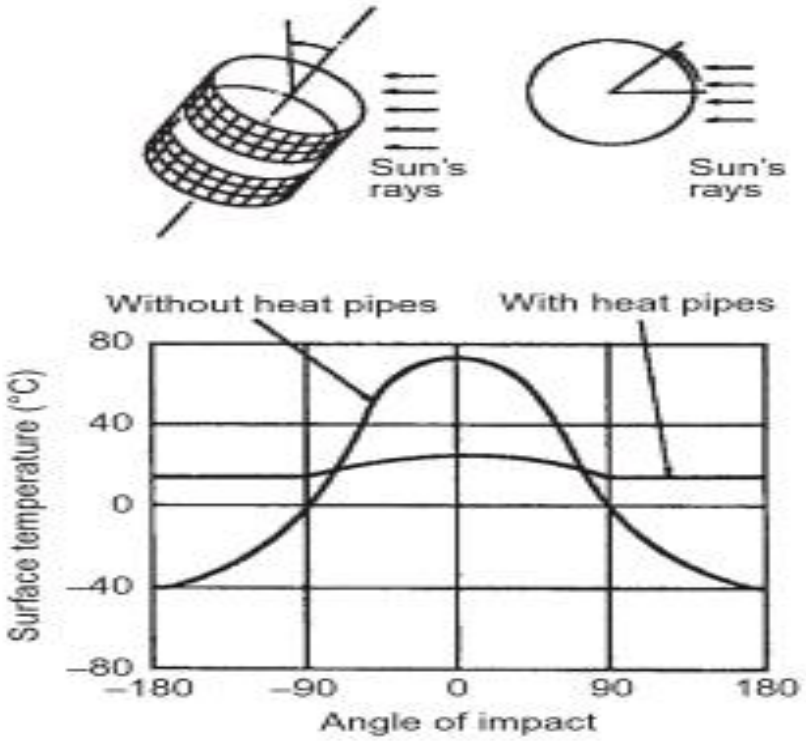

Figure 2.2 Temperature gradient of satellite with/without heat pipes [47]

Another application area is die casting and injection molding. For the die-cast process, during the solidification, dies are generally cooled by water. However, this causes thermal shock for the product, and there can be some defects such as cracks, splitting, draws etc. As an alternative solution, the die is produced from high thermal conductivity materials and heat pipes are attached to certain points of the die. Other ends of the heat pipes are connected to a liquid channel. When the casting is finished, channel is filled up with water. Die starts to cool down rapidly thanks to super conductivity of heat pipes. In this method, even though there is no direct contact with liquid, die is cooled in a short time, and there is no thermal shock. Using heat pipes in injection molding is the reverse process of casting. At the end of the each manufactured product process, injection nozzle starts to cool down. Nevertheless, before the next molding is started, nozzle must be heated in order to prevent plastic or metal from

solidifying at the nozzle outlet. Otherwise, outlet of the nozzle might be blocked. The nozzle is heated up by heaters on the nozzle surface, but this requires an external power, which means extra cost. In order to eliminate external power requirement, heat pipes are placed between the molten plastic/metal reservoir and the nozzle. With the excessive dissipated heat from the molten material, the nozzle can always be kept ready to work for the next product.

Heat pipes are also used in order to prevent waste of energy. With the increase in energy costs, designers and scientists want to use every energy source. For this demand, heat pipes are used in building construction for air-heating. As it is known, the air heating system takes cold air from the atmosphere to the inlet channel of the system. The standard system sucks the air and heats it up with heaters, then heated air is sent to the building ventilation system. If temperature difference between fresh (cold) air and air after heating operation increases, the required energy of heaters increases, which means it needs more power. The solution is generating pre-heating system which uses the waste heat. It is basically an energy recovery operation. Thermal recovery unit is designed using heat pipes. The evaporator sections of the heat pipes are placed into the exhaust air of the heaters, and the condenser section is mounted into the cold air inlet. The inlet air is heated up by the heat pipe system, and this results in reduction in power consumption of the heaters. For example, Firouzfer et al. [48], in 2011, made an investigation of a heat pipe heat exchanger applied to an HVAC system. They observed the performance and the advantages of this HVAC system. This study reaches to the conclusion that there is an increase in air quality in the heated space and reduction in consumed power. This system decreases the relative humidity in the conditioned space (nearly 10%) and reduces the power demand. Another example is that The National Engineering Laboratory and The Shell Research Laboratory have co-operated in applying heat pipes to solve the problem of exhaust emissions of petrol engines. The heat pipe was attached between the intake manifold and the exhaust system. The evaporator is the exhaust and the condenser is the intake. As a result, by using waste heat, the control of lean burn was achieved [49]. Similarly, heat pipes are also used as liquid to liquid heat exchangers.

The most striking example comes from Alaska pipe line, the surrounding, low temperature, is used as the condenser and the transported fluid section is the evaporator[50]. In Alaska, ground has a permafrost layer. The permafrost layer is the layer occurring below 0 ^{o}C at which soil and salt water mixture freezes, and it creates a non-porous ice rock under the surface layer. When pipeline penetrates the ground, heat spreading from the fluid melts this structure, which results in the collapse of the pipeline. In order to eliminate this obstacle, excessive heat dissipation of the fluid is transferred to the atmosphere by using heat pipes. As it is seen in Figure 2.3, the heat pipes used are long and they are used in order to prevent the permafrost layer from melting. 100000 heat pipes are used and their dimensions range in diameter between 5 cm and 7.5 cm, in length between 9 m to 18 m.

Figure 2.3 Heat pipe application in Alaska pipeline with permafrost ground [51]

The most common example of heat pipe application is electronic cooling. In notebooks, the heat pipe is attached on CPU, and its condenser may be located in different sections inside the notebook. For example, Apple MacBook Pro with retina display is the last example for CPU cooling. As it is illustrated in Figure 2.4, the heat pipe is connected to CPU, and its ends are connected to specially designed slim fans.

With all these, the thickness of the notebook is only 18 mm. Also it can be easily seen that heat pipe's middle sections are used as evaporators and the ends are condensers.

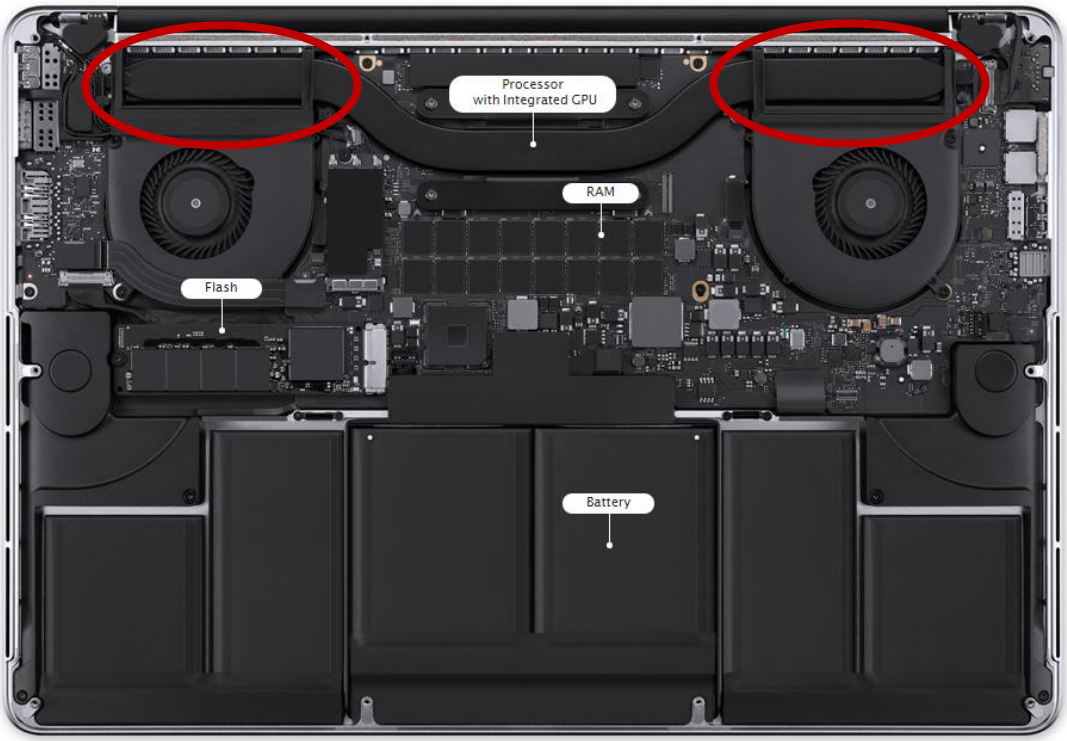

Figure 2.4 Internal design of Apple MacBook Pro [52]

To sum up, applications of heat pipes are widespread. They can be seen in buildings, HVAC systems, space and avionic applications and electronic devices. Heat pipes are preferred for their low cost, infinite life-cycle and high reliability.

2.3 Working Principles of Heat Pipes

Historically, metallic heat sinks are very useful in thermal management of electronic devices. Nevertheless new generation electronic devices have large amounts of heat dissipation, hence metallic heat sinks, which are combined with natural or forced convection are not sufficient against excessive heat dissipation rates. Other limitations are the weight and the required physical volume (size). Due to these limitations, the trend of application of heat pipes is rising.

Heat pipes provide passive and indirect cooling. Because of this, their reliability is very high and their product life is infinite. Working principle of heat pipes comes from

two phase cooling mechanism which combines conduction with convection. Because of this, understanding how heat pipes work and mathematically modelling them are complex and hard. Two phase heat transfer helps a heat pipe gain extremely high thermal conductivity, which is thousands of times higher than the same amount of pure copper rod. Basically, a heat pipe has three main structures; namely, the vessel (outer wall), the working fluid and the wick structure (inner structure). Common types of heat pipe vessels have shapes of cylindrical, rectangular, ellipsoid etc. The vessel material and the working fluid are selected according to each other's material and operational conditions. The inner (wick) structure has an effect on the capillary effect or transport performance.

The heat pipe is a closed envelope device, in other words, its tube is evacuated and charged with the working fluid. Then, internal pressure of the tube is set to vapor pressure of the inside working fluid. As heat is input at the evaporator, the fluid is vaporized, which creates a pressure gradient in the pipe. This pressure gradient forces the vapor to flow along the pipe to the cooler section where it condenses giving up its latent heat of vaporization. The working fluid is then returned to the evaporator by capillary forces developed in the wick structure [53]. The working principle is illustrated in Figure 2.5.

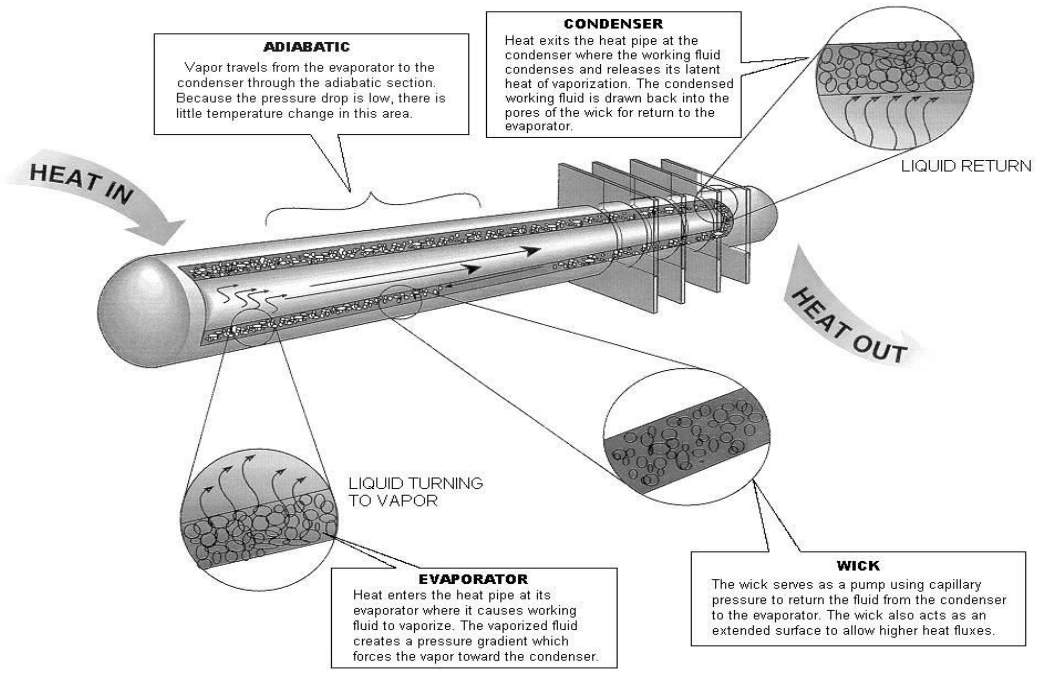

Figure 2.5 The working operation of heat pipe [53]

There are many factors affecting the performance and design of heat pipes. These are length, diameter, bending effect, compatibility of vessel and working fluid, operating temperature range, mounting orientation, power limitation, thermal resistance and connections of ends. During heat pipes are manufactured or designed, all factors should be taken into consideration.

Consequently, heat pipes are designed for a large range of working conditions from cryogenic temperatures (< -243 ^{o}C) to elevated temperatures (> 1500 ^{o}C) by selecting proper vessels and working fluids. In heat pipe operations, there is no external power to drive the mechanism. If there is a 'heat-in' section and a temperature difference between two ends, the mechanism will operate itself. Heat and the temperature difference are driving forces for heat pipe operations.

2.4 Wick Structures of Heat Pipes

Identifying the inner structures of heat pipes is the most critical point in the design of a cooling system supported with heat pipes. The wick type of a heat pipe directly affects performance of the heat pipe. Essentially, wick structures affect capillary pressure inside the heat pipe, which has importance when working against gravity. The most commonly used wick structures are sintered powders, grooves, screens and felts. The sintered type wick has more advantages than the others in terms of manufacturability, cost and performance. In addition to these, it is the simplest one. The most critical advantage of the sintered type is operational orientation. It can be easily used in the against gravity application by placing the condenser section above the level of the evaporator or the heat source. On the other hand, the groove and the screen mesh heat pipes have very limited capillary forces to support the continuous cycle. These types are not suitable for the against gravity application; however, especially the groove type is the most frequently used in space applications due to its minimum irregularity in non-gravitational space. The felt type is not very common because it is produced from knitted metal wire mesh, so it has some composite types.

2.5 Limitations of Heat Pipes

The most important parameter in heat pipe design is the rate of heat that can be transferred by the designed heat pipe, defining the working range as heat transferring capability. A proper design results in increasing performance and increasing heat carrying capability in the order of kilowatts. If a heat pipe is used above its capacity, there will be a drastic reduction in performance and thermal conductivity. In addition to this, if it is not used within its limits, a failure may occur inside the pipe such as dry-out.

Heat carrying capacity depends on several factors, such as the working fluid, the wick type, the working temperatures and the orientation and the dimensions of the heat pipe. All these factors result in five main limits for heat pipe's operations, namely viscous or vapor pressure, sonic, capillary pumping or 'circulation limit', boiling and entrainment/flooding. These limits are given in Table 2.1 together with brief explanations of descriptions, causes and potential solutions.

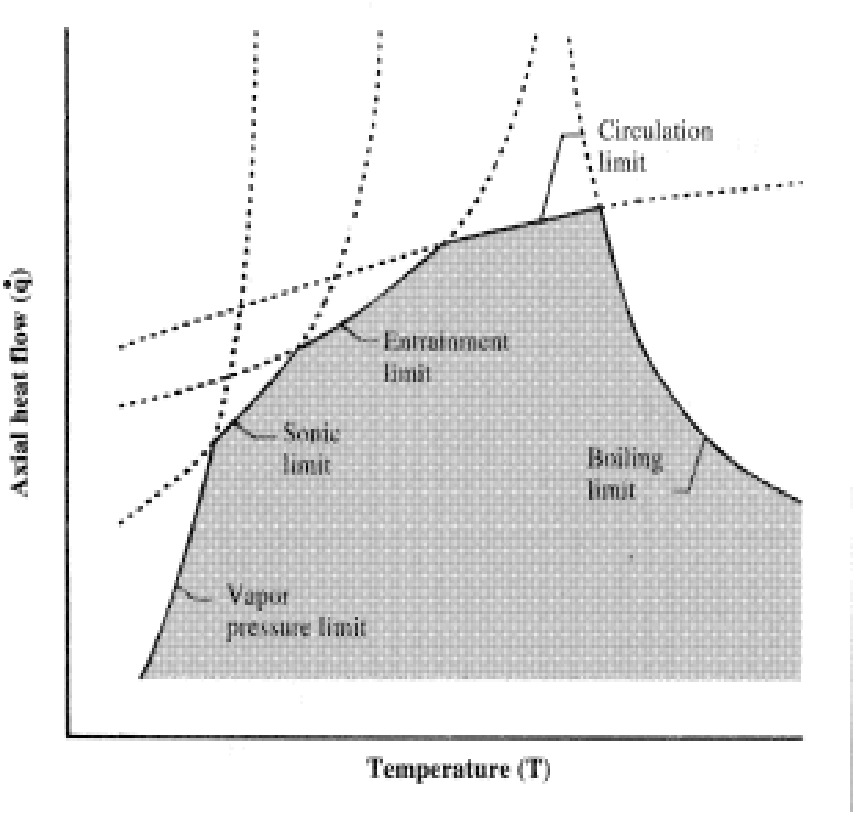

Figure 2.6 Usage Limitations of Heat Pipe, Axial Flux vs Temperature [54]

Figure 2.6 demonstrates the distribution of the limits according to axial heat flow vs temperature. At the design stage, this graph should be taken into consideration. For example, low temperature working conditions are challenged with the vapor pressure (viscous) limit, hence the selection of the working fluid is the most important stage. There are brief explanations about these limits in the following section.

Table 2.1 Heat transport limits of heat pipe [53]

Heat Transport Limit	***Description***	***Cause***	***Potential Solution***
Vapor Pressure (Viscous)	Viscous forces prevent vapor flow in the heat pipe	Heat pipe operating below recommended operating temperature	Increase heat pipe operating temperature or find alternative working fluid
Sonic	Vapor flow reaches sonic velocity when exiting heat pipe evaporator resulting in a constant heat pipe transport power and large temperature gradients	Power/temperature combination, too much power at low operating temperature	This is typically only a problem at start-up. The heat pipe will carry a set power and the large T will self-correct as the heat pipe warms up
Entrainment/Flooding	High velocity vapor flow prevents condensate from returning to evaporator	Heat pipe operating above designed power input or at too low an operating temperature	Increase vapor space diameter or operating temperature
Circulation (Capillary)	Sum of gravitational, liquid and vapor flow pressure drops exceed the capillary pumping head of the heat pipe wick structure	Heat pipe input power exceeds the design heat transport capacity of the heat pipe	Modify heat pipe wick structure design or reduce power input
Boiling	Film boiling in heat pipe evaporator typically initiates at5-10 W/cm^2 for screen wicks and 20-30 W/cm^2 for powder metal wicks	High radial heat flux causes film boiling resulting in heat pipe dry out and large thermal resistances	Use a wick with a higher heat flux capacity or spread out the heat load

2.5.1 Viscous Limit

This limit is also known as the vapor pressure limit. At the start-up range of the heat pipe, which is the low temperature range, vapor pressure difference between the evaporator and the condenser of the heat pipe can be too small. This results in an increase in the viscous force of the working fluid, which means the viscous force within the vapor region can be larger than the pressure gradient at the working temperature. Occurrence of the viscous region prevents the vapor flow inside the tube and vapor stays stagnated [55]. This limitation is a big problem for cryogenic heat pipes, heat pipes with a long condenser and operating temperatures below the freezing point of working fluid.

Busse (1973) made an experimental study and created a mathematical model. The mathematical relation giving the maximum axial heat transfer rate reaching viscous limit [56] is

$$q_{app} < q_{vis} = \frac{A_v . r_0^2 . \delta . \rho_v . P_v}{16 . \mu_v . L_{eff}} \qquad \textbf{(2.1)}$$

where P_v and ρ_v are respectively vapor pressure and density at the evaporator end of heat pipe. 'δ' is the enthalpy of vaporization, A_v is area of the vapor section and μ_v is the dynamic viscosity of the vapor phase. Finally, L_{eff} is the effective length of the heat pipe, which can be calculated from

$$L_{eff} = \frac{1}{2} l_{condenser} + l_{adiabatic} + \frac{1}{2} l_{evaprator} \qquad \textbf{(2.2)}$$

The solution for eliminating this limit is changing the working fluid or increasing the operational temperature.

2.5.2 Sonic Limit

In a heat pipe of constant vapor space diameter, vapor flow accelerates and decelerates because of vapor addition in the evaporator and vapor removal in the condenser. The changes in vapor flow also change the pressures along the heat pipe. As more heat is applied to the heat pipe, vapor velocities generally increase. A choked flow condition

will eventually arise, where the flow becomes sonic. At this point, vapor velocities cannot increase and a maximum heat transport limitation is achieved. The heat flux that results in choked flow is considered as the sonic limit [57]. The recommended heat transfer rate for avoiding sonic limit is given with

$$q_{app} < q_{sonic} = 0.474 A_v . \delta . (\rho_v . P_v)^{1/2} \quad \textbf{(2.3)}$$

On the other hand, a high vapor velocity also results in quick response of the heat pipe.

2.5.3 Entrainment / Flooding Limit

Vapor velocity increases with temperature and may be sufficiently high to produce shear force effects on the liquid return flow from condenser to evaporator, which cause entrainment of the liquid by vapor. Restraining force of liquid surface tension is a major parameter in determining the entrainment limit [54]. The existing vapor blocks the motion of liquid to evaporator section, in other words condensed flow cannot reach evaporator section. This situation concludes in 'dry-out' phenomena. The corresponding heat transfer rate causes this procedure, called entrainment limit. This limit is calculated using Formula 2.4.

$$q_{ent} = A_v . \delta . \sqrt{\frac{\rho_v . \sigma}{x}} \quad \textbf{(2.4)}$$

Where 'σ' is surface tension of working liquid and 'x' is characteristic dimension of wick structure.

$$x = 2 r_\sigma \quad \textbf{(2.5)}$$

Where 'r_σ' is effective radius of pure structure.

Flooding limits are valid for gravity aided operations due to the existence of excess liquid. The wick structure is saturated and the excess fluid results in a "puddle" flow on the surface of wick structure. The flooding limit, likewise the entrainment, happens when high vapor velocities preclude the fluid that is flowing on the surface of wick to return to evaporator. The shear force of vapor prevents the condensed fluid from reaching to evaporator and leads to a flooding condition in the condenser section [57].

Shortly, this is known as accumulating excess water at condenser section. This also causes ‘dry-out’ like entrainment limit.

These limits can be solved by applying procedure below;

- Increase in vapor space (Large diameter heat pipe)
- Change in operating temperature
- Use gravity advantage to give direction to fluid towards the evaporator

2.5.4 Capillary Limit

The driving force of heat pipe liquid circulation is capillary force. Depending on the wick structure of the heat pipe, capillary pressure exists which relies on the pore radius of the wick and surface tension of the working fluid. Total capillary pressure created by the wick must be greater than the sum of the gravitational losses and fluid flow losses through the wick. Liquid and vapor pressure drops depend on pipe and wick structure geometries, physical properties such as wick thickness, effective length, vapor space diameter, etc and fluid properties such as latent heat, density, viscosity, etc. A critical heat flux exists which balances capillary pressure with pressure drop associated with fluid and vapor circulation. For horizontal or against gravity operations, which means evaporating section at a higher level than the condensing section, heat pipe is limited by capillary limit. For gravity aided orientations, capillary limitation may be neglected, in this case flooding limit should be taken into consideration if the heat pipe can have an excess fluid accumulation [57] [58]. The maximum capillary pressure can be calculated depends on where ‘σ’ is surface tension of working liquid and ‘r_σ’ is effective radius of wick.

$$\Delta P_{cap} = \frac{2\sigma}{r_\sigma} \qquad \textbf{(2.6)}$$

If capillary limit is experienced, it should be eliminated by changing the wick type and reducing the heat load at the evaporating section (heat input).

2.5.5 Boiling Limit

If excessive heat load is applied to the evaporating section of the heat pipe, the liquid inside the pipe can produce bubbles in the evaporator wick. Formation of vapor bubbles in the wick is undesirable because they can cause hot spots and obstruct the circulation of the liquid. In other words, it is defined as a drastic decrease in thermal conductivity. With the increase of heat flux, more bubbles come out. At a certain heat flux limit, bubble formation completely blocks the liquid flow, at that point fluid flow stops and heat is only transferred on the wall of the heat pipe. In this case, the heat pipe does not function as a super conductor, and its conductivity becomes equal to that of the wall material. Hence, this limitation is associated to a radial heat flux, which means heat is applied to the perimeter of the heat pipe or outer shell. The boiling limit generally occurs at high temperature working conditions [54] [57] [59].

By increasing the heat flux at the evaporator, the critical point is reached when the temperature difference exceeds the degree of superheating sustainable in relation to nucleate boiling conditions. When most of the liquid transforms into vapor, the first dry out occurs. '*Dry-out'* exists due to an unbalanced ratio between vapor and liquid. If high heat flux is still applied, the evaporator section loses all fluid itself, and this phenomena is known as *'burn-out'.* When 'burn-out' occurs, heat pipe starts to act like a metal rod.

Boiling limits can be prevented by using a wick with a higher heat flux capacity or spreading out the heat load. Among the type of wicks, the sintered wick is the best way of dealing with boiling limits. This type has significantly more area inside the pipe, hence it can deal with high fluxes. The basic understanding of whether dry-out occurs or not is done by taking temperature measurements on the heat pipe wall between the end of the evaporator and the top of the condenser. If the temperature differences are large then the adiabatic assumption is not correct, and the dry-out exists.

2.6 Heat Pipe Arrangement and Operations

The performance of a heat pipe does not only depend on the working fluid, the wick type, the working temperature, the dimensions of the heat pipe, etc. but also depends on mechanical operation on it and arrangement of usage. The arrangement of heat pipe has 2 different ways which are vertical and horizontal usage. Vertical usage can be named according to position against gravity. Mechanical processes are collected in 2 different methods. One of them is bending, and the other one is squeezing.

Bending is the most common application in the use of heat pipes, because system packaging can make it harder to design a cooling system. Hence, the heat pipe can be shaped according to the mechanical design of the system. Bending causes reduction in performance. Heat pipe manufacturers suggest a rule of thumb: every 90^{o} bend results in 1 ^{o}C performance loss [57]. Another suggestion is about bending radius. Bending radius should be 3 times larger than the heat pipe diameter. Tighter bend results in drastic reduction in conductivity of the heat pipe. Another problem for bending of brass and aluminum shell heat pipes is crack due to shrinkage.

Another mechanical process on heat pipe is squeezing, which is faced during the mounting process. Hence the tolerance between pipe and mounting detail is very important. Suggested tolerance detail is transition fit. Clearance fit causes gap between pipe and its mounting detail, on the other hand, interference fit causes squeezing of pipe, which results in performance reduction. As a rule of thumb, heat pipe should be flattened by reducing pipe diameters only 1 mm. Over squeezing can destroy the wick structures, and this results in hitting transport limitations.

The pressure difference due to hydro-static head of working fluid can be positive, negative and zero, which means heat pipe can be located as horizontal and vertical. The pressure drop (ΔP_g) due to gravity effect can be calculated from [60].

$$\Delta P_g = \rho_l . g . l_{eff} . \sin\theta \qquad \textbf{(2.7)}$$

where θ is the angle between heat pipe and horizontal plane. It is positive when the condensed section is below the evaporator section.

The working orientations will be summarized in the following three subsections. Detailed information about working orientation will be in Chapter 3, as a part of the heat pipe selection guide.

2.6.1 Horizontal Orientation

The horizontal orientation of a heat pipe is the most common one, especially in notebooks. In this orientation, the performance of the heat pipe is limited by capillary limit. This limit depends on heat pipe dimensions such as diameter and length. Larger diameter can carry more heat load; in contrast, a longer heat pipe carries less heat load. Besides, gravity effect and wick type directly affect the capillary limit. For horizontal orientation, gravity effect can be ignored, hence designer should accordingly select the wick type [57].

The heat pipe length which affects capillary limit is not the full length of the pipe. It must be the effective length, which is given with Equation 2.2.

Grooved wick type is good for horizontal applications because this kind of heat pipes has large pore radius with a high permeability, which do not cause drastic pressure drop. By contrast, powder (sintered) wick has small radii and relatively low permeability. Hence, sintered wicks are limited by pressure drop in horizontal operation [53].

2.6.2 Gravity Aided

In gravity aided orientation, evaporator section is located below the condenser section, hence the angle between horizontal plane in Equation 2.7 is negative. Gravity aided or gravity assist configuration is the best configuration for heat pipe applications. Gravity helps to return condensed fluid to evaporator section. Flooding and boiling limits are the critical transport limits for gravity aided orientation [57].

2.6.3 Gravity Against

In gravity against orientation, evaporator section is located above the condenser section, hence the angle measured from the horizontal plane in Equation 2.7 is positive. Gravity against configuration is a problematic configuration for heat pipe applications. The main limitation is capillary limit, similar to the horizontal configuration [57]. Gravity can be ignored for horizontal placement, in contrast for gravity against placement gravity effect should be taken into consideration. To eliminate the disadvantages of this orientation, the dimensions of heat pipe must be carefully selected. As the elevation between evaporator section and condenser section increases, the performance of heat pipe decreases proportionally.

2.7 Heat Pipe – Heat Sink Performance [57]

Up to this section, theory of heat pipe and its performance have been summarized. This section is related to cooling performance of the cooling system. A cooling system with heat pipes has 3 main sections. It starts with evaporator base (heat in), continues with heat pipe (heat carrying) and ends with condenser section (heat dissipation). Resistance network is given in Figure 2.7. This network is placed between evaporator and condenser.

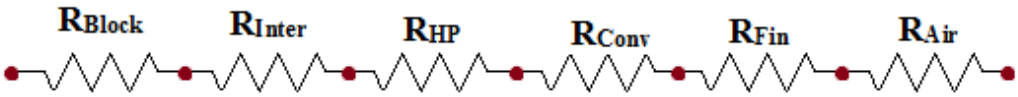

Figure 2.7 The Resistance Network of Heat Pipe

Each resistance can be found to calculate an associated temperature change. The calculation starts with the block section. The governing equation comes from Fourier's Law of conduction, in order to calculate R_{block}.

$$\Delta T_{block} = \frac{Q.t_{block}}{k_{block}.A_{block}} \qquad \textbf{(2.8)}$$

Another resistance is the interface between heat pipe and its mounting detail. To eliminate gap between these two, thermal pad or grease can be used, which creates interface resistance, 'R_{inter}'.

$$\Delta T_{inter} = \frac{Q.R_{inter}}{\pi.D_{HP}.L_{evap}} \quad \textbf{(2.9)}$$

The detailed mathematical model of heat pipe is too complex, hence heat pipe internal resistances are simplified as evaporator, axial and condenser resistance. These are respectively R_{evap} , R_{axial} and $R_{condenser}$.

$$\Delta T_{HP} = \frac{Q.R_{evap}}{\pi.D_{HP.}L_{evap}} + \frac{Q.R_{axial}}{0.25\pi.D_{VS}} + \frac{Q.R_{condenser}}{\pi.D_{HP.}L_{condenser}} \quad \textbf{(2.10)}$$

The resistance of heat transferring from fin to ambient (R_{air}) is calculated from convection term.

$$\Delta T_{conv} = \frac{Q}{h.A_{fin}} \quad \textbf{(2.11)}$$

The conduction loss of fin is calculated from fin efficiency (R_{fin}).

$$\eta_{Fin} = \frac{\tanh(m_{fin}L_{fineff})}{m_{fin}L_{fineff}} \quad \textbf{(2.12)}$$

Where,

$$m_{fin} = \sqrt{\frac{2h}{k_{fin}.t_{fin}}} \quad \textbf{(2.13)}$$

Then,

$$\Delta T_{fin} = \Delta T_{conv}(1 - \eta_{fin}) \quad \textbf{(2.14)}$$

The change in air temperature is calculated from bulk air properties,

$$\Delta T_{air} = \frac{Q}{m.C_p} \quad \textbf{(2.15)}$$

The overall performance of heat sink is calculated with summation of all temperature changes.

$$\Delta T_{Total} = \Delta T_{block} + \Delta T_{inter} + \Delta T_{HP} + \Delta T_{conv} + \Delta T_{fin} + \Delta T_{air} \quad \textbf{(2.16)}$$

The thermal resistance of the sink to surrounding is calculated with.

$$R_{s-a} = \frac{\Delta T_{Total}}{Q} \quad \textbf{(2.17)}$$

If calculation above is followed, designers can estimate the performance of heat sink with heat pipe system.

CHAPTER 3

PRELIMINARY DESIGNS AND NUMERICAL ANALYSIS

This chapter includes the starting point of the conceptual design. First, preliminary design is defined according to four main parameters. These are the system requirements, reliability, environment conditions and the configuration cost. Then, a numerical investigation is done in order to make corrections and optimization in the preliminary design.

The preliminary design consists of two different designs. Main differences between the designs are the type of cooling surface (rectangular plate fins versus pin fins). The type of cooling surface is also determined by the operating conditions. Numerical analyses are done for both designs, but the numerical model is validated only for the pin fin configuration using the results from the conducted experiments.

Chapter 3 includes the details about the purpose of using rotary platforms, explanations about the software used (PTC Creo and FloEFD), heat pipe selection, and CAD designs with numerical calculation.

3.1 Military Rotary Platforms

Military product design is done based on environmental conditions (cold, hot, rain, salt fog, high pressure etc.), operating conditions (land, naval, and air), minimum dimensions and ergonomics. Some devices are out of action (stagnant) such as detectors, walkie-talkies, mission computers, LRUs etc. which have simple designs due to not having moving parts. However, radars, antennas, weapon systems, target detecting systems etc. can move in x-, y- and z- directions and rotate around an axis; this movability makes design procedure difficult due to movements.

Military systems often require special designs such as rotary platforms, launching systems and lifting systems to perform their missions successfully. Vehicles with rotating turrets and rotating carriers are obvious examples of critical rotating platforms. The systems with rotating components are generally used in radar applications, target detection and destruction systems and unmanned vehicles. All types of rotating platforms require power, signal exchange and a cooling fluid with the stationary vehicle hull. The turret to hull interface must often transmit electrical power, as well as safety interlocks, digital data, video data, other signals (RF, control etc.) and coolant of the system. These functional requirements must be satisfied in a mechanical package that meets battlefield environmental requirements [66]. To transmit all required things from the stationary section to the rotary section, slip rings are generally used. As it is defined previously, slip ring is an electromechanical device that allows the transmission of power, electrical signals and mechanical interface from a stationary part of the system to a rotating structure. The slip ring is a high-tech device, nevertheless its reliability is very low because of its complexity.

A traditional rotary slip with fluid interface assemblies contains discrete precious metal rings for each electrical circuit and corresponding sliding wipers (or brushes) to conduct power and signals from rotating rings to a stationary member [61]. In the middle of some slip rings, there is a circular gap which supplies the fluid passing channel during rotation. This channel is specially designed, and it is a sealed section of slip rings against leakage and break down. A sample of military rotary joint is given in Figure 3.1 with electrical and fluidic interfaces.

Rotary joints with only an electrical interface cost between 10,000 and 60,000 dollars in military applications. However, rotary joints with electrical and fluidic connections cost more than hundred thousand dollars in military applications. These high prices come from the military standards. Despite military standards, there is always a malfunction possibility due to complexity. The most critical problem is the leakage of coolant, which causes permanent and inevitable results. However, military designs must be reliable and long lasting under harsh conditions. Military product designers generally suggest that slip ring must not be used if it is not really necessary.

Figure 3.1 SPINNER High-quality hybrid rotary joints are mainly used in military radar systems, fire control systems, rotating vehicle-mounted camera systems and in mobile battlefield communication systems [62]

3.2 Used Software

In this study, two different commercial software packages are used, which are PTC Creo 2.0 Educational License and FloEFD with Electronic Cooling. PTC Creo 2.0 is a parametric CAD program and FloEFD is a commercial CFD program, which works with CAD integrated and has its own solver.

PTC Creo 2.0 is a Computer Aided Drawing (CAD) program. This program is used for creating 3-D models for the parametric study. ASELSAN rotary platforms are simplified for the experimental setup and for the numerical investigations by using PTC Creo 2.0. The first design procedure is to create a 3-D CAD model by simplifying the real design. Then, model's parameters are identified. Finally, these parameters are identified for later use in parametric optimization according to identified sections which affect the results of experiments and numerical simulations.

FloEFD is a CFD program which is highly focused on heat transfer and flow problems. Many companies including the leaders of defense and automotive industries use FloEFD for analysis of heat transfer and fluid flow problems in their designs because of its reliable results and reduction in solution time of analyses. FloEFD has a

capability of solving both external and internal fluid flows, steady-state and time-dependent fluid flows, compressible gas and incompressible fluid flows, free, forced and mixed convection problems, HVAC operations, fluid flows with boundary layers, including wall roughness effects, laminar and turbulent fluid flows, radiation heat transfer, electronic cooling applications such as heat pipes and joule heating, flows of non-Newtonian liquids, flows of compressible liquids, real gases, two phase flows etc.[63].

In this study, FloEFD with electronic cooling module is used. Electronic cooling module provides additional capabilities for analysis by specialists who support electronic cooling applications. FloEFD Electronic Cooling Module contains joule heating effect, PCB generator, electronic materials such as components, fans, single- and multi-stage thermo-electric coolers, interface materials, etc. and compact modules such as heat pipe module and two resistor module. FloEFD is working with CAD integration, which means that it takes geometrical data from a CAD program directly, hence it is suitable for parametric analysis. Another advantage of FloEFD is that it has its own mesh generator inside the software. The auto-mesh generator creates structural Cartesian mesh, which is the only mesh type inside it.

CFD software packages numerically calculate flow behavior, temperature and pressure data for designers. For reliable results, there must be selected methodologies and algorithms behind all calculations and approaches. Behind the solver of FloEFD, Finite Volume Method (FVM) is used for solving the governing equations. FVM is a method for representing and evaluating partial differential equations in the form of algebraic equations. The values are calculated at discrete places on a meshed geometry. The unknowns in the discretized equations for calculation are obtained by Semi-Implicit Method for Pressure –Linked Equations (SIMPLE). SIMPLE depends on guesses and corrections. First, the point is guessed, then the result is corrected. Procedures behind SIMPLE algorithm are listed below [64]:

- Estimation of pressure field
- By predicting the pressure field, velocities in x, y , and z- direction are calculated from the momentum equations

- After initial guess calculation, pressure is corrected by correction equation. Then, velocities are again calculated with new 'corrected' pressure value
- Temperature value is found by correct pressure and velocity components with solving of energy equation.
- If convergence of temperature does not occur, new estimation must be done, which means all steps are given above must be repeated
- If convergence occurs, stop the calculations.

FloEFD has only one turbulence model, which is *k-ε* turbulence model. *k-ε* turbulence model is reliable enough for thermo-fluid problems. This turbulence model is also known as 'two equations model' which means it includes two extra transport equations to reflect turbulence properties of the fluid. The first transported variable is turbulent kinetic energy '*k*' and the second one is turbulent dissipation '*ε*', which defines the scale of turbulence [65]. There is an important notice that *k-ε* turbulence model should not be used in a large adverse pressure gradient, hence this model is not suitable for a compressor inlet [66]. Mathematical model of *k-ε* turbulence model is obtaining by given below equations. The general equations for turbulent kinetic energy '*k*' and turbulent dissipation '*ε*' respectively are [67]

$$\frac{\partial k}{\partial t} + U.\nabla k = \nabla.D_k\nabla_k + Production - Dissipation \qquad \textbf{(3.1)}$$

$$\frac{\partial \varepsilon}{\partial t} + U.\nabla \varepsilon = \nabla.D_\varepsilon\nabla_\varepsilon + Production - Dissipation \qquad \textbf{(3.2)}$$

If above equations are solved, these two main equations are (given in index form) obtained.

$$\rho\frac{\partial k}{\partial t} + \rho U_j\frac{\partial k}{\partial x_j} = \frac{\partial}{\partial x_j}\left(\left(\mu + \frac{\mu_t}{\sigma_k}\right)\frac{\partial k}{\partial x_j}\right) + \tau_{ij}\frac{\partial U_i}{\partial x_j} - \rho\varepsilon \qquad \textbf{(3.3)}$$

$$\rho\frac{\partial\varepsilon}{\partial t}+\rho U_j\frac{\partial\varepsilon}{\partial x_j}=\frac{\partial}{\partial x_j}\left(\left(\mu+\frac{\mu_t}{\sigma_\varepsilon}\right)\frac{\partial\varepsilon}{\partial x_j}\right)+C_{\varepsilon1}\frac{\varepsilon}{k}\tau_{ij}\frac{\partial U_i}{\partial x_j}-C_{\varepsilon2}\rho\frac{\varepsilon^2}{k} \qquad \textbf{(3.4)}$$

where μ_t is eddy viscosity,

$$\mu_t=\frac{\rho C_\mu k^2}{\varepsilon} \qquad \textbf{(3.5)}$$

and all constants are given below. These constants are calculated by a semi-empirical procedure and optimization procedure.

$$C_{\varepsilon1}=1.44 \quad C_{\varepsilon2}=1.92 \quad C_\mu=0.09$$

$$\sigma_k=1.0 \quad \sigma_\varepsilon=1.3$$

Actually, there is no certain answer to the question of which turbulence model must be chosen and how reliable it is. As a rule of thumb, the *k-ε* turbulence model should not be used in large pressure gradient problem.

As it is indicated above, FVM requires calculation nodes, hence computational domain must be divide into small control volumes. FloEFD prepares these small volumes with its mesh generator. It uses structured Cartesian mesh. With the changes of geometry or domain, mesh is automatically updated. Another feature of the mesh is solution adaptive mesh refinement. Mesh numbers and dimensions can be automatically or manually refined according to convergence criteria or user's demand, which also reduces meshing and solving time. Therefore, mesh mechanism of FloEFD is easier than the most of other similar software. Level of mesh which refers to the cell number of mesh and the level of mesh refinement can be done by user and the rest of the work is done automatically by FloEFD. If mesh refinement is active during the study, the total cell number of the mesh can change during the calculation.

In FloEFD, there are three different mesh types; namely, these are fluid cell, solid cell, and partial cell. Fluid cell is the mesh at fluid regions, similarly solid mesh is the mesh at solid regions. Partial mesh is used for solid and fluid interface regions. The sum of the fluid, solid and partial cells numbers gives the total mesh for analyses.

FloEFD with electronic cooling is a good choice for modeling and analyzing the cooling system of an electronic package when design process and solving time for analysis is taken into consideration.

3.3 Selection of Heat Pipe

Heat pipes are generally used when conventional cooling methods are insufficient. At that point, selection of heat pipes considering their working range, the fluid inside them, diameter and shape, inside structures etc. becomes very important and critical. However, this is not an easily manageable task that is why designers must follow some procedures. Manufacturers of heat pipes are the best consultants for the designers. Thermacore, Enertron Inc. and Advanced Cooling Technologies (ACT) are the most popular heat pipe manufactures. The selection steps of heat pipes are explained in detail below.

3.3.1 How to Select a Heat Pipe?

The procedure is quite complicated and grueling; however; if the steps below are applied, selection will be simplified. The heat pipe selection guide or Enertron [68] is used as a reference.

1) Identify the operational parameter
    - Geometry and heat load capacity of the heat source.
    - To determine heat sink structure and locations. It gives the shape of distance and orientation from the heat sink to heat source.
    - To create expected temperature profile for ambient, heat source and heat sink
    - To investigate environmental conditions in order to create temperature gradient and to protect from corrosion.
2) Select heat pipe's material, fluid inside it and wick structure inside it. (The best way at that point is to consult manufacturers.)

- To choose fluid inside the heat pipe. Main consideration is the purpose of heat pipe used such as extreme heat loads, naval applications, working place at pole region, space applications, etc.
- To select outer material of heat pipe. It must be compatible with the fluid inside it.
- To select wick structure for operating conditions.
- If it is necessary, protecting coating must be identified.

3) Determine the design parameters of the heat pipe such as length, size and shape.

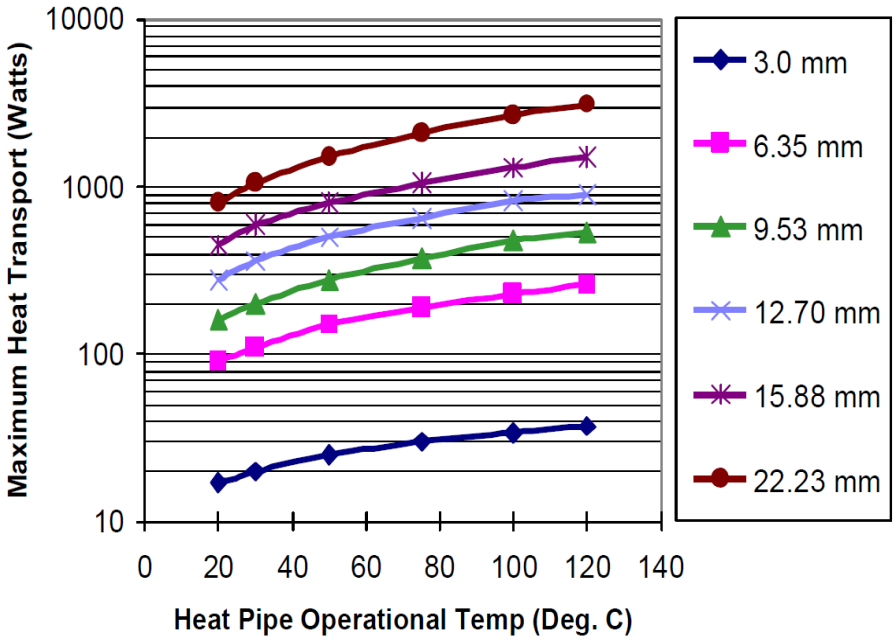

Figure 3.2 Diameter effects on heat pipe performance. Heat pipe is water copper groove type and at vertical orientation (gravity assist) [68]

Important parameters are diameter, orientation and length. Orientation affects the gravity effect on the heat pipe. Diameter is the most important step in choosing heat pipe. With an increase in diameter, heat carrying capacity increases as it is shown in Figure 3.2.

3.3.2 The Construction Material of Heat Pipe

The working fluid is functional in a certain temperature range due to changes at different temperatures. In addition to this, working fluid needs to be compatible with the shell of heat pipe to prevent corrosion and chemical reaction. If chemical reaction or corrosion occurs, non-condensable gases appear, which decreases the performance of the heat pipe. Hence, corrosion effect and compatibility of the vessel material must be considered. Some examples for the compatibility between the fluid and the vessel material are given in Table 3.1.

The most commonly used heat pipe type is water as a working fluid and copper as a vessel. It is generally used in electronic cooling applications within the range of 5 ^{o}C to 230 ^{o}C. Due to working range, liquid nitrogen and liquid ammonia heat pipes are used in special areas such as cryogenic applications, space applications, etc. Liquid ammonia with aluminum vessel heat pipe is very common popularity in space applications due to lightweight of aluminum.

Functionality of a heat pipe is restricted by the freezing point of the working fluid. Under the freezing point, heat pipe's sealed joints can be damaged, and flow inside can have discontinuity, which directly affects the performance of the heat pipe.

Table 3.1 Typical Operating Characteristics of Heat Pipes [68]

Temperature Range (°C)	***Working Fluid***	***Vessel Material***	***Measured Axial Heat Flux at Certain Temperature (kW/cm^2)***	***Measured Surface Heat Flux at Certain Temperature (W/cm^2)***
-200 to -80	Liq. Nitrogen	Stainless Steel	0.067 @-163 °C	1.01 @-163 °C
-70 to +60	Liq. Ammonia	Nickel, Aluminum, Stainless Steel	0.295 °C	2.95 °C
-45 to +120	Methanol	Nickel, Copper, Stainless Steel	0.45 @100 °C	75.5 @100 °C
+5 to +230	Water	Copper, Nickel	0.67 @200 °C	146 @170 °C
+190 to +550	Mercury(0.02%) Magnesium(0.001%)	Stainless Steel	25.1 @360 °C	181 @750 °C
+400 to +800	Potassium	Nickel, Stainless Steel	5.6 @750 °C	181 @750 °C
+500 to +900	Sodium	Nickel, Stainless Steel	9.3 @850 °C	224 @850 °C
+900 to +1500	Lithium	Niobim (1%), Zirconium	2.0 @1250 °C	207 @1250 °C
+1500 to +2000	Silver	Tantalum (5%), Tungsten	4.1 °C	413 °C

3.3.3 Wick Structure of Heat Pipe

Wick structure selection is the hardest part of heat pipe selection. There is no certain information about heat pipe's inner wick structure. The most important effects are determining the wick structure, operational condition and manufacturability. There are four wick types which are commonly used such as groove, wire mesh, powder metal and fiber/spring. These four types have no certain advantages. The performance can easily change with operating conditions. Designers should proceed with the help of manufacturers at that point and should receive performance documents of manufacturer's products. Figure 3.3 and Figure 3.4 give some examples of Enertron's heat pipe laboratory test results. They show the effects of operating conditions.

As it is seen in Figure 3.3 and Figure 3.4, groove wick type has the lowest thermal resistance in vertical operation, which is condenser is above the heater level and this operating type is also known as gravity assist orientation [68]. The main reason behind this behavior is low capillary limit which directly affects wick type selection. Besides, in space applications, ammonia groove heat pipe is generally used for its suitability to ammonia specifications and groove's weak capillary limits.

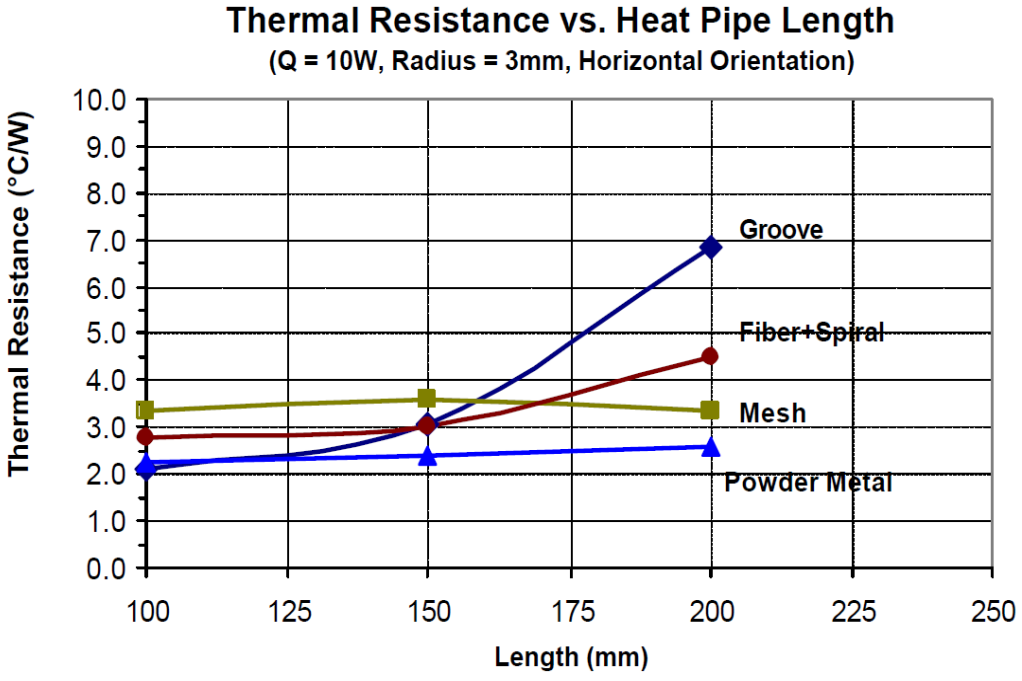

Figure 3.3 Enertron's actual test results of heat pipe with different wick structure at horizontal (gravity against) orientation [68]

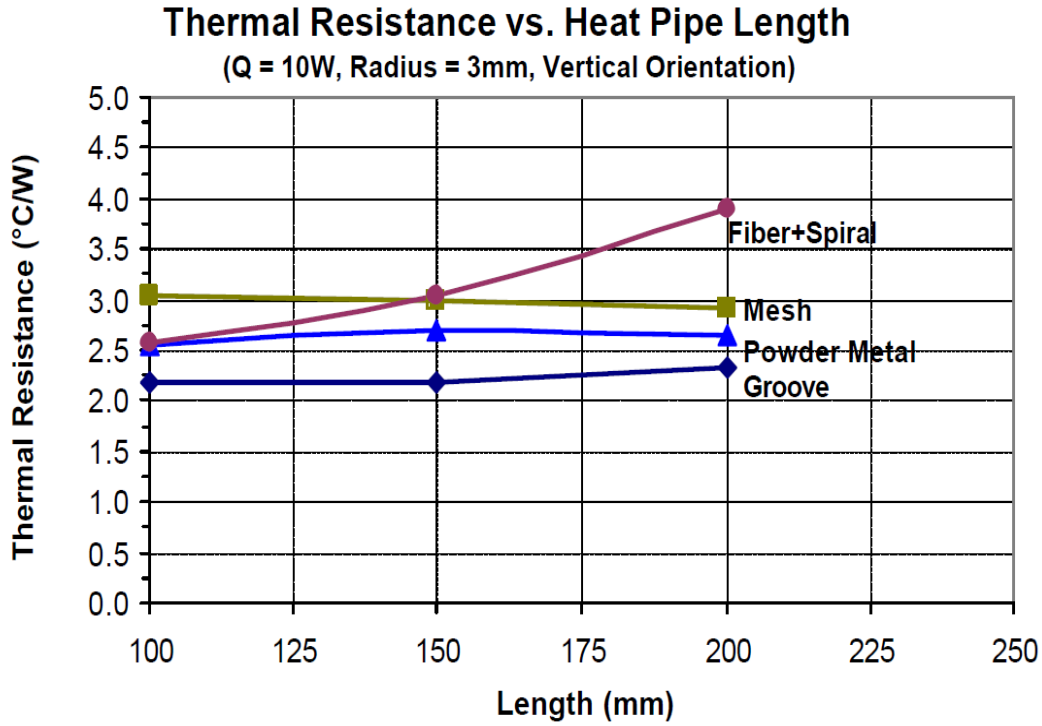

Figure 3.4 Enertron's actual test results of heat pipe with different wick structure at vertical (gravity assist) orientation [68]

3.4 CAD Design of the Whole Structure

This study is inspired from ASELSAN's radar project. Radar systems are usually placed on rotating platforms. These platforms generally rotate around the z-axis. Rotating platforms in ASELSAN are used in radars, tracking and weapon carrying applications. Generated platform is designed based on a real system. Dimensions are close enough to implement the gathered information from this study to real applications.

Most of the rotating platforms generally are 'U- shape'. There is a planar base for connection to rotating base, and it has support walls on two sides. Rotating platforms do not carry only the main system, but they also carry controller sections, RF units for radar applications, power amplifiers, power controller etc. Hence at the first step of design stage, platforms should be designed for satisfying the requirements.

In this study, one of the mass produced ASELSAN rotary platforms is simplified to implement a cooling method for it. Experimental platform is generated by PTC Creo

with real dimensions. The platform's dimensions are respectively height, width and length as 650 mm, 375 mm and 460 mm. In addition to these, there are two different cooling structures, one of them is pin fin type, and the other one is rectangular channel type as they are illustrated in Figure 3.5 and Figure 3.6

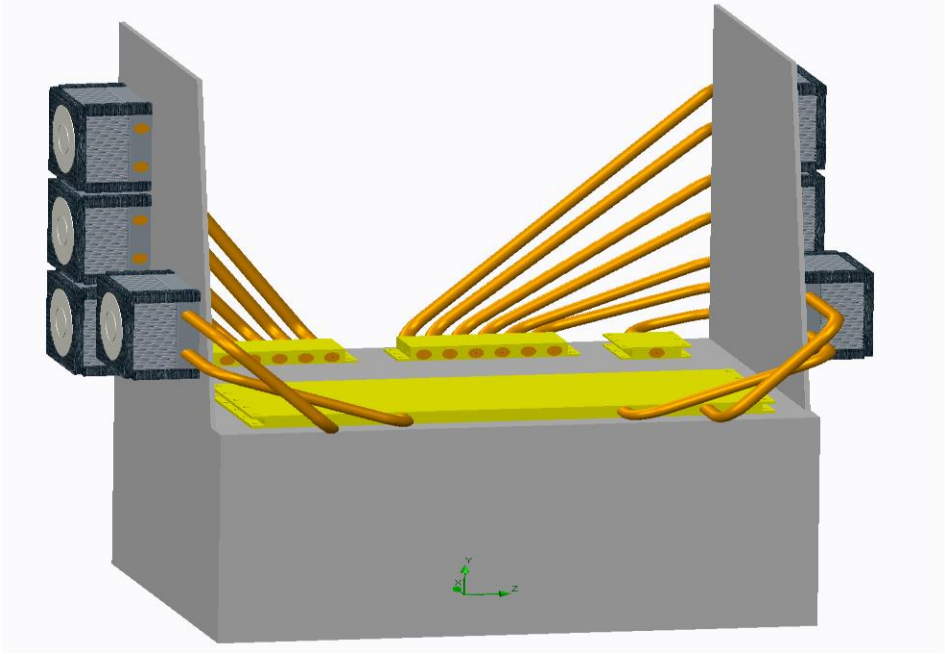

Figure 3.5 CAD model of Pin Fin Configuration, which will be used in experiment

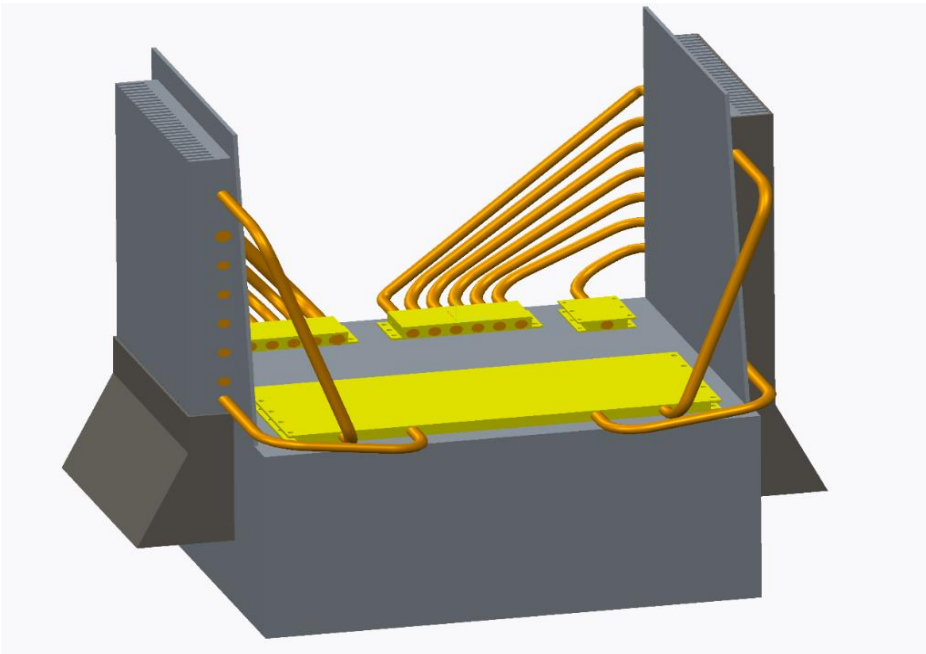

Figure 3.6 Sample CAD model of Rectangular Channel Type Configuration

During the CAD design, the parameters which affect performance of cooling method are identified and parameterized as a preparation for the numerical analysis stage. The CAD model is directly updated and the updated model is analyzed by FloEFD. The update methodology of CAD models and preliminary procedures are given in Figure 3.7. According to capability of numerical results, the next step will be defined.

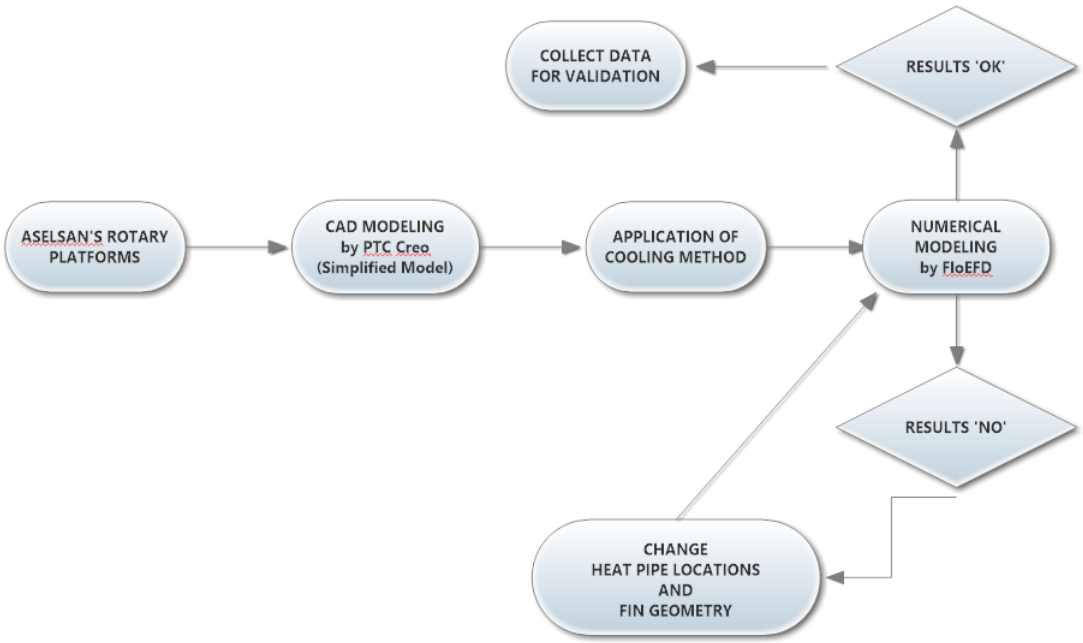

Figure 3.7 Flow Chart of Preliminary Procedures

3.5 Preliminary Numerical Analyses

Aim of this section is to collect data for the experimental procedure and optimization. There will be two types of heat sinks, namely pin fin structured and rectangular plate fin with duct structured. Numerical investigations are done in FloEFD, which are explained in Section 3.2.

Analyses are done at 25 ^{o}C and 50 ^{o}C environmental conditions which come from MIL-STD-810 test procedure. During the analysis, radiation effect is ignored; however, natural convection is considered. Also, flow supplied by the fans does not

have a constant flow rate, for each condition flow rate is directly obtained from the fan performance curve (see Figure A.4 in Appendix A).

These runs will be used for making comparisons with the experiments and improving the design. Numerical analysis procedure will be explained in detail in following headlines.

3.5.1 Procedures of Numerical Analyses

The first step of starting numerical runs is 3-D CAD design of the system which will be manufactured to be used in the experiments. Numerical runs are done under 1atm pressure and 25 ^{o}C and 50 ^{o}C environmental conditions. During the analyses, inputs of the runs such as turbulence parameters, environmental properties, boundary conditions etc. always remain the same. All geometrical upgrades are done in CAD, then the numerical model is re-generated.

The next step of numerical runs is configuration analysis. FloEFD needs some settings, in other words, beginning input. These are flow type such as internal or external flow, modes of heat transfer considered during the run such as conduction, convection or radiation, types or materials and fluids, flow type such as laminar, turbulent or mixed flow, turbulence parameters and initial state in terms of temperature, pressure, velocity etc. After all these settings are done, boundary conditions and tools are defined.

In this study, flow type is set to external flow. For all cases of analyses, radiation is ignored. Conduction in solids and natural convection in fluids are considered. In addition to these, flow is considered as laminar first and then as turbulent. As it is mentioned before, FloEFD only uses k-ε turbulence model, hence solver needs only the parameters of k-ε model. There are two different setup configurations about turbulence parameter. One of them is turbulence intensity (%) and turbulence length (m) configuration, which is selected in this study. Another one is turbulent energy (J/kg) and turbulent dissipation (W/kg) combination. Turbulence parameters in terms of turbulence length and turbulence intensity are calculated from the following equations [69].

Turbulence length (l_s);

$$l_s = 0.07 D_h \tag{3.6}$$

Turbulence intensity (I);

$$I = 0.16 Re_{Dh}^{-1/8} \tag{3.7}$$

where Re is the Reynolds Number which is the ratio of inertial forces to viscous forces defined as

$$Re = \frac{\rho \vartheta D_h}{\mu} \tag{3.8}$$

In Equations 3.6, 3.7 and 3.8, D_h is the *hydraulic diameter*.

After the calculations, the turbulence intensity of 5.4% and the turbulence length of 0.525 mm are defined as initial values. As the fluid, air is chosen at 25 ^oC and 50 ^oC depending on the case. During the analyses, solver needs thermodynamic properties, hence initial temperature and pressure are defined. Temperature is changing with analyzed conditions (25 ^oC or 50 ^oC) and pressure is always constant at 1 atm.

After all of the definitions above the configuration step is completed. Then the computational domain and boundary conditions must be defined. First step here is to define the calculation domain; in other words, calculation envelope. The dimensions of the envelope are given in Table 3.2.

Table 3.2 Dimensions of Computational Domain

Dimensions of the Computational Domain	
x axis	0.5 m
-x axis	-0.5 m
y axis	0.75 m
-y axis	-0.15 m
z axis	0.65 m
-z axis	-0.65 m

The material definitions are made. All solid parts are defined as Aluminum 5052. Except the outer shells of fans that are defined as insulators, because they are plastic materials. Al 5052 is chosen for its accessibility and economy. Generally, in military applications Al 6061 and Al 6063 are used; however, they are expensive and hard to obtain. In terms of thermal conductivity of these materials, the differences are quite large, and it affects the performance of system and experiments. Al 5052 has the conductivity of 138 W/mK, Al 6061 has the conductivity of 180 W/mK and Al 6063 has the conductivity of 218 W/mK at room temperature, 25 ^{o}C. The selection of Al 5052 for the mock-up guarantees the performance of the final product that will be made out of Al 6061 or Al 6063.

Then, the boundary conditions are defined. The heaters representing the electronic chips are defined as constant heat sources, which are classified as surface heat sources. Powers of the sources are given in Table 3.3. These sources simulate the real TWT and PA modules of the radar electronics.

Table 3.3 Heat Source of the System

Source	***Quantity***	***Dimension (mm)***	***Power (W)***	***Heat Flux (W/cm^2)***
Heater 1	2	50 x 126 x 10	600	10
Heater 2	1	152 x 400 x 10	350	0.58
Heater 3	1	68 x 54 x 10	70	1.91

Next step is to create heat pipes. In FloEFD, there is an electronic cooling module, and this module has some special components for electronics cooling. Heat pipe is one of them. In literature, there are some mathematical models for heat pipes; however, these may not work with all systems. Hence, heat pipes are commonly modeled as super conductive rods in axial direction. Radial direction conductivity is ignored. During the analyses, requirements for creating heat pipes are identifying condenser and evaporator sections as heat in / out sections and guessing effective thermal resistance of the heat pipe. The first assumption for the effective thermal resistance value is 0.25 ^{o}C/W or K/W. This is only a prediction, and corrected values are defined after the

experiments. Actually, thermal resistance must be found by the experiment and resistance curve must be captured. FloEFD can also receive thermal resistance as a continuously changing graph. According to explanations from the FloEFD guideline, heat conduction through the heat pipe is calculated using specified effective thermal resistance to heat conduction from object being cooled to evaporator section of heat pipe and calculated thermal resistance of a solid component [70]. As it is mentioned before, initial values are guessed, but they are not made up. They are results of a basic calculation which is explained below. The temperature difference between the evaporator and condenser sections of heat pipe is calculated approximately from

$$\Delta T = Q_t . R_{tot} \tag{3.9}$$

where, Q_t is the heat transferred along the heat pipe and R_{tot} is the total heat pipe thermal resistance, consist of resistance of conduction inside and resistance of outer shell (wall) as in

$$R_{tot} = R_{cond} + R_{wall} \tag{3.10}$$

$$R_{wall} = \frac{L}{A.k} \tag{3.11}$$

where L is the length of heat pipe, A is the cross-sectional area of heat pipe. k is the conductivity of heat pipe, it is taken as a large number because of the assumption about heat pipe behavior as a directionally super conductive material.

Moreover, a heat pipe has three sections which are evaporator, adiabatic and condenser sections. In the numerical model, adiabatic section is also defined. In order to do this, heat pipe wall surfaces other than evaporator and condenser sections are classified with infinite resistance, which means there is no heat transfer from the adiabatic section of the heat pipe to its environment. This assumption will be proved during the experimental procedure.

The last set of conditions to be defined are flow conditions. These conditions are not defined as constant values. Flow occurring during the analyses is gathered from the fan performance curve. Flow rate and pressure drop are checked from the fan curve,

which is supplied from the manufacturer. The fan that is used is Ebm Papst 8214JH3, and its specifications are given in Appendix A.

During the analyses, mesh is automatically generated and refinement levels are always active. The mesh independence is also studied, which will be given in Section 3.5.2. There, different cell numbers of mesh are tried then, optimum mesh number and level is selected.

A summary of preliminary procedures can be given as

- Real rotary platform is simplified in PTC Creo.
- Two types of cooling techniques are modelled.
- All models are parameterized in CAD to prepare CAD models for FloEFD.
- Working conditions are identified from MIL-STD-810.
- Numerical modeling is done in FloEFD.
- Heat loads, boundary conditions and some assumptions are defined.
- Optimum mesh is obtained.
- Results are collected. The results which are above the thermal shut-down range are ignored and the designs leading to these results are eliminated for being inadequate.
- If a result is above thermal shut-down point, heat pipe locations and geometry of fins are changed.
- For the experimental procedure, hot spots are identified. The measurements in experiments will be taken from these hot spot points.

3.5.2 Results and Discussions of Numerical Analyses

Configurations of analyses are summarized in previous sections. This section covers the results of preliminary analyses and their discussions. Some of these results will be validated in the experiment which is in Chapter 4. Finally, gathered knowledge will be used for correcting the model and optimizing the rectangular plate fin model in Chapter 5. The investigations will be started with the pin fin configuration because this system is also used in the experiments.

The first numerical study is for mesh convergence in pin fin configurations. During this process, FloEFD's performance and the numerical model parameters and the mesh are optimized. As it is known, duration of numerical analyses directly depend on the performances of the solver and the computer, complexity of numerical modelling, quantities of inputs and outputs etc. Hence, the first step is identifying optimum solution condition for analyses, which is directly affected by mesh or cell numbers.

For the mesh convergence study, one goal is defined, which is the surface temperature of Heater 1. The reasons for the selection of Heater 1 are listed below;

- It simulates the critical component.
- It has a higher importance in the electronic system.
- It has the highest heat dissipation with 600 W and the highest heat flux with 10 W/cm^2.

Table 3.4 Mesh Independence Study: the change of Heater 1 average surface temperature with the number of cells in the model at 50 ^oC ambient temperature

Number of Total Mesh Cells	***Number of Solid Mesh Cells***	***Number of Fluid Mesh Cells***	***Number of Partial Mesh Cells***	***Average Temperature on Surface of Heater 1 (^oC)***	***Duration (hour)***
173546	12468	64252	96826	102.54	1.66
307384	19968	89152	198264	102.05	2.42
421751	20567	99782	301402	102.76	3.86
682101	39535	150252	492314	102.61	5.29
734660	43724	178562	512284	102.70	6.18
896478	59570	231977	604711	102.60	6.94
1200778	63642	312516	824614	102.62	9.13
1572110	84656	486158	1001296	102.59	11.34

Mesh convergence study is done at 1atm pressure and 50 ^{o}C environmental temperature. According to the results in Table 3.4, working point in terms of mesh number is identified. During the preliminary runs, the computer that was used has INTEL Core i7-4771 CPU @ 3.50 GHz and installed memory (RAM) of 32 GB. The runs are made under 64-bit Windows operating system. From Table 3.4, the selected mesh has nearly 700000 initial cells with refinement level 4. At the selected mesh, one run lasts approximately 5.5 hours.

The numbers above are selected out of 20 runs with different mesh numbers in which all conditions and definitions are the same except the mesh numbers. According to optimum duration of solution, mesh numbers between 600000 and 700000 is selected. Mesh types in Table 3.4 are explained in the previous section related to FloEFD. All of these numbers are captured at the beginning of analyses, at the end of the analyses these numbers increase due to adaptive cell refinement. For all cases, cell refinement level is 4.

Then, second study is related to pin fin configuration at 50 ^{o}C ambient temperature. The total mesh number in the analysis is 684248 and refinement level is 5. The effective thermal resistance of heat pipes is defined as 0.25 ^{o}C/W or K/W. All solid to solid interfaces are defined as full contact.

According to the results illustrated in Figure 3.8, temperature distributions at 50 ^{o}C are below the thermal shut-down point. Heaters 1 (identical heaters with 600 W heat generation) have nearly 103 ^{o}C average temperatures. Maximum point temperatures on them are 104.05 ^{o}C and 104.15 ^{o}C. Heater 2 and Heater 3 have nearly the same temperature distributions with the average of 88 ^{o}C. From the figure, it can be easily seen that there is no hot spot region, hence distribution of heat pipes is guessed well.

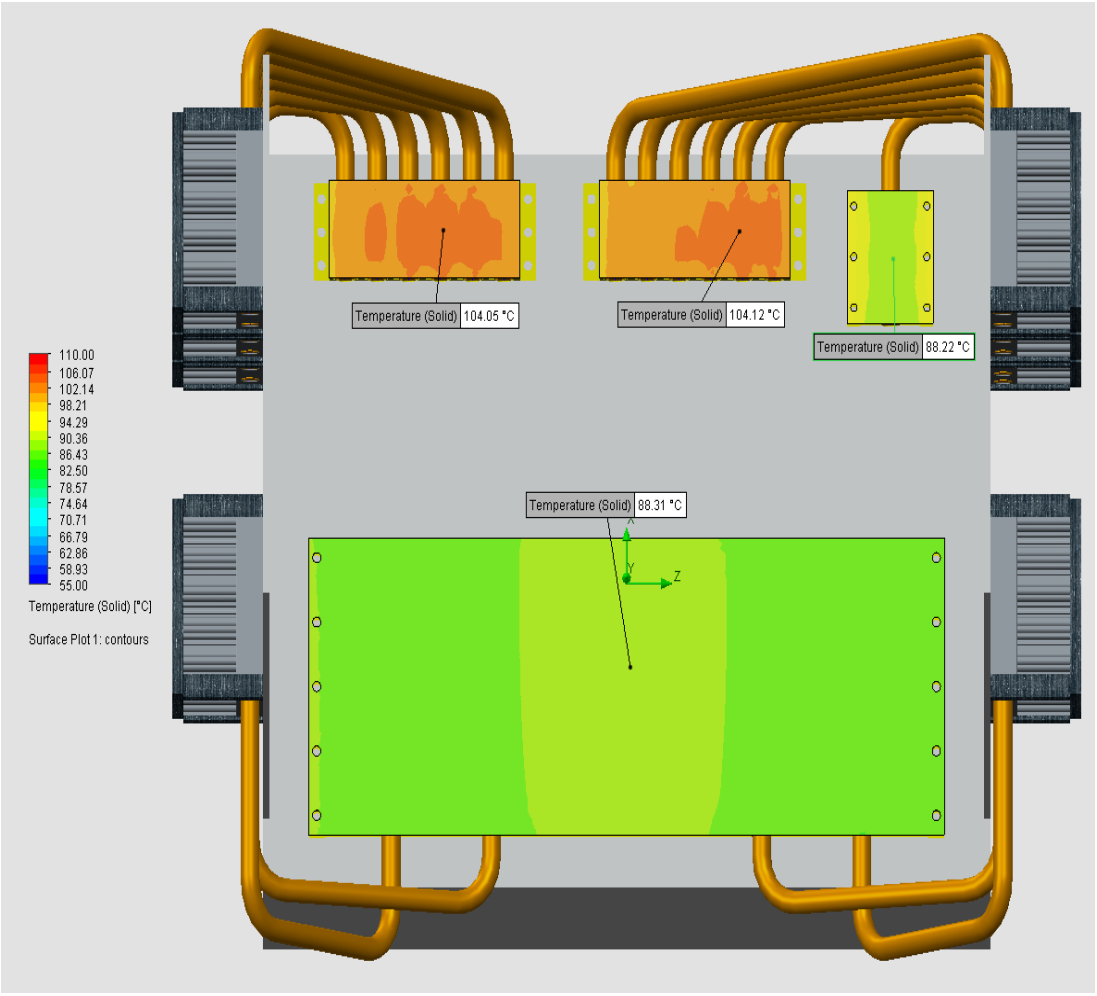

Figure 3.8 Temperature Distributions on Heaters (50 ^{o}C ambient, pin fin configuration)

During the analysis, mesh distribution on the system is also observed. Meshes become more frequent at natural convection regions, above the heater surfaces, the surfaces of pin fins and the connections of heat pipes with the bodies. As can be seen from Figure 3.9, the temperature distributions on fins are nearly isothermal.

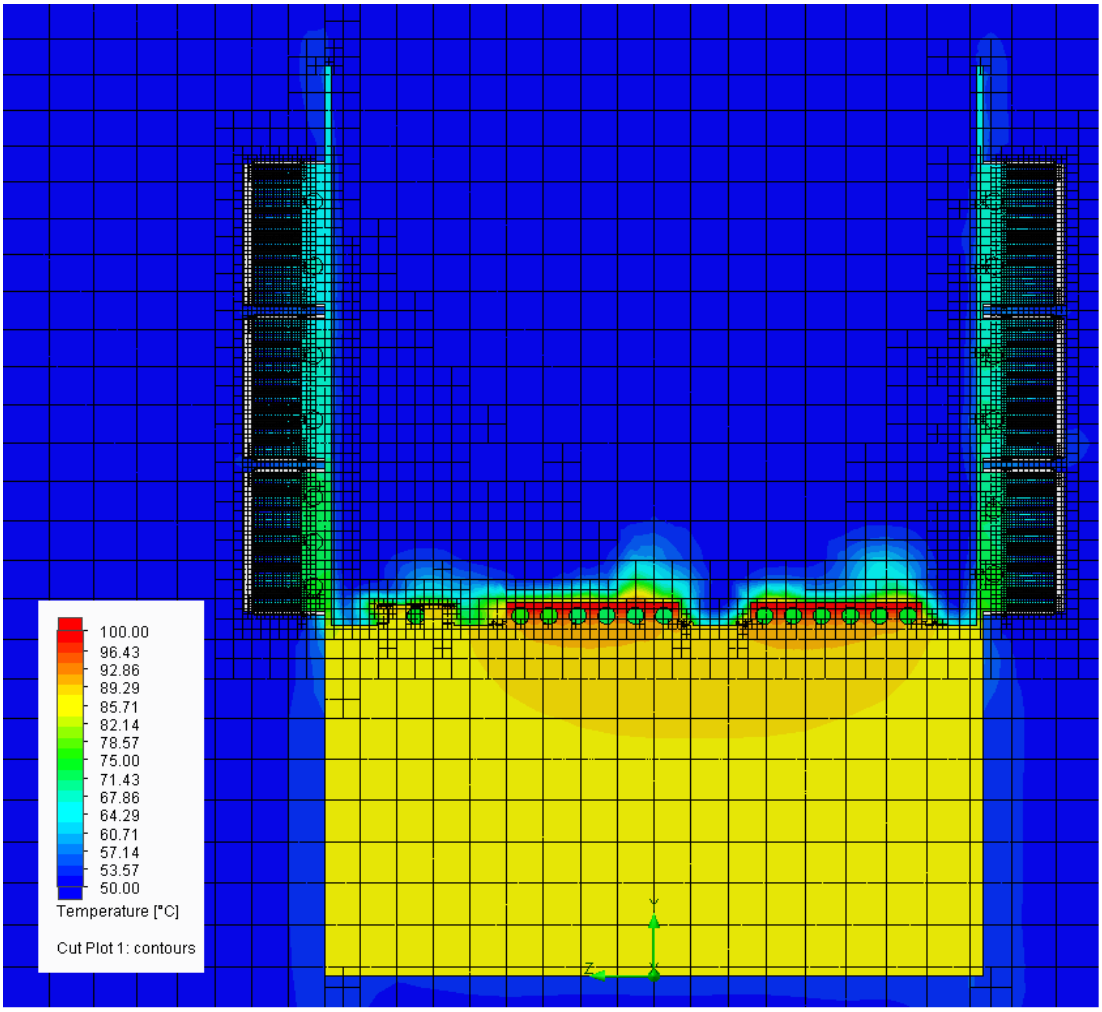

Figure 3.9 The Cut-View of Platform, with mesh and temperature distribution

The third study is for the pin fin configuration at 25 ^{o}C ambient temperature. Total initial mesh numbers in the analysis are 548624 and refinement level is 6. The effective thermal resistance of heat pipes is defined as 0.25 ^{o}C/W or K/W. All solid to solid interfaces are defined as full contact. As it is seen in Figure 3.10, temperature distributions on heater surfaces are close to isothermal distribution. Nearly 76 ^{o}C average temperature is captured on Heaters 1 (600 W). For heater with 70 W, this value is close to 64 ^{o}C and Heater 2 (350 W) has nearly 61 ^{o}C average temperature on its upper surface.

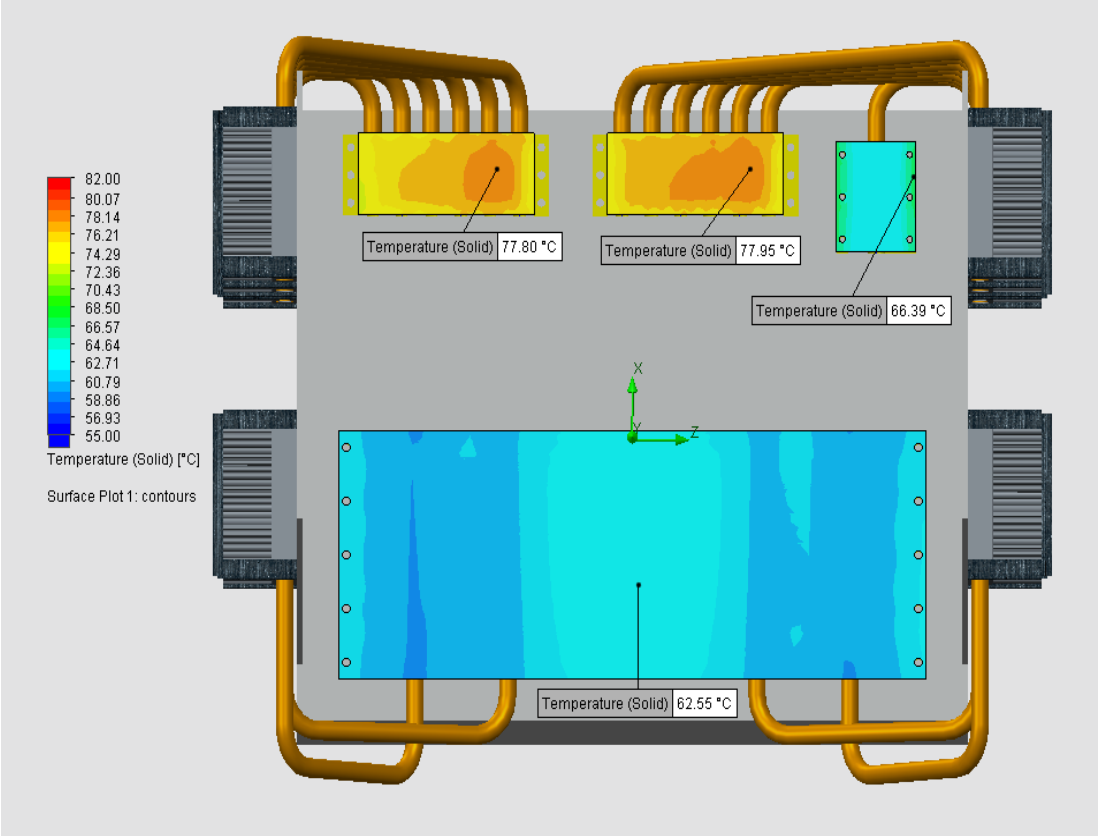

Figure 3.10 Temperature Distributions on Heaters (25^{o}C ambient, pin fin configuration)

During the analysis, convergence of results for temperature distributions on heaters with 600 W are monitored. First 190 iterations are illustrated in Figure 3.11 from which it can be seen that convergence occurs around 55 iterations.

Results of 25 ^{o}C ambient temperature with pin fin configuration is important for this study. After all numerical analyses are completed, this model will be validated with experiments. After the experiments, the numerical results will be compared the experimental results. Finally, corrected models will be created to simulate the experimental case better. Experiments also prove the assumptions made in the analyses.

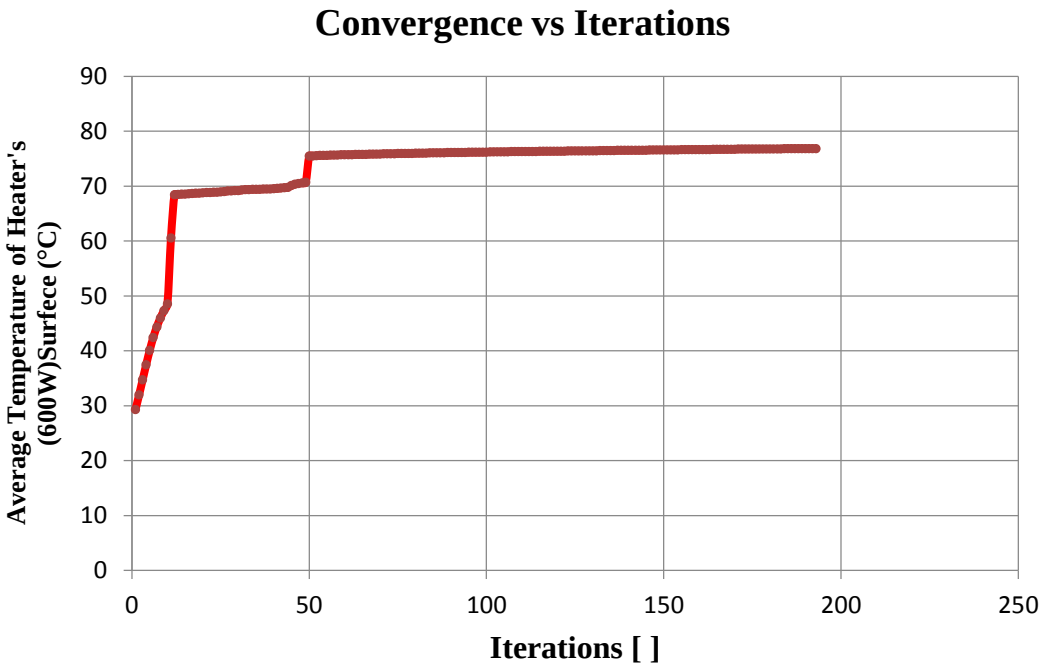

Figure 3.11 Iteration Numbers vs Iterations for Pin Fin Configuration @ 25 ^{o}C

After that point, the second configuration, rectangular plate fin heat sink with duct structure is studied. All parameters and inputs are the same as the pin fin case. At the preliminary stage, this configuration is prepared by general design assumption. There are several runs which were done; however, one sample will be selected among these, and it will be explained and discussed. Sample analyses given have mesh numbers between 450000 and 500000 with refinement level 3.

Dimensions of platform are the same as pin fin configuration for rectangular plate fin heat sink with duct structure. Rectangular fins have 248 mm width and 350 mm length. The base thickness of the heat sink is 14 mm, it is identified by diameter of heat pipe used which is 12 mm. The length of the fin plates is 25 mm with 5 mm thickness and 4 mm spacing. These numbers are selected by getting information about manufacturing techniques and considering manufacturability. For CNC Milling machines, there is a suggested ratio of length to fin spacing, which is close to 6. In that part, only 5 mm thickness and 4 mm spacing fin is considered. In Chapter 5, there will be another configuration for rectangular plate fin heat sink with duct structure.

Figure 3.12 is given for basic illustration of temperature distributions for this configuration at 50 ^{o}C ambient. The maximum temperature occurs at the surface of heaters with 600 W, which is nearly 122 ^{o}C. This number is in critical range for real product form of heaters. These devices make thermal shut-down at 120 ^{o}C base temperature distribution. This system is cooled by 6 fans, each duct has 3 fans inside.

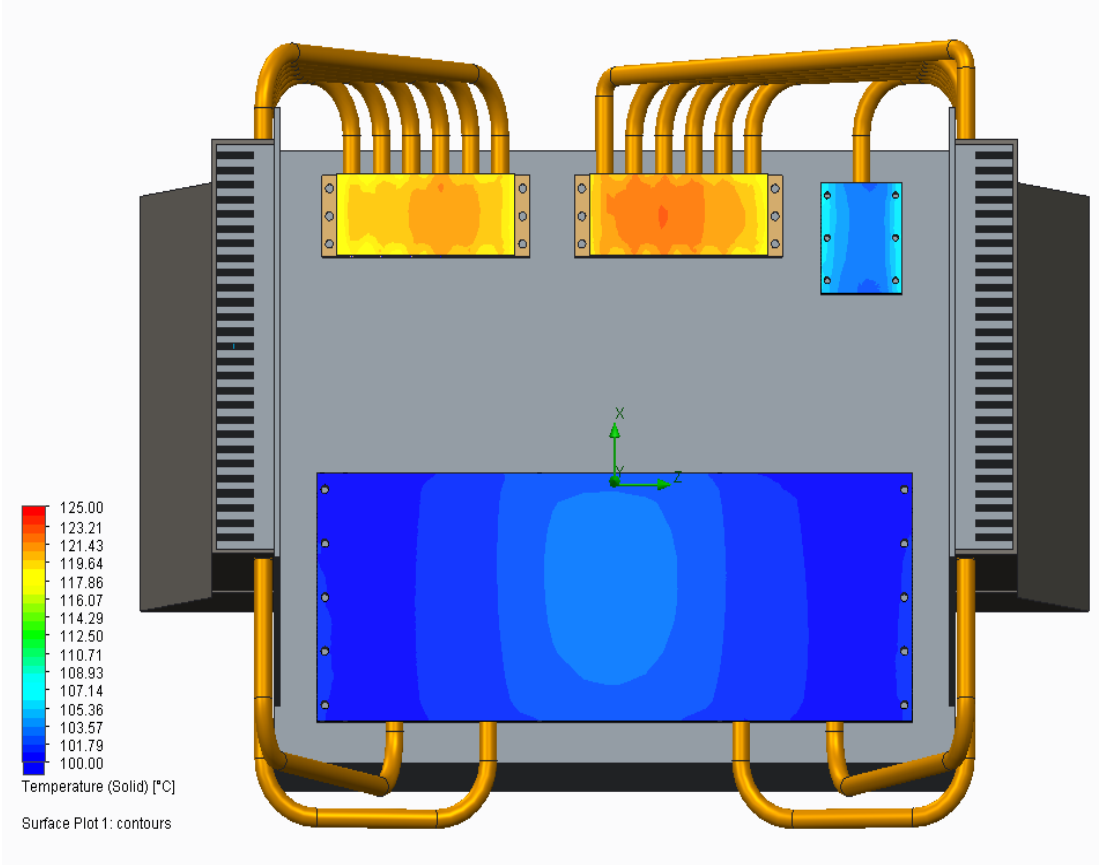

Figure 3.12 Temperature Distributions on Heaters (50 ^{o}C ambient, rectangular plate fin with duct structured)

Same study is also done for 25 ^{o}C ambient temperature. This configuration will be optimized in Chapter 5. The used plate fin heat sinks are the same as the ones in the analysis above. Moreover, there are some observations related to flow on fin plates and temperature distribution on fins, located on two sides. Figure 3.13 gives the temperature distributions on heater surfaces, the heaters with 600 W have temperatures close to 95 ^{o}C. Heater 2 and 3 have average temperatures of 74 ^{o}C and 78 ^{o}C, respectively. Figure 3.14 and Figure 3.15 demonstrate temperature distributions on heat sinks, average solid temperatures. When these figures are examined, heat pipes

locations can be easily identified from temperature distributions. In order to gather close to isothermal surfaces on fins; heat pipe locations are studied. Locations of heat pipes are adjusted iteratively. Suggested method is to keep more powerful heat pipe close to air flow. Another suggestion about placement of pipes is that, pipes must be embedded to the base of the heat sink because heat pipes transfer heat by conduction at evaporator and condenser sections. Average temperature on fins is approximately 58 ^{o}C. Finally, air flow temperature is considered. The heat sink at the left side, which has 9 heat pipe connections exhausts the air at a temperature 3 ^{o}C hotter than the other heat sink. Another observation can be made from Figures 3.14-3.17 is the mesh density on heat sinks. When the figures are examined in detail, there are some additional divided cells seen around the connections of fluid flow and the fins. These are the refined cells occurring during the calculation, which is an advantage of the adaptive mesh mechanism of FloEFD.

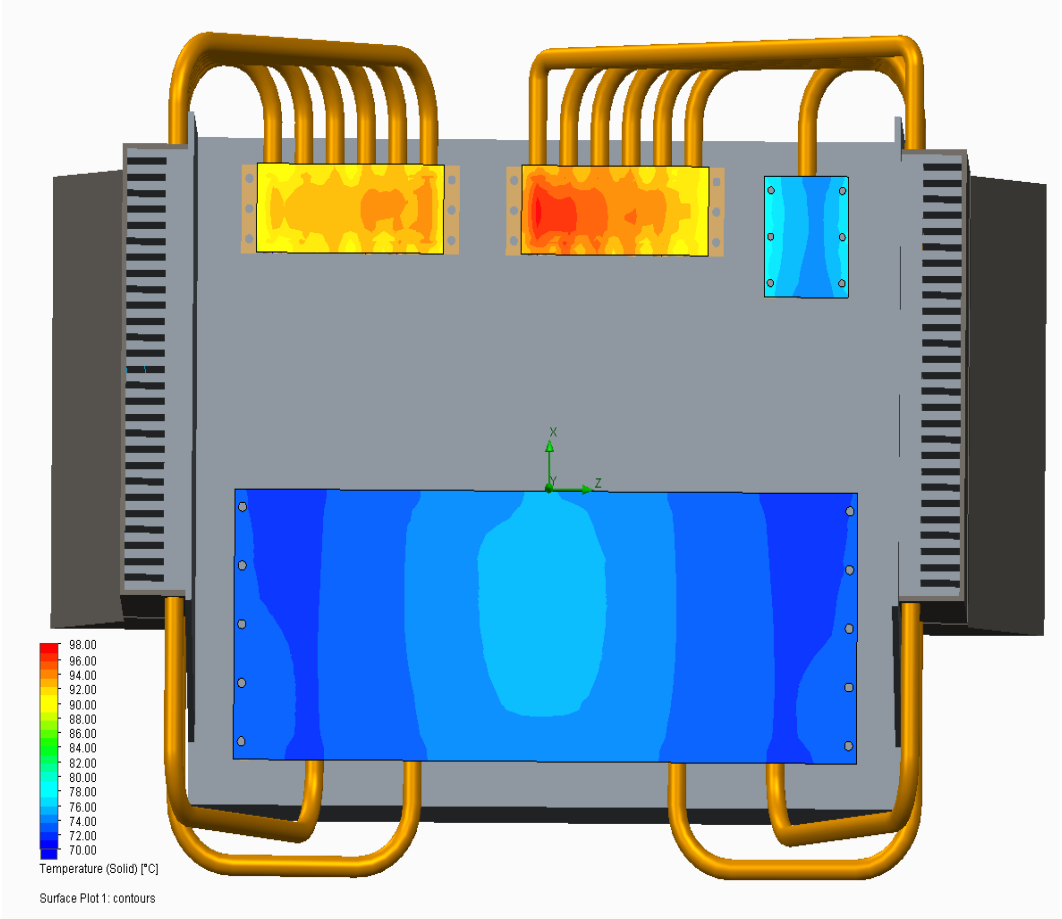

Figure 3.13 Temperature Distributions on Heaters (25^{o}C ambient, rectangular plate fin with duct structured)

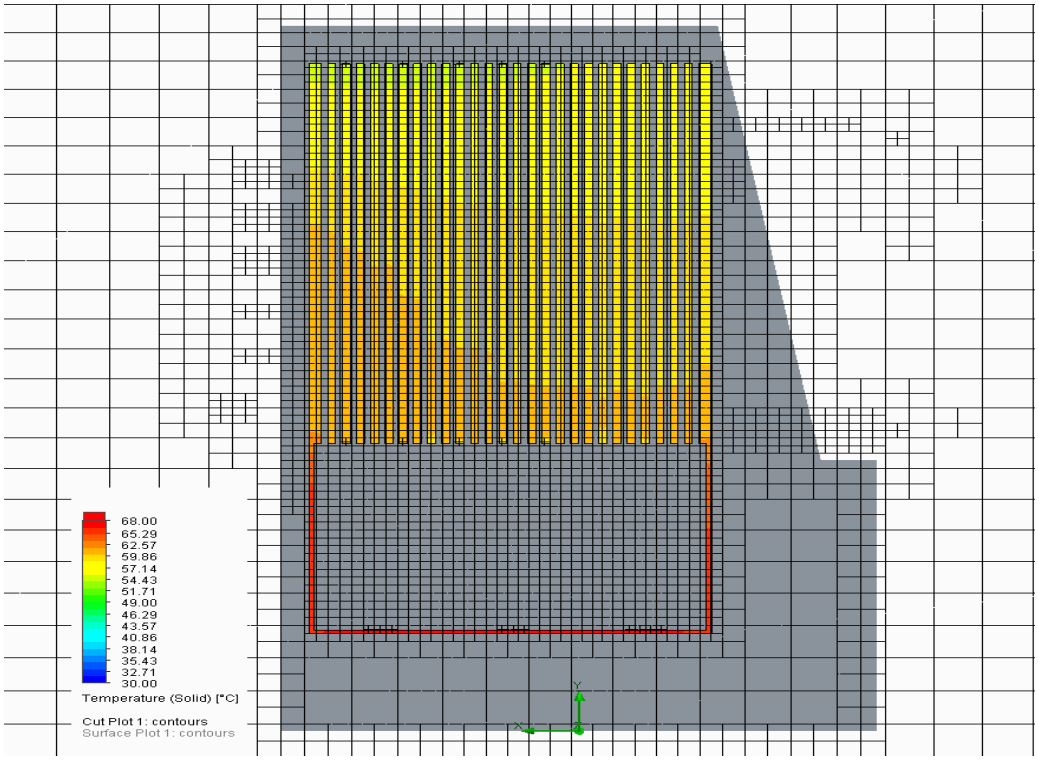

Figure 3.14 Temperature Distribution on Right Fin (8 heat Pipes Connected)

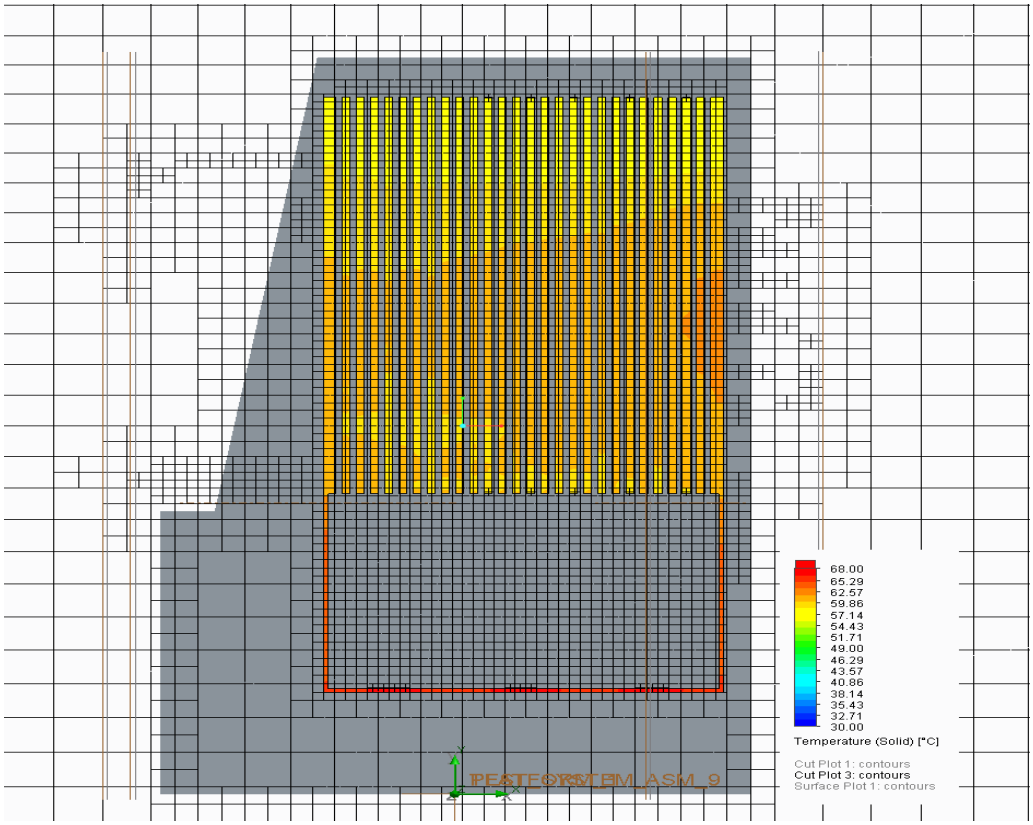

Figure 3.15 Temperature Distribution on Left Fin (9 heat Pipes Connected)

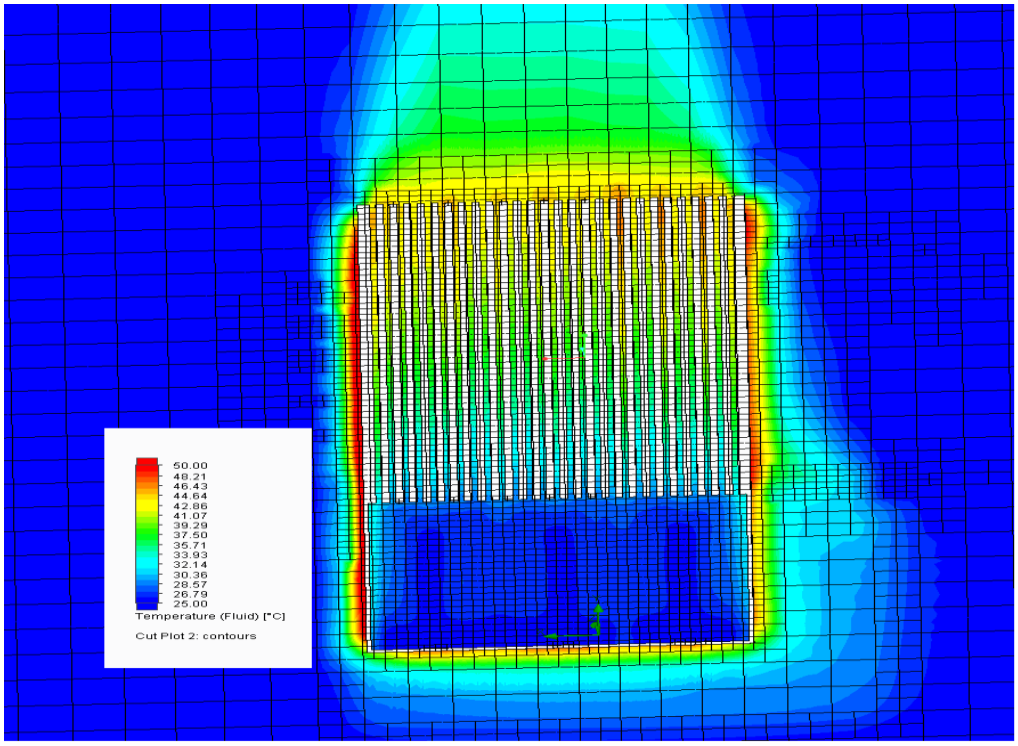

Figure 3.16 Exhaust Air Temperature Distribution on Right Fin (8 heat Pipes Connected)

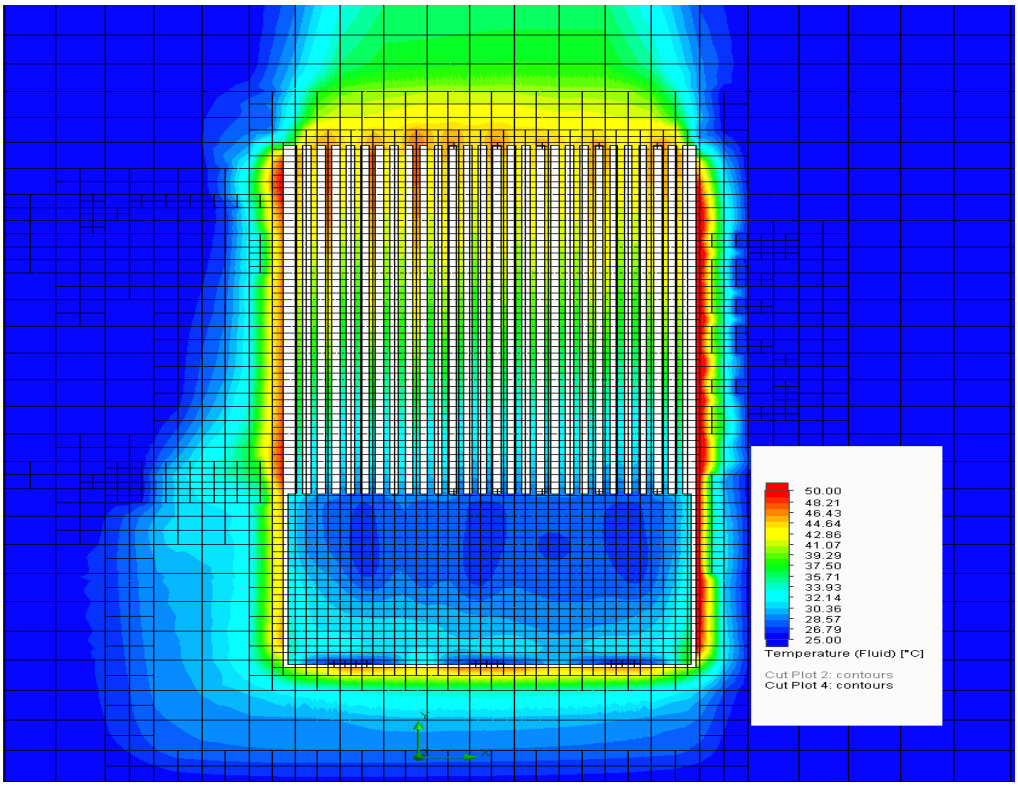

Figure 3.17 Exhaust Air Temperature Distribution on Left Fin (9 heat Pipes Connected)

Finally, these runs are done in order to gather a general idea about the usage of heat pipes. Collected results will be validated experimentally for the pin fin heat sink case. This validation will prove the performance of heat pipe and show the real characteristic of system such as thermal and contact resistances. In this case, effective thermal resistance for all heat pipes is defined as 0.25 ^{o}C/W or K/W. This number will be checked by experiments and re-calculated. The next chapter covers the experimental procedures and comparisons of experimental and numerical analyses. After that, plate fin heat sink optimization in terms of thickness and spacing will be done in Chapter 5.

CHAPTER 4

EXPRIMENTAL PROCEDURES AND RESULTS

This chapter includes the experimental setup and the experimental results at operating conditions. After the preliminary design is developed, the experimental setup is manufactured. With the manufactured setup which reflects the preliminary design of the pin fin heat sink configuration, the numerical model will be validated and according to results, numerical model will be updated in the final design. These experimental results have also demonstrated the capabilities of the heat pipes specifically designed and manufactured for the setup.

4.1 Manufacturing of Experimental Setup

The experimental setup includes the manufactured experimental platform, which is designed according to the real product dimensions, hence it represents the real rotary platform's shape. The heaters are manufactured to simulate the heat loads of power amplifiers and they have the dimensions of the actual chips. The heat pipes are designed using the numerical analyses and they are manufactured according to the exact specifications in the numerical model. The experimental setup is manufactured according to the design in Figure 3.5 of Chapter 3.

Design procedure started with generating CAD model. Then dimensions are identified. Basically, platform's dimensions are respectively height, wide and length 650 mm, 375 mm and 460 mm with H-shape design. There are four heat sources, three of them are different from one another. These are powered with 70W, 350W and two of them are powered 600W. These sources simulate the power amplifier in radar application. 15 different heat pipes are generated from the knowledge of heat source locations. Heat pipes are sintered wick type with water as working fluid, a sample cross-sectional view of the wick structure is given in Figure 4.1. Heat pipe's one end is connected to the

designed condenser cold plate and the other end is attached to the pin fin heat sink assembly.

Preparation of the experimental setup will be explained step by step. In addition to the platform, the measurement devices and techniques will also be explained.

Figure 4.1 Cross-section of sintered wick heat pipe

First step is the manufacturing of the dummy platform. Real dimensions are used in order to manufacture the dummy rotary platform with dimensions 650 mm x 375 mm x 460 mm. Platform is produced from an Aluminum 5000 series sheet with 5 mm thickness. The assembled platform is illustrated in Figure 4.2.

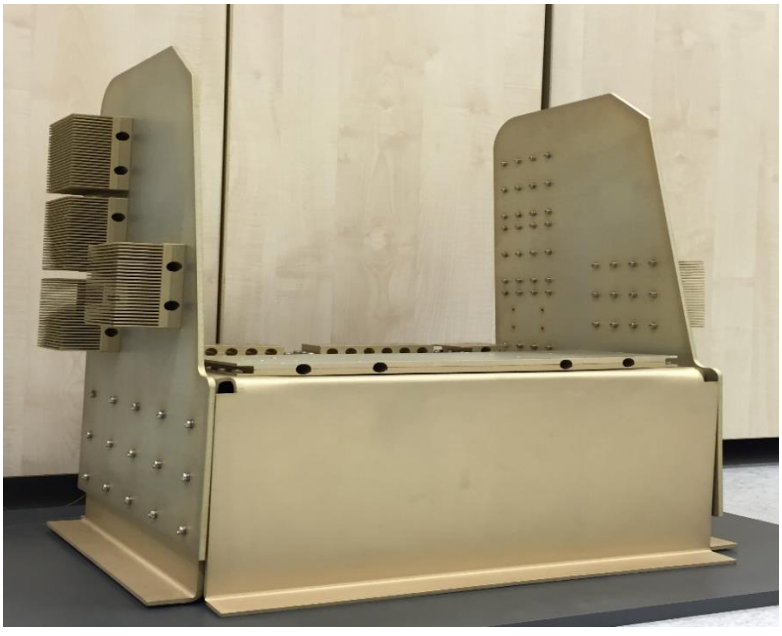

Figure 4.2 Manufactured dummy rotary platform

Heat pipes are imported and they are produced in Taiwan by Enertron Inc. There are 15 different size heat pipes and all have the same U-shape with 90^{o} bends. The dimensions and quantities of heat pipes are given in Table 4.1. Bending of the heat pipe directly affects the performance, hence during the bending process, decrease in quality of the wick structure and the cracks due to shrinkage of the bending edge should be prevented.

Table 4.1 Dimensions and quantities of used heat pipes

Name of Heat Pipe	***The Amount of Heat Pipes***	***Length (mm)***
Heat Pipe – 1	2	522.78
Heat Pipe – 2	2	551.55
Heat Pipe – 3	1	276.5
Heat Pipe – 4	1	319.7
Heat Pipe – 5	1	381.4
Heat Pipe – 6	1	430.7
Heat Pipe – 7	1	495.85
Heat Pipe – 8	1	545.8
Heat Pipe – 9	1	586.95
Heat Pipe – 10	1	539
Heat Pipe – 11	1	479.4
Heat Pipe – 12	1	434.6
Heat Pipe – 13	1	388.15
Heat Pipe - 14	1	356.9
Heat Pipe - 15	1	300.5

Heat pipes are generally manufactured from copper. Designers should consider corrosion effect. In order to eliminate the corrosion, all structures except for heat pipes are coated with yellow alodine according to MIL-STD-5541 Type II and Class-1A. Pin fin heat sinks are off the shelf products, which is ALPHA Novatech S20100-40W, aluminum square pin fin heat sink. The detailed information about pin fin heat sinks is given in Appendix A. These standard heat sinks are further machined in a CNC

milling machine. Assembly connection holes and heat pipe connection locations are prepared.

The heat pipes that are used have 12 mm diameter with different lengths, as shown in Table 4.1. Hence the machined heat sinks have 12 mm diameter assembly holes for heat pipes with close-fit tolerances. The gap between the heat pipe and its connection location is the most important design criteria in manufacturing process due to the resulting thermal resistance caused by the clearance gap. To eliminate a high thermal contact resistance, an interface material is used for filling the clearance between the heat pipe and its hole. As a filler material, Artic Silver 5 is used, which is high density polysynthetic silver thermal compound (Appendix A). This filler material is spread in the form of a thin layer, as illustrated in Figure 4.3. Then, heat pipe is attached to the interface hole. During the assembly steps, this filler also behaves like lubricant for heat pipe's fitting. The fitted heat pipe is shown in Figure 4.4.

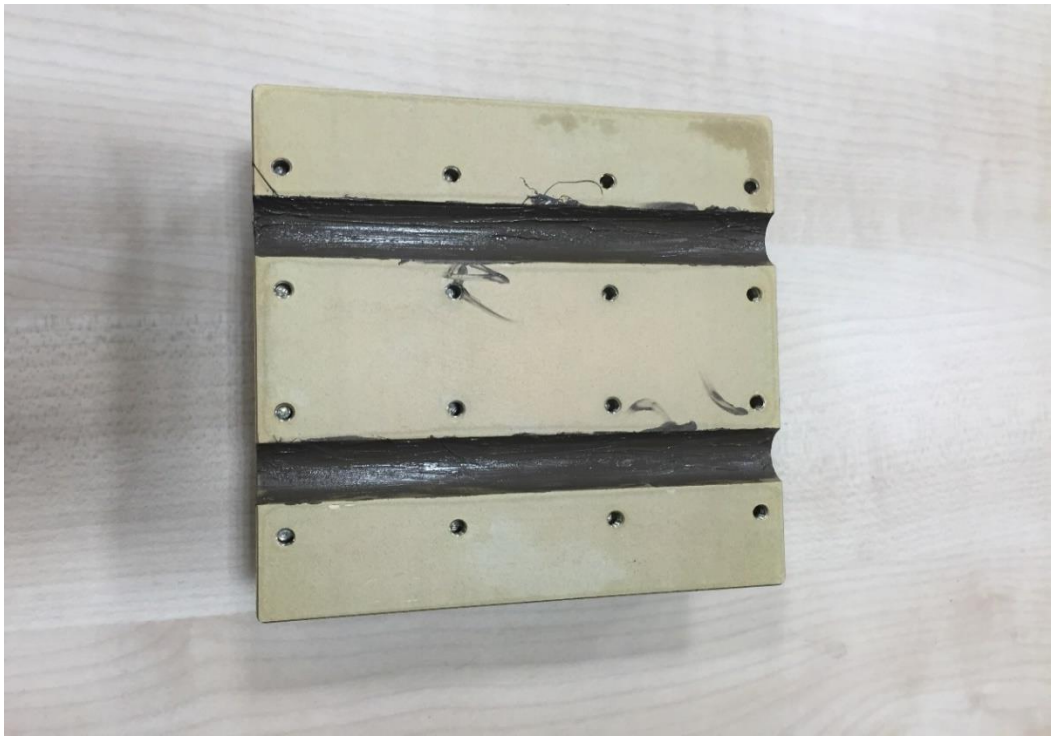

Figure 4.3 Filler material is applied to mounting holes

During the design steps, accessibility and maintenance procedures are also considered. Hence, the condenser section is designed as a cooling module. This part includes the pin fin heat sink, the fan and its holder, the mounting back plate, and the heat pipes.

The final form of the module is shown in Figure 4.5. All assemblies are readied to easily connect them to the platform. The main idea behind this is to decrease the replacement time and the maintenance duration.

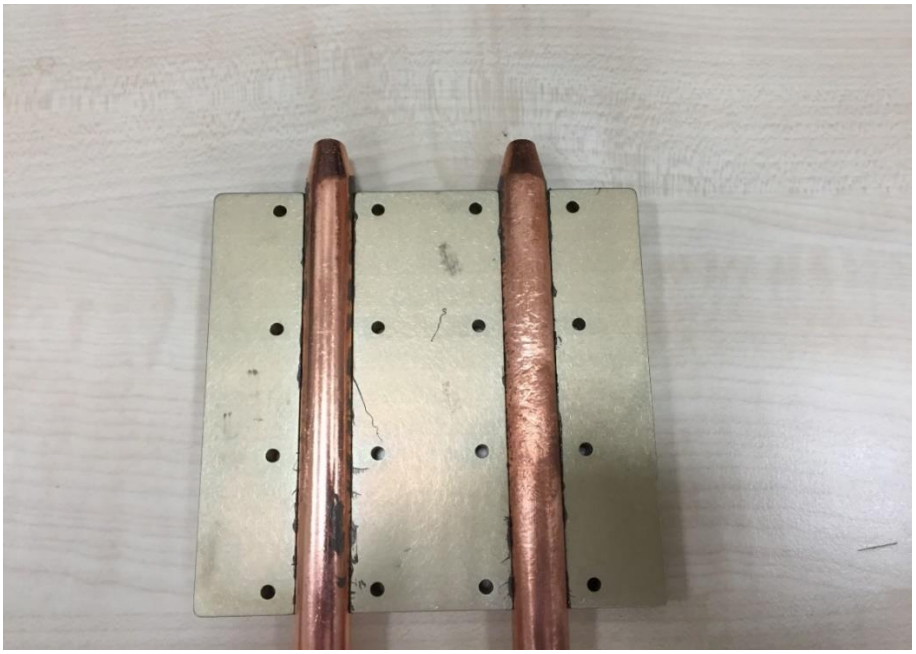

Figure 4.4 Heat pipes are mounted into mounting holes of pin fin

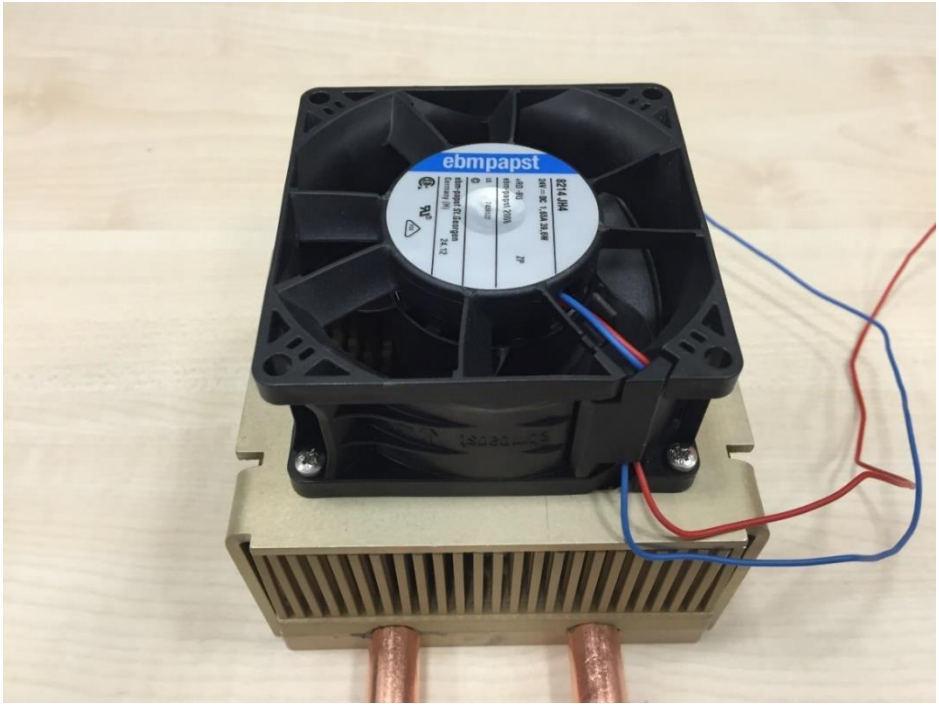

Figure 4.5 Condenser module

The selected fan is EbmPapst 8214 JH4, whose specifications are given in Appendix A. Ebm 8214JH4 is very close to military standards and it is a high speed fan. There is only one negative side, which is noise at maximum speed. During the experiment, fans are driven with external DC power supply. This fan is produced from plastic material, hence it is only 0.2 kilograms. It is very important for the overall system weight.

Finally, cooling module is screwed the side walls of platform. This configuration is appropriate for desert environment. Because there is no suction or exhaust to the normal of the ground. If there is blow or suction, the critical damage may occur due to sand particles. The evaporator ends of the heat pipes are attached to heater base plates. These plates are produced from the same material with the platforms and they used for the connection between heat pipes and power sources. Fans can be under operation independent from the cooling module, which means it can be easily replaced. However, the cooling module and platform's heater base must be attached at the same time. The final mounting of the heat pipes is given in Figure 4.6.

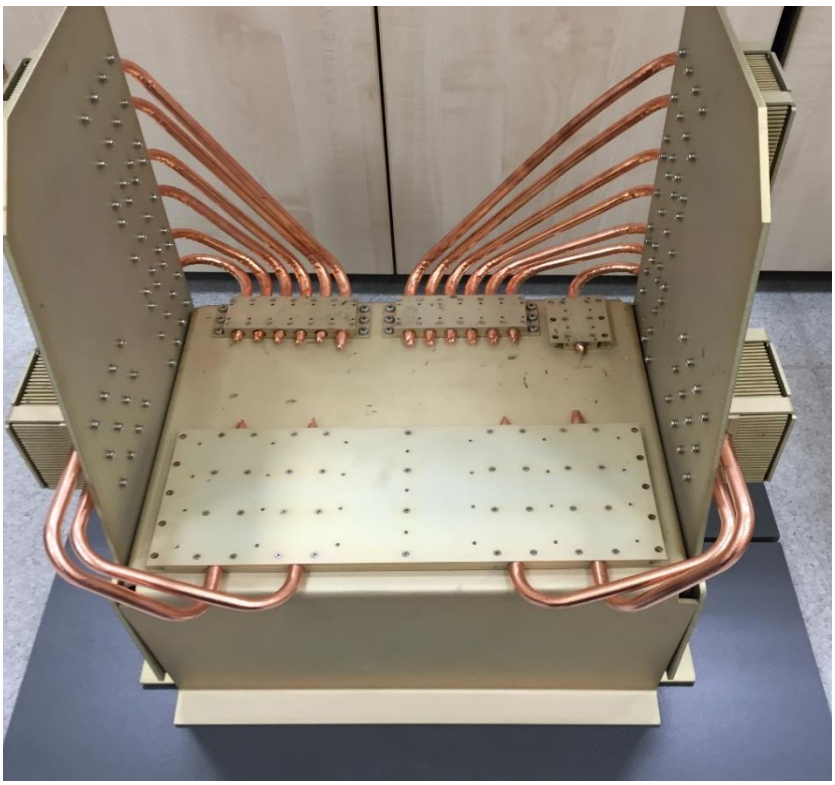

Figure 4.6 The final mounting of heat pipes

4.2 Preparation of Experiment Setup

Final experimental setup shown in Figure 4.6 is prepared for the experiment procedure. Heat loads, power supplies, measurement devices and monitoring equipment for the experiment are mounted or placed on relevant places.

The first step is the preparation of heat loads. Heat loads are custom made heaters for this study with powers of 600 W, 350 W and 70 W. There are 3 different but 4 total heaters. Heaters are produced from stainless steel casting. They operate with maximum 24 VDC current and they are prepared for easy mounting. They are connected to the system with screws and their electrical interfaces are easy-plug banana sockets. The dimensions of them are given in Table 4.2 and they are illustrated in Figure 4.7. They simulate power amplifiers (PA) and travelling wave tube (TWT) modules, hence dimensions and power ratings are the same with real components.

Table 4.2 Specifications and dimensions of heaters

Name of Heater	***Quantity***	***Dimension (mm)***	***Power (W)***	***Heat Flux (W/cm^2)***
Heater 1	2	50 x 126 x 10	600	10
Heater 2	1	152 x 400 x 10	350	0.58
Heater 3	1	68 x 54 x 10	70	1.91

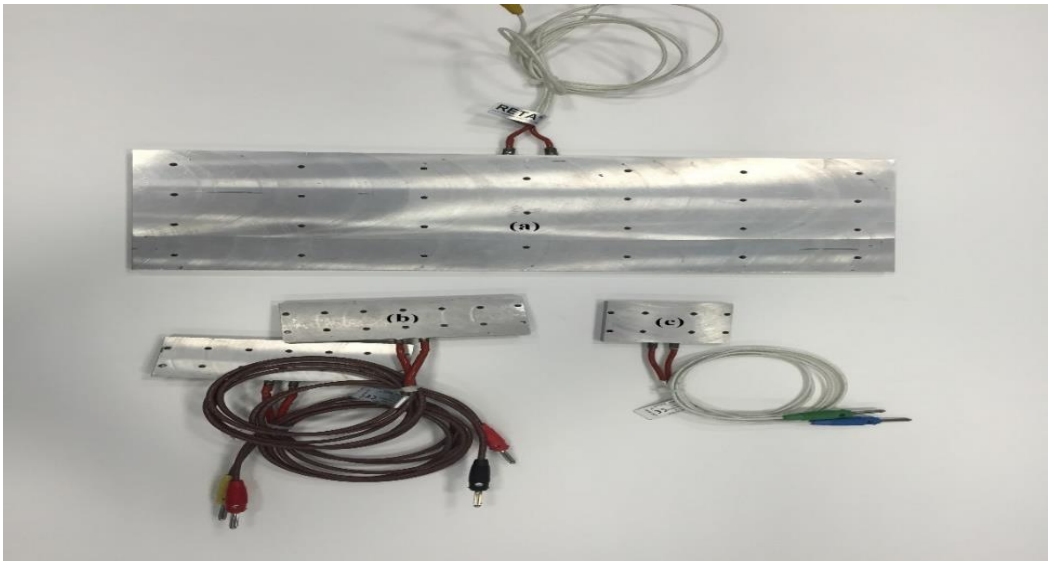

Figure 4.7 Heaters (a) Heater 2 (350W) (b) Heater 1(600W) (c) Heater 3 (70W)

The second step is preparation of the data logging system for the test setup. The main parts of this system are the data logger, the multiplexers for data-logger, the thermocouples and the computer. The thermocouples are used for receiving temperature data as electrical input, hence they are used as thermal sensor. During the experiment, 'Type-J' thermocouples are used. 'Type-J' is nickel alloy thermocouple and it has iron–constantan couple. 'Type-J' thermocouples have a restricted measurement range (-40 ^{o}C to 750 ^{o}C) compared to other types, however they have higher sensitivity than the other types with 50 µV/^{o}C. Upper limit 750 ^{o}C comes from iron's properties. Thermocouples generate a voltage difference due to temperature change, hence receiving data must be converted. This conversion can be done with a calibration based on 'Type-J voltage to temperature transformation catalogue'. However, during the experiment they are calibrated automatically by the data logger. Thermocouples are prepared at ASELSAN Thermal Laboratory. 2 m length thermocouple wires are cut. Then, the junction weld is done by thermocouple welder 'Omega TL-WELD', this device is listed in Table 4.3. After the thermocouples are finalized, they are connected to their measurement points by pieces of thermally conductive 3M^{TM} Aluminum adhesive foil tape. All thermocouples are numbered as illustrated in Figure 4.8. In total, twenty nine thermocouples are placed and 3 of them are connected to the platform body to monitor the platform wall temperatures. These thermocouples are placed according to identified hot spot points from the numerical simulation results at the preliminary stage.

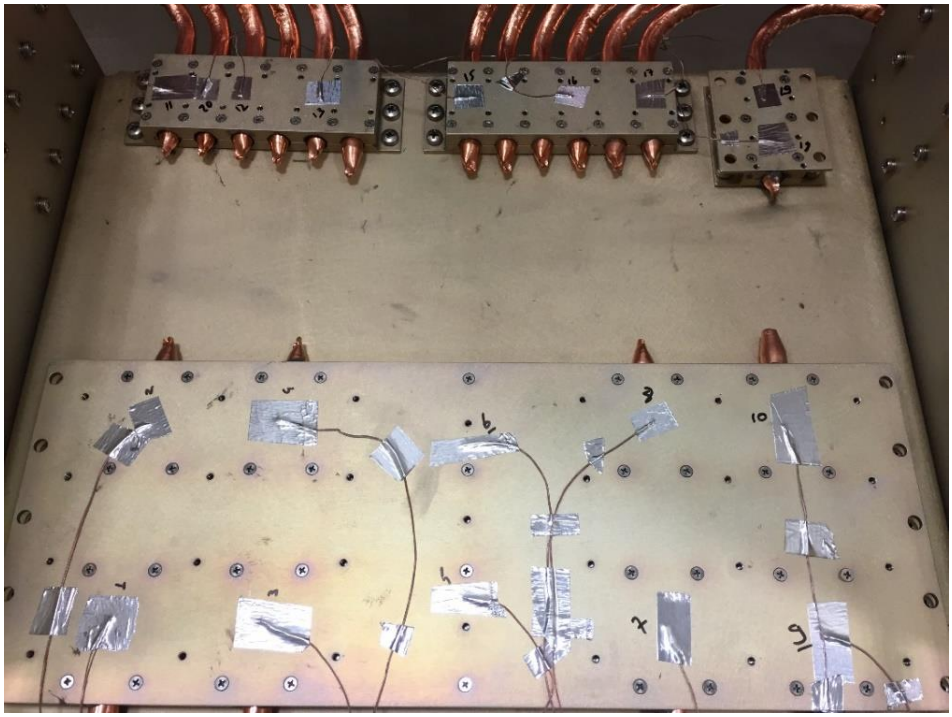

Figure 4.8 Sample view of thermocouple's location

In order to process the data coming from thermocouples, Agilent 34970A Data Logger device is used. These thermocouples are connected to the data logger with two Agilent 34903A 20-Channels Switch Unit Multiplexer Boards. A single board has twenty channels, which means twenty inputs can be collected by one multiplexer. A computer is used for screening the data coming from the data logger and collecting the data with certain time intervals. All measurement devices are tabulated and explained in Table 4.3.

The third and final step of the setup is mounting the heaters to the upper-side of heat pipe's heat collecting plates. The heaters are not installed directly. Because of the manufacturing tolerances and presence of thermocouples on the surface, there might be gaps between the heaters and the heat collecting plates. Existence of a gap can cause to thermal contact resistance and it can obstruct the conduction between heaters and their sitting place. To eliminate this obstacle, a thermal interface material is used. The used material is Laird Tflex 640. It is boron nitride filled silicone elastomer with 3W/mK thermal conductivity. It is also adhesive, so it can easily be applied, which is shown in Figure 4.9. It is elastic material, hence it can be compressed by mounting load due to screws.

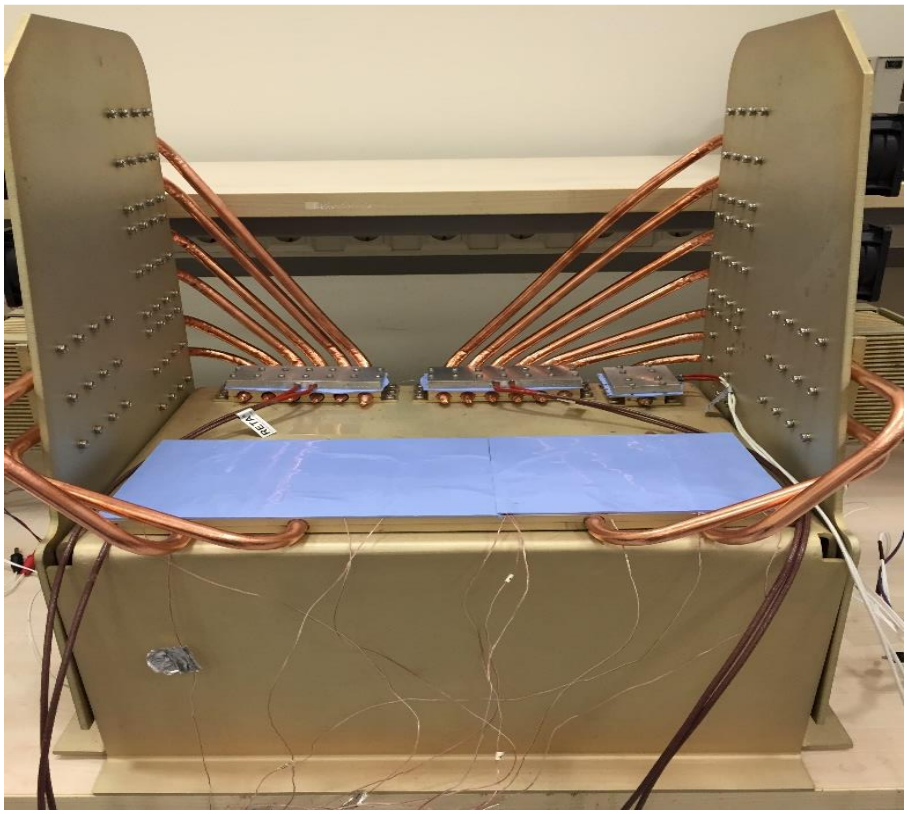

Figure 4.9 Heater mounting with gap filler ‘Laird Tflex 600’

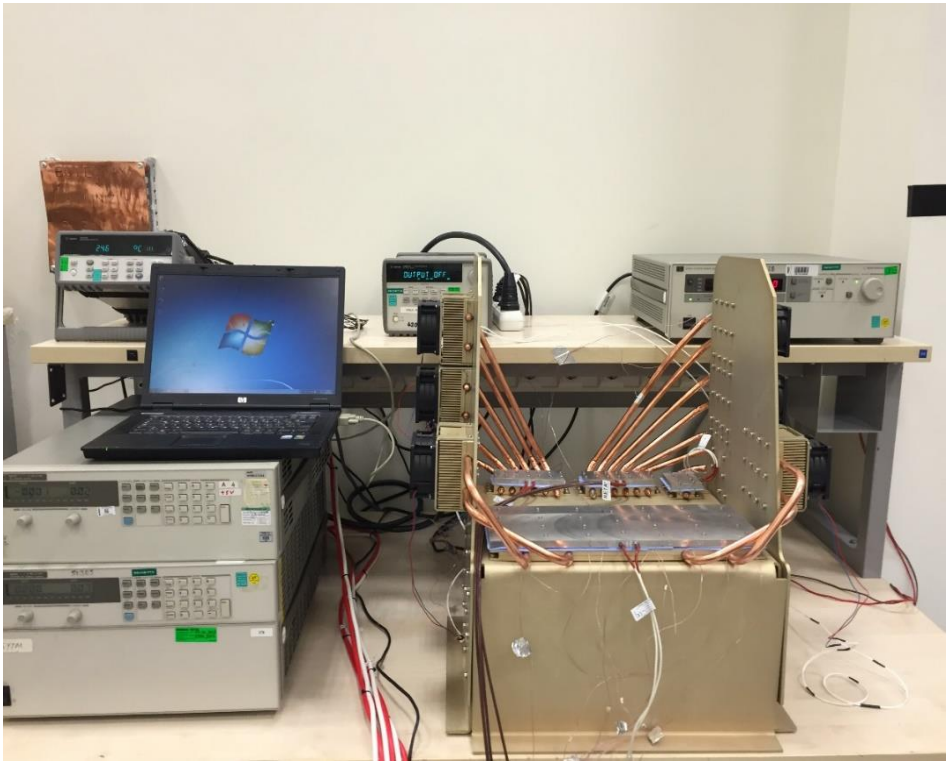

Figure 4.10 Experimental setup with dummy platform

Another data collection approach used is thermal imaging. The system is monitored with a FLIR E60 thermal camera. Detailed specifications of the camera are given in Appendix B. Before capturing images, the thermal camera must be calibrated. The thermal camera is calibrated with a 3M matt black tape, which has ($\varepsilon = 0.95$) emissivity. It is seen attached to the wall on the right side of the equipment in Figure 4.10. The calibration is done manually, by holding the camera at a 0.5 meter distance.

While preparing the setup, four different AC to DC power supplies are used. Three of them run the heaters and one of them runs the fans. Fans are powered with Agilent 6032A System Power Supply 0-60V /0-50A, 1000W. EbmPapst 8214 JH4 works with 24VDC and 1.65A, hence eight fans require 317 Watt. Heaters are controlled with three different power supplies. Heater 1 (2 pieces) is controlled by Agilent 6692A DC Power Supply 0-60V /0-110A. Heater 2 is controlled by HP 6573A System DC Power Supply 0-35V /0-60A. Heater 3 is controlled by Agilent E3634A DC Power Supply 0-25V, 7A / 0-50V, 4A. All supplies are tabulated in Table 4.3 and their specifications are given in Appendix B. Due to the risk of electricity because the required current is too high for running heaters, all power supplies are grounded with a ground terminal, a copper sheet, which is seen on the left, in Figure 4.10.

The experimental setup is prepared as shown in Figure 4.10 and the experiment is done at ASELSAN Thermal Laboratory. As it is mentioned above, the validation of the numerical model will be at 25 ^{o}C environmental temperature. Hence first limitation is to obtain the same environmental condition in the real case. Before starting the experiment, the laboratory's temperature is set to 25 ^{o}C by the air-conditioner system in one day.

To conclude, the steps of the experimental procedure are given below.

- Numerical results are interpreted.
- From the numerical runs and specifications of the modules, hot spots and the points that thermocouples are attached are identified.
- The manufactured platform is mounted.
- Cooling modules (heat pipes + heat sink + fan) are attached to the platform. Mounting holes are filled with thermal grease.

- Gap filler is spread on mounting plates.
- Under the filler material, thermocouples are attached to certain points defined from numerical runs and technical documents of modules.
- Heaters are mounted on cold plates.
- System is prepared as shown in Figure 4.10.
- Room temperature is stabilized by air-conditioning system by 2 hours.
- Measurements are captured from thermocouples and thermal camera.
- Measurements are stopped when system reaches steady conditions.
- Results should be compared with numerical runs.

Table 4.3 Used devices during the experiment

PRODUCT		***PURPOSE OF USE***
NAME	***IMAGE***	
Omega TL-WELD		Arc weld for thermocouples
Agilent 34970A Data Logger		Collecting data
Agilent 34903A 20-Channels Switch Unit		Multiplying Data Logger's channels

Table 4.3 (cont'd)

Agilent 6032A System Power Supply 0-60V /0-50A, 1000W		Feeding fans
Agilent 6692A DC Power Supply 0-60V /0-110A		Feeding heater 1
HP 6573A System DC Power Supply 0-35V /0-60A		Feeding heater 2
Agilent E3634A DC Power Supply 0-25V, 7A / 0-50V, 4A		Feeding heater 3

4.3 Results of Experiment

Results are obtained in nearly 25 ^{o}C laboratory environment. As it is mentioned in the previous part, the laboratory's temperature is set to 25 ^{o}C by air-conditioner system in one day before start to experiment.

Measurements taken from setup are results of the worst case scenario. As it is explained before, heaters simulate real TWT and PA modules and they only work in extreme case of TWT and PA modules' working conditions, which means the full power case is studied.

Results are divided in to two sections, one of them is thermocouple data and the other one is thermal imaging data. In this part, results and their explanations are covered, in addition to this the summarized discussions are in Chapter 6.

4.3.1 Results Collected From Data Acquisition System and Discussions

These results are collected by the data logger from thermocouples. They are calibrated and controlled by Agilent 34970A Data Logger. The idea behind the thermocouple use is obtaining the temperatures of the heaters. Hot spot temperatures on the heaters are important because the investigated devices make thermal shut-down above 120 ºC temperature. All heaters' average base temperatures are given in the following pages. In Figure 4.11, heaters are labeled in order to show which graph belongs to which heater.

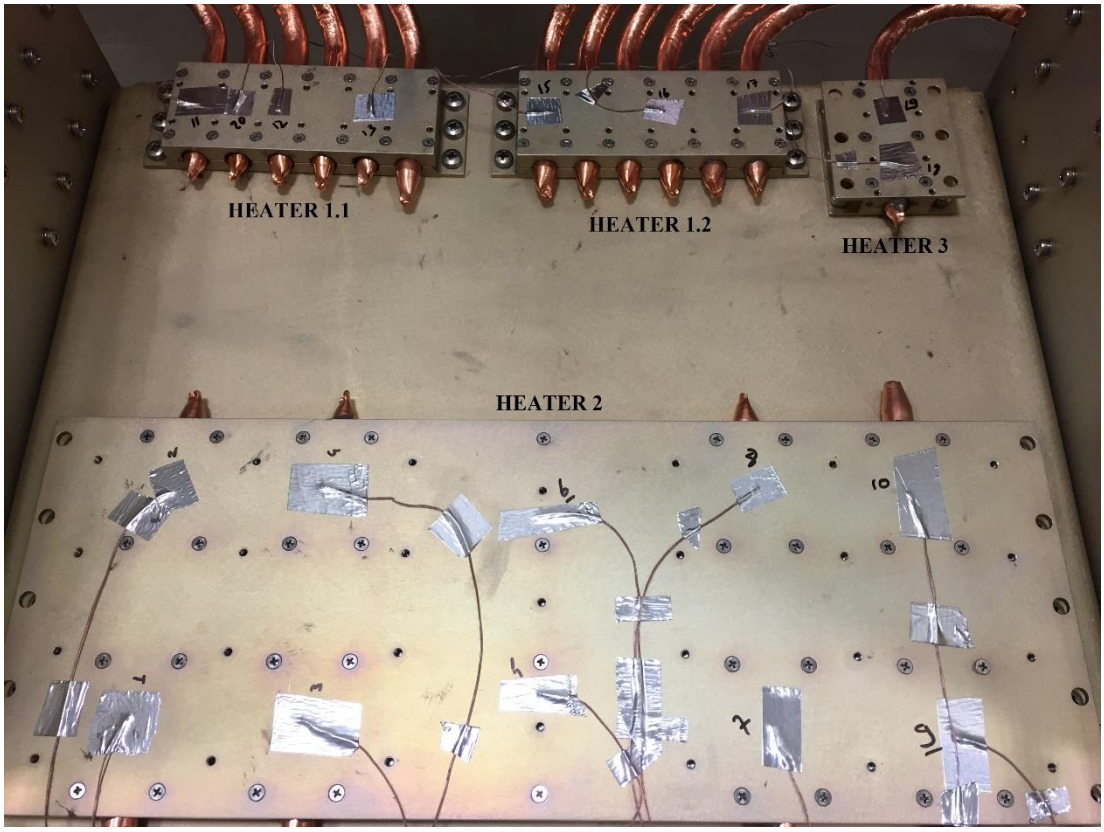

Figure 4.11 Illustration of labeled heaters

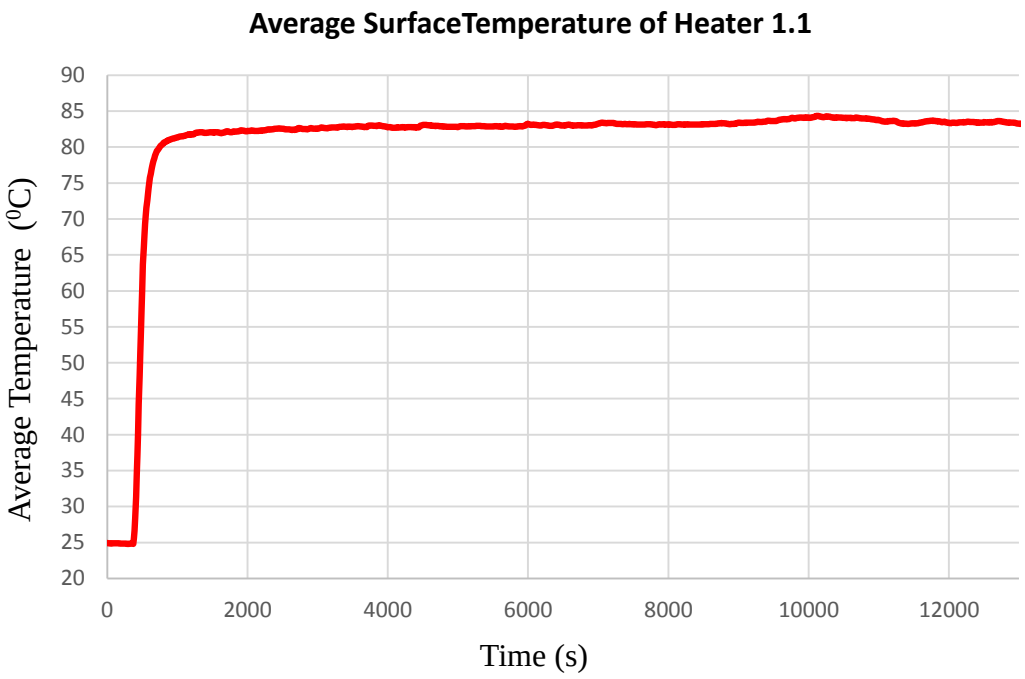

Figure 4.12 Average surface temperature of Heater 1.1

From Figure 4.12, the average surface temperature of Heater 1.1's base plane is nearly 82.75 ºC. Heater 1.1 reaches steady state conditions in approximately 1000 seconds. The highest point temperature on the surface is 86.27 ºC.

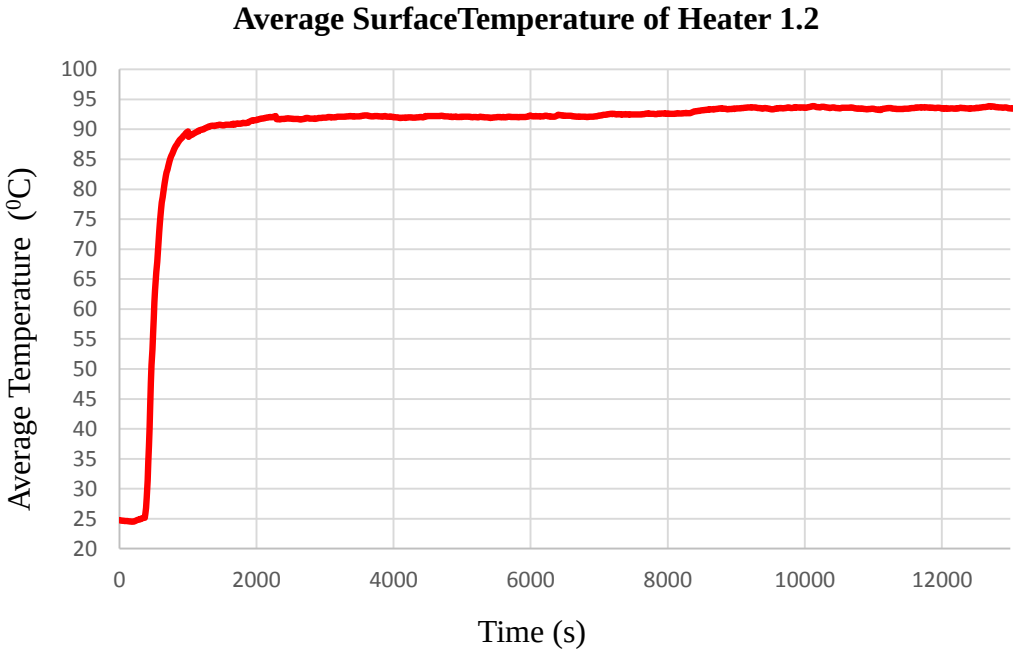

Figure 4.13 Average surface temperature of Heater 1.2

From Figure 4.13, the average surface temperature of Heater 1.2's base plane is nearly 92.5 ^{o}C. Heater 1.2 reaches steady state conditions in approximately 1000 seconds. The highest point temperature on the surface is 94.73 ^{o}C

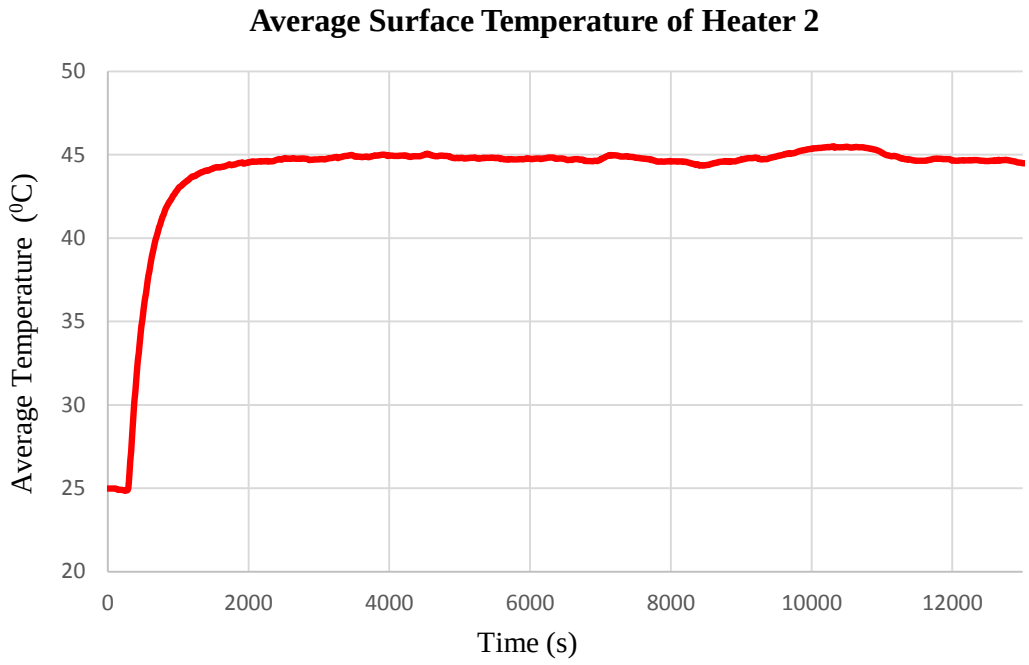

Figure 4.14 Average surface temperature of Heater 2

From Figure 4.14, the average surface temperature of Heater 2's base plane is nearly 45.80 ^{o}C. Heater 2 reaches steady state conditions in approximately 2100 seconds, which is due to large dimensions of the heater. The highest point temperature on the surface is 58.76 ^{o}C. This point is located in near middle section, where thermocouples 5 and 6 are attached.

From Figure 4.15, the average surface temperature of Heater 3's base plane is nearly 46.75 ^{o}C. Heater 2 reaches steady state conditions in approximately 1000 seconds. The highest point temperature on the surface is 47.55 ^{o}C.

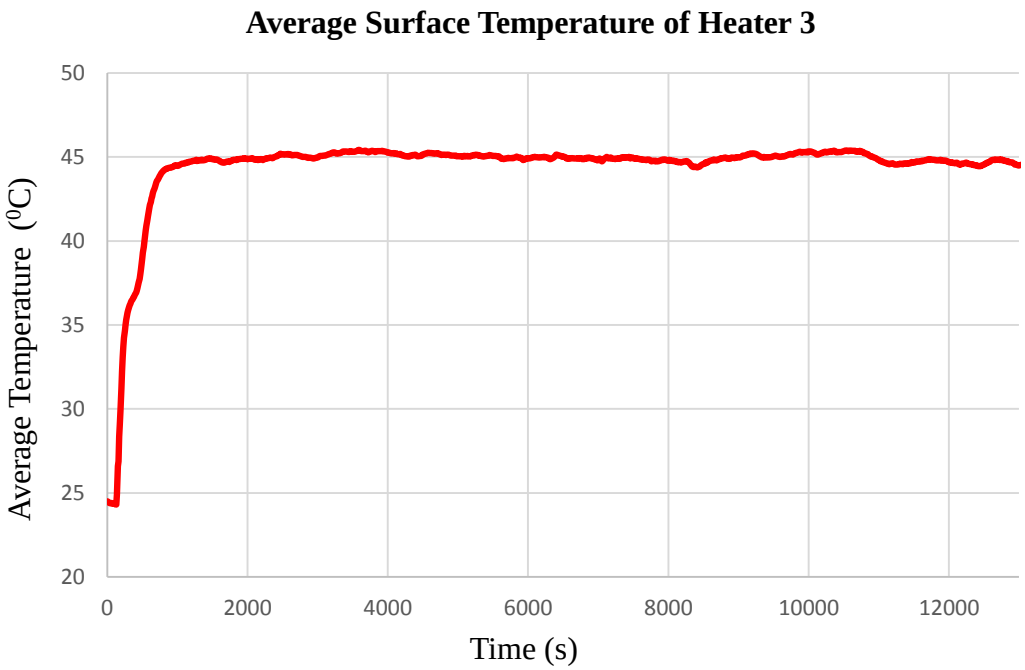

Figure 4.15 Average surface temperature of Heater 3

During the experiment, heat pipes' properties are also considered. One of the most important assumption about the heat pipe is the existence of the adiabatic section. 5 different thermocouples are placed along the longest heat pipe in use to measure the temperature differences on the heat pipe wall as shown in Figure 4.16. Figure 4.17 proves the existance of an adiatic section. If the graph is observed, the temperature difference between evaporator and condenser is quite small. It is less than 3 ^{o}C, hence this difference is so small. The assumption of adiabatic section is also true in real life application. This figure is the proof that there is no dry-out in the heat pipe. The meausement of dry-out detecting is explained in Chapter 2.

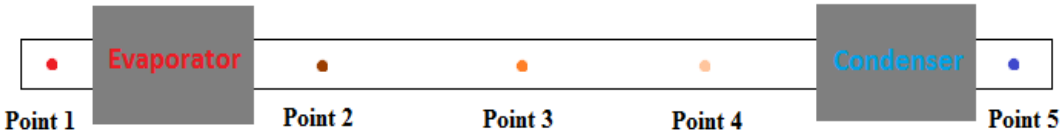

Figure 4.16 Illustration of Thermocouple couples' place on heat pipe

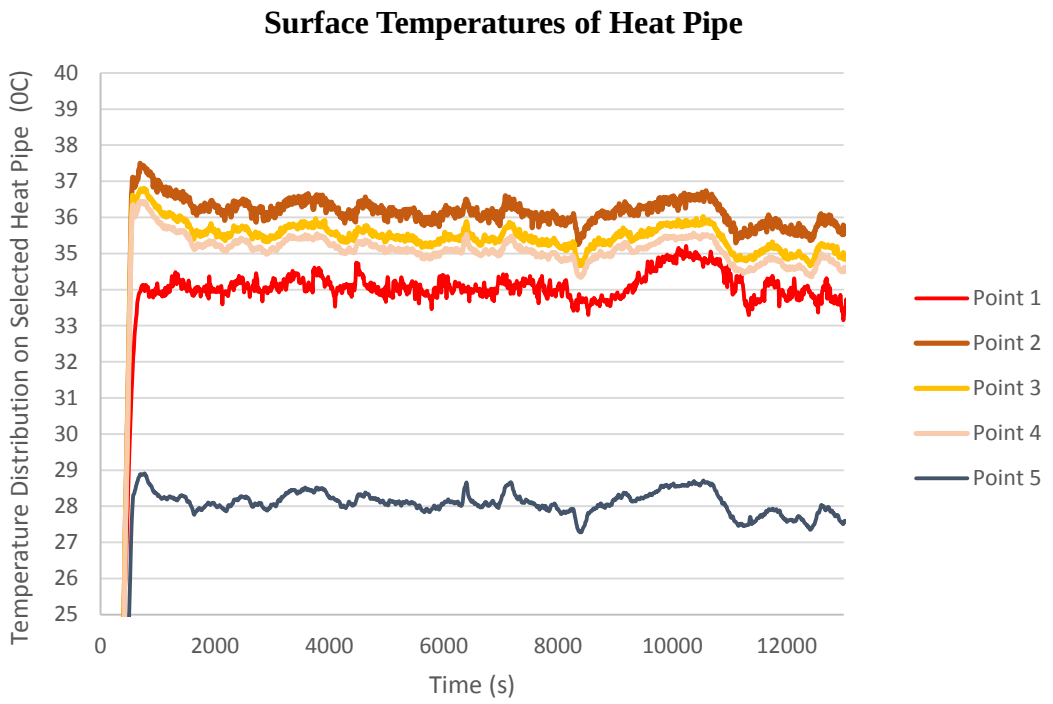

Figure 4.17 Temperature Distributions of Longest Heat Pipe

To sum up, measurements show the performance of cooling system. It can be said that heat pipes are used as alternative solutions. When it comes to discuss the results, the surprising result is the difference between Heater 1.1 and Heater 1.2. These two sources are identically the same, but results show nearly 11 ^{o}C temperature difference. According to analyses in the previous chapter, this gap is as small as nearly 4 ^{o}C. Hence, this difference is expected; however, it should not be quite large. This results in manufacturing tolerances of pin fins and their connection bases. Because of the existence of gap between connection holes and pipe, thermal resistance is increased, which is the main reason behind the surface temperature difference between Heater 1.1 and Heater 1.2. Another contradiction is about the surface temperatures of Heater 2 and Heater 3. The results in previous chapter are nearly 12 ^{o}C larger than the results of experiment. Probably main reason of this is the difference between heat pipe's performance in analysis and its performance in real life. This will be observed after corrected analysis is done in further chapter. The last inference of the experiment is the validations of heat pipes' performance. Figure 4.17 proves the existence of adiabatic section.

4.3.2 Results Collected From Thermal Camera and Discussions

Before starting the screening, thermal camera must be calibrated in order to capture correct and reliable visual data. The thermal camera (Flir E60) works based on thermal radiation. Hence, it must be calibrated with the surface, which has high emissivity. The calibration parameters are given in Table 4.4.

Thermal camera is used for visual observation. The purpose of using thermal camera is to identify the defects of mounting parts and gather information about the surfaces whose surface temperature distributions cannot be measured by thermocouple. The visual results are more understandable and clearer than numerical data for engineers. They can easily define the defects and solve the problem.

Table 4.4 Calibration parameters of thermal camera

Calibration Parameters Of FLIR E60 Thermal Camera

Emissivity (ε)	**0.95**
Distance (m)	**1**
Atmospheric Temperature (^oC)	**25**
Relative Humidity (%)	**50 %**

The results of thermal visualization are very close to data from the thermocouples. When Figure 4.18 is considered, point SP1 is on the Heater 1.2, and as it is measured by thermocouples, it is close to 94 ^oC. Another point is SP2, which is on Heater 1.1 and it indicates nearly 82 ^oC. SP4 belongs to Heater 3 and it shows around 48 ^oC. SP3 and SP5 are on Heater 2 and values can be easily seen in Figure 4.18.

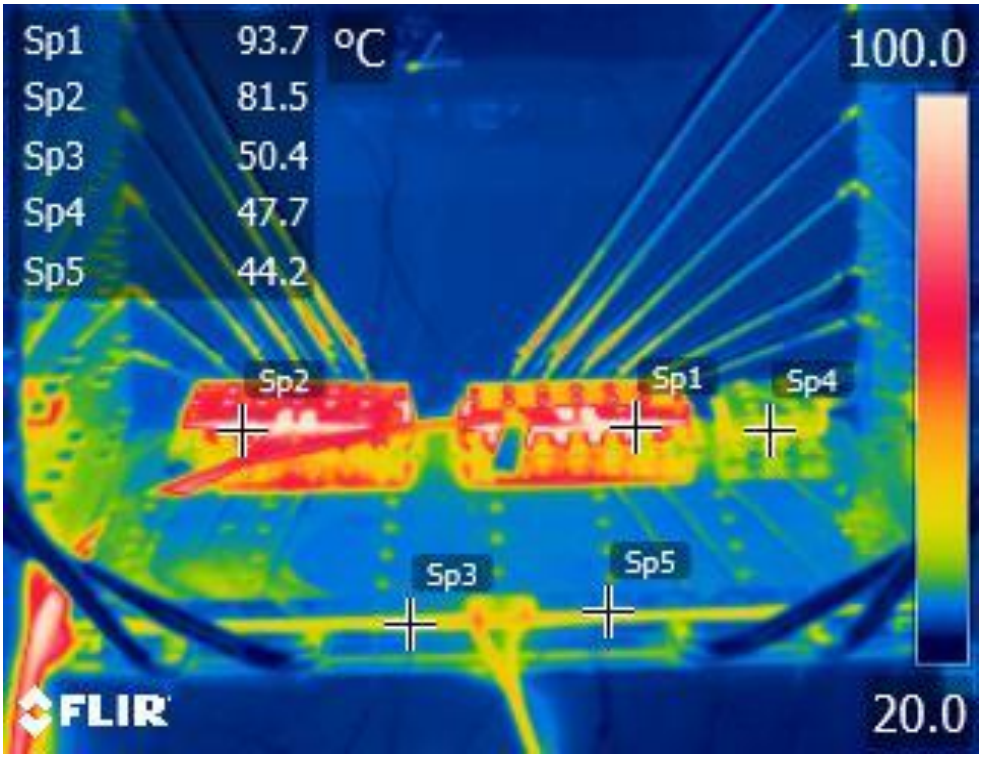

Figure 4.18 Temperature distributions on all heaters

The difference between SP1 and SP2 (see Figure 4.18) is not expected, because these heaters are identical, hence the temperature distributions on these heaters are supposed to be equal or close. However, this difference quite large, which is more than 10 ^{o}C difference. The main problem behind this is the manufacturing tolerances. The manufactured pin fin heat sinks for Heater 1.2 has clearance fit, which is that the mounting hole has slightly larger than diameter of heat pipe. The gap between heat pipes and mounting holes is filled up with thermal grease. However, increase in thickness of grease layer causes increase in thermal resistance, which explains this temperature difference. There will be one further iteration for the experiment and transition fit pin fin heat sink. In Figure 4.19, the average temperature distributions on heaters are simulated in FLIR Image Process Tool. Li1, Li2, Li3 and Li4 are the average calculation runs. The calculated data is very close to figures from 4.12 to 4.15. Li1 and Li2 have attention triangles due to high maximum temperatures. These high points are the connections of heaters wire, which should be neglected.

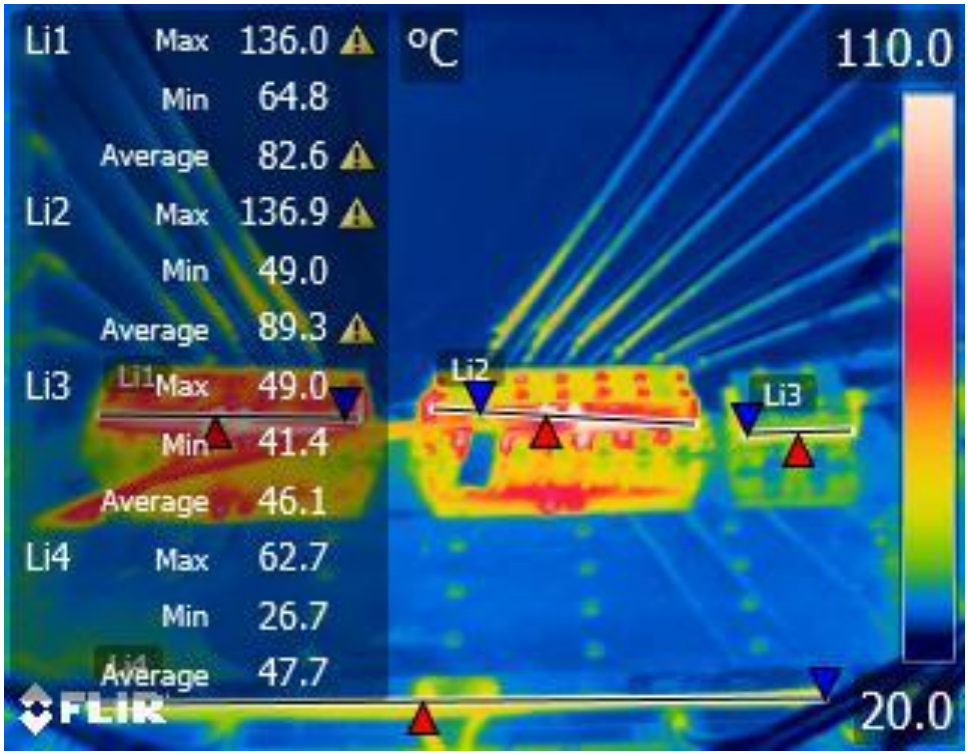

Figure 4.19 Average temperature distributions on heaters

Figure 4.20 and 4.21 illustrate temperature on pin fin heat sink and heat pipe connections. The shown heat sink is attached to Heaters 1.1. From Figure 4.20; SP1 indicates the connections of basal plate and pin fin heat sink. The temperature for this connection is measured nearly 35 ^{o}C. SP2 shows temperature of fin's pin and SP3 is for air inside the fin. When the figure is observed, it can be seen that there is nearly isothermal distribution on pin fin heat sinks. The important issue for the thermal visualization is reflection. The thermal camera works based on radiation, hence it also measures reflection and shows like mirror image (see Figure 4.20 and 4.21). Figure 4.21 illustrates heat pipe's connections and average temperature distribution along the connection of basal plate and heat sink. The average temperature around connection of heat sink and its basal plate is close to 32 ^{o}C. At it is demonstrated, the temperature around heat pipe rises up to more than 35 ^{o}C. This is due to thermal resistance around the pipe. The existence of thermal grease around the pipe directly affects the performance in terms of thermal resistance. The most critical point about that is the thickness of the grease layer. The suggested layer thickness is less than 0.01 inch (0.254 mm), which is equal to 0.3 mm. To eliminate this, manufacturing details must be evaluated.

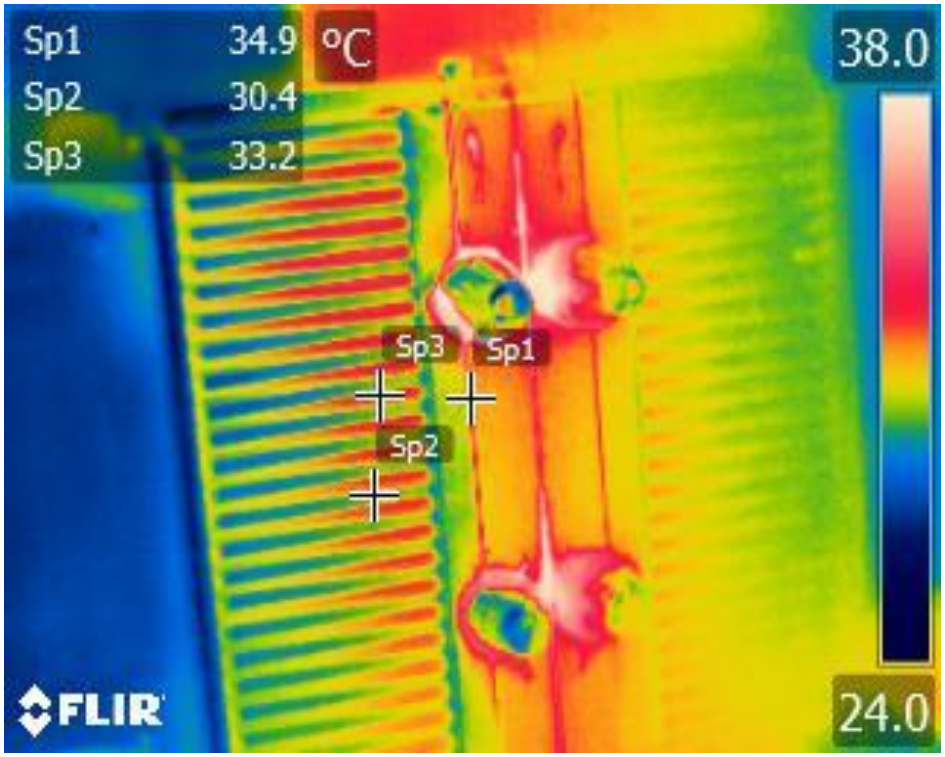

Figure 4.20 Temperatures on a pin fin heat sink

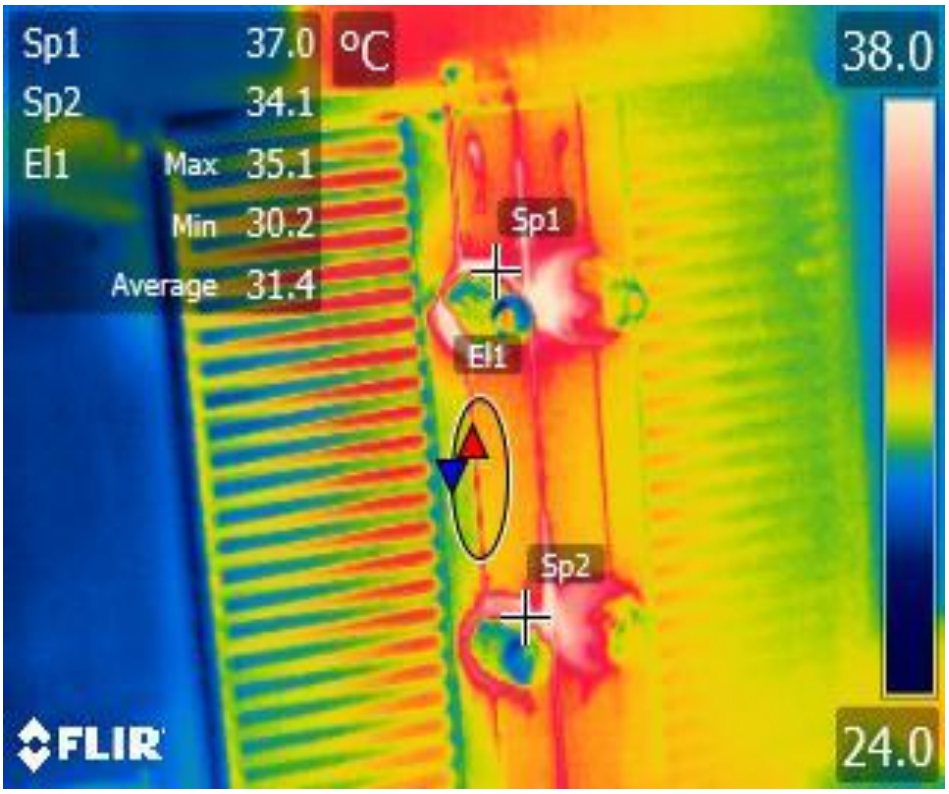

Figure 4.21 Temperatures of connections on a pin fin heat sink

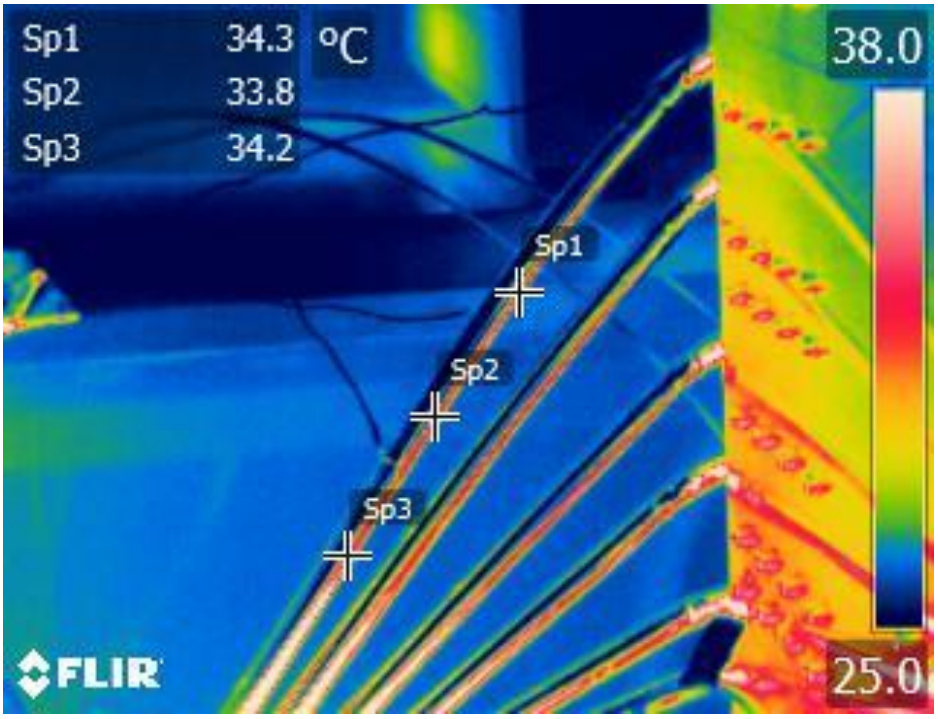

Figure 4.22 Axial temperature distribution on selected heat pipe

Performance of the longest heat pipe is measured and it is also shown in Figure 4.17. The visual proof 'Figure 4.22' has the equal number with Figure 4.17. From the illustration, it is easily seen that the temperature difference along the pipe is so small.

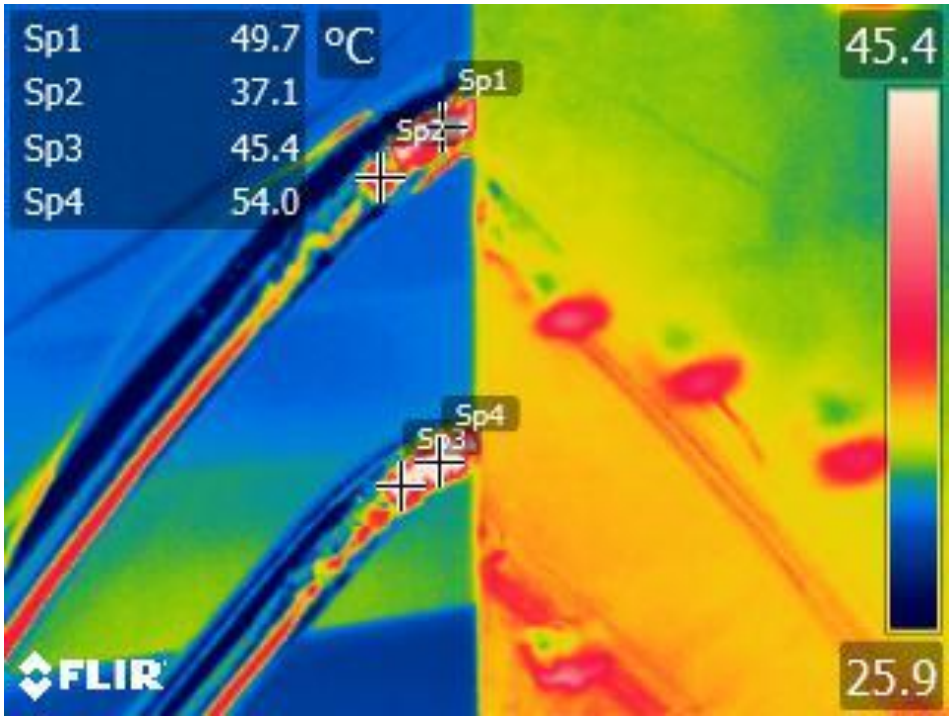

Figure 4.23 Bending effect on the performance of heat pipe

The last comment is related to bending effect. In Figure 4.23, bend regions are quite hotter than other areas. Bend increases the thermal resistance of heat pipe's inner section. From the general knowledge of heat transfer theory, if resistance increases, temperature around the resistance region also increases. The more the bend increases, the less the performance of heat pipe will be as it is mentioned in theory section. As a rule of thumb, every 90^{o} bends causes 1 ^{o}C performance loss.

After the experimental validation, numerical analysis will be updated. In the previous chapter 'Preliminary Design', thermal resistances are not identified in analyses, however these thermal resistances will be taken into consideration in the following section, corrected numerical model.

4.4 Uncertainty Analysis

For calculation of uncertainty of the system measurement, three sets of data are captured experimentally. The results of these three experiments are shown in Table 4.5.

Table 4.5 Results of experimental runs

Number of Run	*Heater 1.1 (^{o}C)*	*Heater 1.2 (^{o}C)*	*Heater 2 (^{o}C)*	*Heater 3 (^{o}C)*
1	76.92	86.28	47.23	51.46
2	77.85	85.64	45.15	52.32
3	77.32	85.84	46.26	51.84

Uncertainty can be calculated with equation below.

$$U_j = \left| \frac{M_{i+1,j} - M_{i,j}}{M_{i,j}} \right| x100 \qquad (4.1)$$

Then, average relative percentage uncertainty is found by,

$$\bar{U} = \sum_{J=1}^{n} \frac{U_j}{n} \tag{4.2}$$

By using formula 4.1 and 4.2, Table 4.6 is calculated, which is average percentage uncertainty of all heaters.

Table 4.6 Average percentage uncertainty of temperatures of all heaters

$U_{1.1}$	$U_{1.2}$	U_2	U_3
0.95 %	0.49 %	3.43 %	1.29 %

From the data sheets of thermocouples and thermal camera, the measurement errors are respectively 0.75 % and 2 %.

CHAPTER 5

OPTIMIZATION

This chapter deals with the corrected numerical model and optimization procedures of design. In this section, pin fin heat sink configuration will be analyzed by corrected parameters taken from initial analyses and experiment. Then, with the information gathered about the heat pipes performance, plated fin heat sink design will be upgraded and optimized. Optimization is done by FloEFD 'What if' analyses.

In 'What if' analyses, optimized section in CAD model must be identified and parametrized. Then, FloEFD automatically solves problem for all conditions. Finally, it can be easily seen which point displays the best performance.

5.1 Corrected Analysis of Pin Fin Heat Sink Configuration

After initial analyses and experiment, problematic points are round out. Numerical modelling is created again. Thermal resistances are added and heat pipe's connection and internal resistances are recalculated.

In initial runs, all heat pipes have same internal resistance; however, experiment showed that this assumption is only used in the beginning. For real life situations, different length heat pipe has different effective thermal resistance. Hence, all effective thermal resistances are recalculated by looking at the results of experiment. At the beginning of analyses, they are defined as 0.25 ^{0}C/W or 0.25 K/W. This value is updated to 0.084 ^{0}C/W or K/W for heat pipes connected to Heater 1.1 (600 W) and Heater 1.2 (600 W), 0.015 ^{0}C/W or K/W for heat pipes connected to Heater 2 (350 W) and 0.002 ^{0}C/W or K/W for heat pipes connected to Heater 3 (70 W).

Another updated value is material contact resistance. As it is mentioned in the experiment, thermal grease is used between pipe and its mounting hole, and thermal pad is used to eliminate gap between heaters and surfaces of evaporators. Thermal grease ‘Artic Silver 5’ is defined according to its specification in user guide. Thermal pad ‘Tflex 640’ is also defined in the same way. (Properties in Appendix A)

Heat sources are also changed. At the beginning, they were defined as surface constant heat generation, new form is volumetric heat source with the real dimensions of heaters. By looking at the results of experiment, the assumption of adiabatic section is considered again. Between all heat pipes’ wall and environment, infinite thermal resistance is defined to prevent convection heat transfer to surroundings. In addition to this, heat dissipations of fans are defined as 38 W. Corrected runs show the validation of the experiment and upgraded values support the validity of the numerical analysis.

After all corrections, results of analysis are getting closer to the results of experiment. Other parameters except for the ones above remain the same. As a calculation domain, the numbers of Table 3.2 in chapter 3 are used. Mesh level is created manually with number of 582344 total mesh cells. During the analysis, mesh refinement is also active, and its level is 4. In order to understand mesh refinement mechanism, Figure 5.1 is given. From the figure, mesh density changes according to the importance of region. FloEFD does not generate dense mesh at surrounding air; however, if Figure 5.1 is observed, mesh density increases at heat pipe connections and fins in order to solve equation of convection and conduction more precisely, and it also increases at outer shell of sources due to consideration of natural convection. One important advice is optimizing the mesh around the pin fin heat sinks because irrelevant increase in mesh cell numbers only extend the solving duration and does not create big differences.

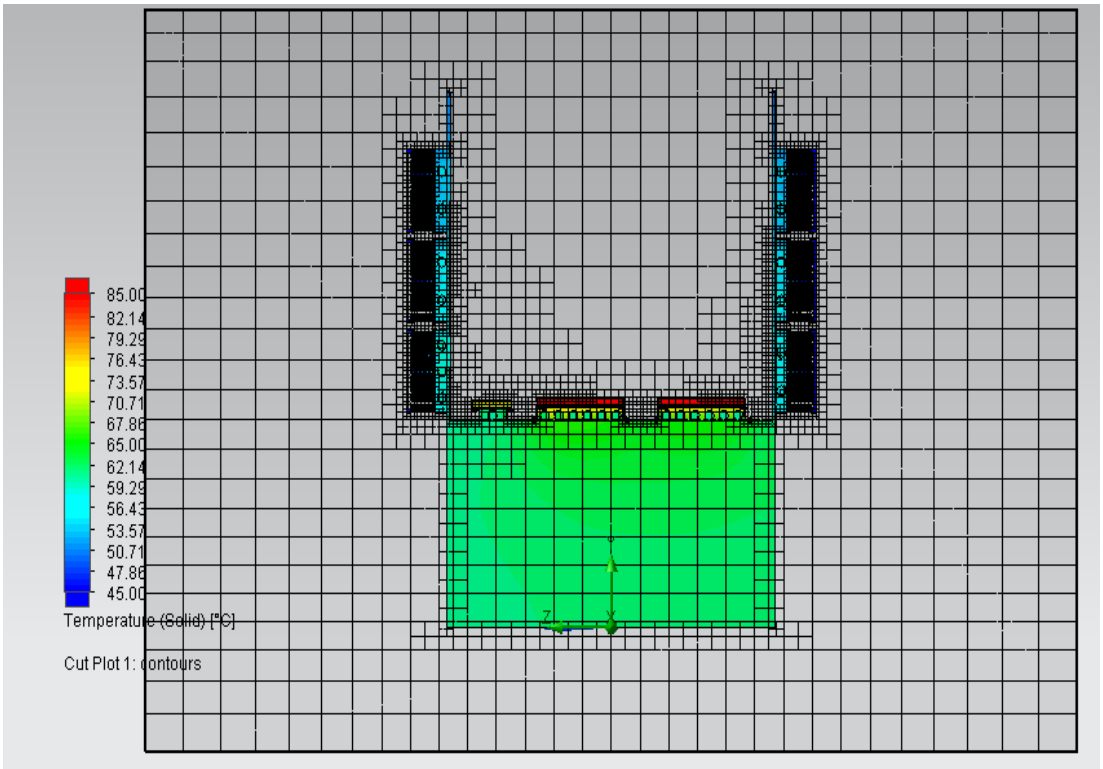

Figure 5.1 Mesh refinement of FloEFD and Cut View of Mesh Distribution from the Back Side of Platform

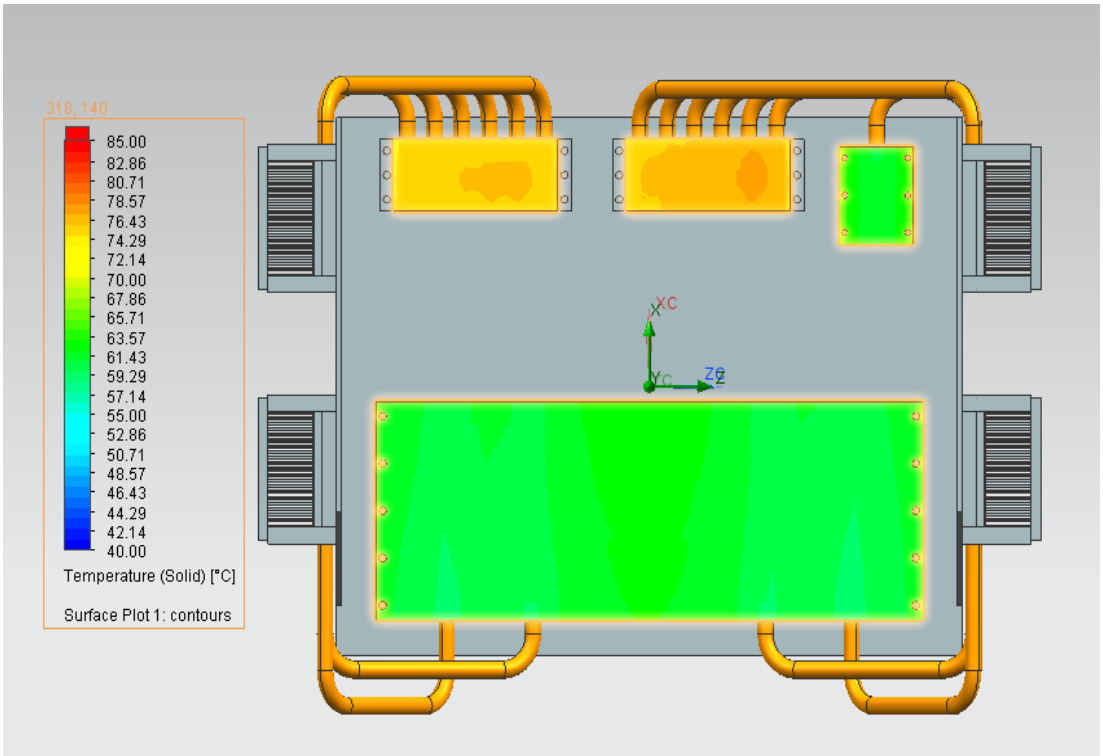

Figure 5.2 Final Temperature Distributions on Heaters

The updated results are illustrated in Figure 5.2. Average surface temperatures of Heater 1.1 and Heater 1.2 are respectively around 79 ºC and 81 ºC, which matches up with the result of experiment. Average temperature distributions of Heater 2 and Heater 3 are also respectively 58 ºC and 62 ºC. These are a bit larger than the results captured in experiment. This deviation is nearly % 20 in ºC unit, which is quite large. This difference results in specifications of heat pipe. In numerical analysis, heat pipes are modeled as super conductive rods, the real performance of pipes cannot be modelled for that kind of large models. Experimental values show us the real performance of heat pipes. In the selection stage of heat pipe, pipes are selected with large margin in order to eliminate the dry-out phenomena. Selected pipes have 12 mm diameter and 120 W heat carrying capacity. To conclude, this difference comes from the performance of heat pipes. In order to eliminate this gap, change in pipe's diameter and heat carrying capacity should be studied.

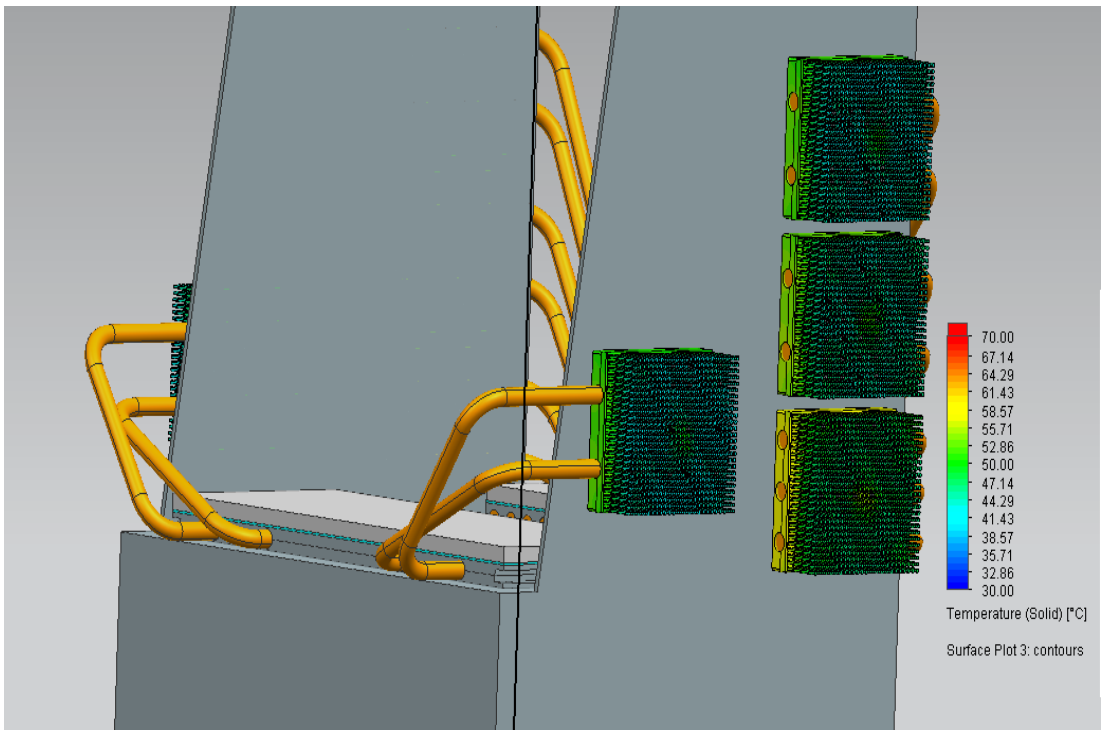

Figure 5.3 Temperature Distributions on Pin Fins (Left Side of Platform)

The last observation is about the temperature distributions on heat sink surfaces. Aim of this criteria is capturing isothermal distribution on surfaces. Nearly isothermal distribution is obtained, one critical point is the connection of pipe and its mounting hole. Designers should consider the connections. If gap cannot be eliminated, thermal

resistance occurs high and the performance of system directly decreases. Figure 5.3 shows the left side of platform and Figure 5.4 illustrates the right side of platform.

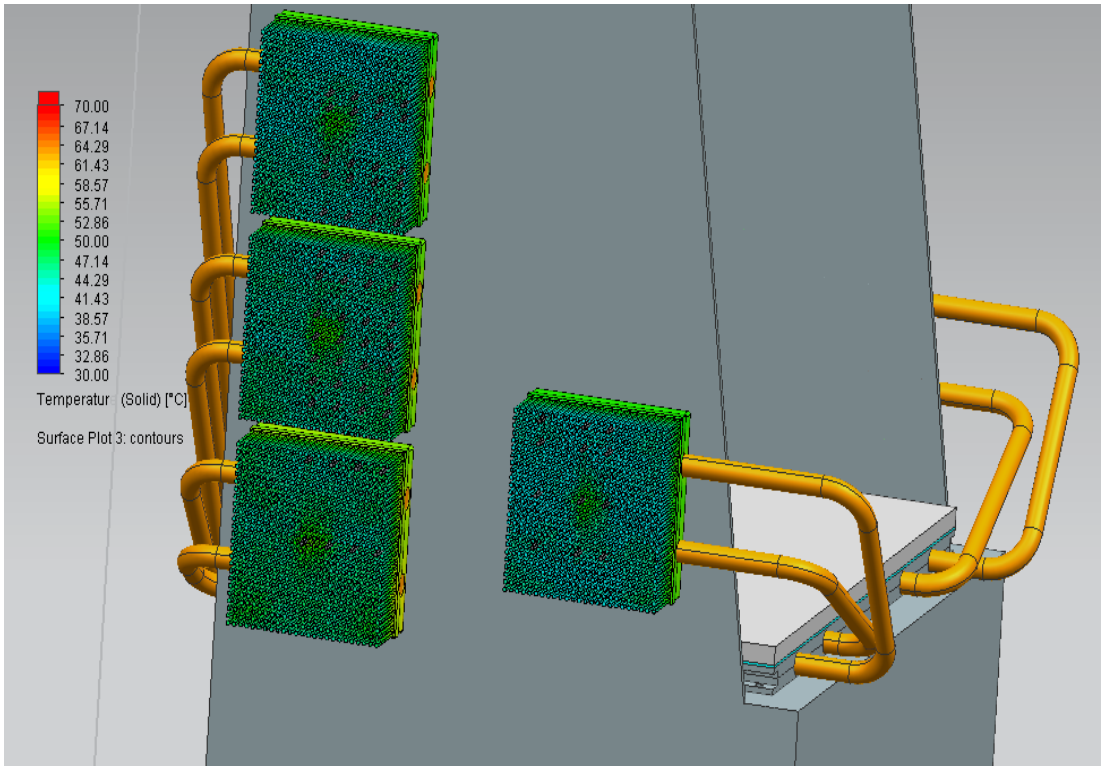

Figure 5.4 Temperature Distributions on Pin Fins (Right Side of Platform)

From the figures above, nearly isothermal distribution is captured, which is obtained through proper decision of pipes' locations and proper selection of heat sink geometry. The temperature distributions on fins are between 45 ^{o}C and 53 ^{o}C. Disproportionate regions are locations of fan's rotor, and in Figure 5.4 pin fin with 3 heat pipes connections. Rotor problem cannot be solved because it comes from the nature of fan. However, if these three pipes' connection are separated, the problem will be solved. In this case, there will be a spacing problem for the design of platform.

In order to compare the results of corrected numerical runs and experiment, Figure 5.5 should be examined. If Figure 5.2 and 5.5 are compared, it can be easily seen that isothermal surfaces are very close to each other. In corrected runs, hot spots on Heater 1.1 and 1.2 are respectively 79.86 ^{o}C and 83.14 ^{o}C. In Figure 5.5, these points have respectively hot spots at 81.25 ^{o}C and 85.34 ^{o}C. These results are also proof of coinciding with the results of corrected numerical runs and experiment.

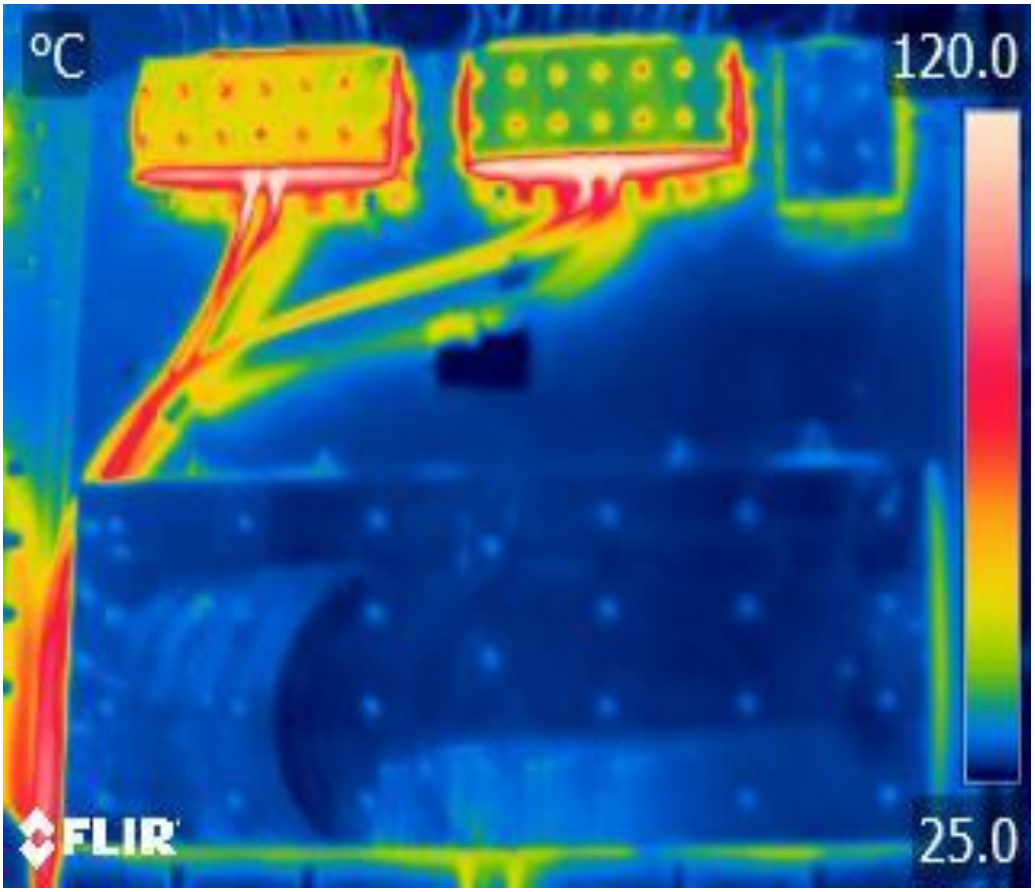

Figure 5.5 The view of isothermal temperature distributions on heaters at experimental stage

Finally, well defined conditions make numerical runs more reliable. Engineers should model every single detail in the runs with simplifications. However, in order to eliminate calculation duration and decrease the calculated equations by CFD program, engineering assumption must be considered. After the regeneration of numerical model, the results get closer to the ones in the experiment, which means numerical results correspond to real life applications.

5.2 Optimization of Plate Fin Heat Sink Configuration

Up to this point, it has been dwelled on numerical modeling and experimental procedure. From the numerical modeling, expected values of average temperatures of heaters' surface were obtained. After that, validation of these values and performance estimations of heat pipes such as effective thermal resistance of heat pipes, the thermal

resistance between the heat pipe and its connections were obtained from the experimental procedure. Also, pin fin heat sink configuration was validated, and with the help of the information gathered, corrected numerical model is created as it is explained in part 5.1. Consequently, corrected model helps the numerical model to match up with the real life conditions. However, the second configuration which is the rectangular plate fin heat sink with duct structured model has not been validated yet under the real life conditions. The second model will be optimized according to surface temperatures of heaters. Changing optimization parameters are fin thickness and the spacing between two fins.

A mechanical design optimization is a challenge in which certain design parameters needed to be determined to achieve the best measurable performance (i.e. objective function) under given constraints. Hence, the selection is done by the best average temperatures distributions on the surfaces of heaters. The set of design variables is composed of fin thickness and spacing between two fins. The main constrain during the optimization step is getting hot spot temperature below thermal shut-down (critical) point. This optimization procedure is done by 'What If ? Analysis ' module of FloEFD.

One of the most powerful features of FloEFD is the ease with which engineers can conduct "what-if?" analyses. FloEFD makes it simple to clone/ modify your models and analyze design variations. The process is very simple. First step is creating base model in 3D with parametric modelling. Then, the setup of a numerical analysis should be generated. . After that multiple variations of analyzed design should be created by modifying the solid model without having to reapply boundary conditions, material properties etc. When the analysis is complete, FloEFD makes it easy to compare the results among the many options to choose best possible design automatically [71].

5.2.1 Procedures of 'What If' Analysis

The starting point of the 'What If' analysis is creating parametric CAD, which is generated by PTC Creo. Geometrical properties and dimensions are the same as preliminary section.

After the modelling is finished, numerical setup must be created in FloEFD. All procedures are the same as procedures explained in Chapter 3 (3.5.1 Procedures of Numerical Analyses). Numerical runs are done at 25 ^{o}C environment temperature and 1 atm pressure. The numbers of fans are increased to 8, there are 4 fans inside each ducts. Another difference from the preliminary conditions is effective thermal resistance of a heat pipe, which was identified as 0.25 ^{o}C/W or K/W. The new value is selected as 0.05 ^{o}C/W or K/W. This value is assumed by the results of experiment as an average of thermal effective resistance of a heat pipe.

Rectangular fin heat sink has 248 mm width and 350 mm length. The base thickness of fin is 14 mm, it is identified by diameter of heat pipe used which is 12 mm. The placements of heat pipes and fin connection are obtained in preliminary stage. There are two identically powered sources, hence placement is done with nearly symmetry condition. Two pipes which are connected to 350 W heater are mounting to top and bottom side of fin. They are placed in a 40 mm distance from horizontal edges of fin (top edge and bottom edge). All other heat pipes are attached to every 40 mm after the first heat pipe. Length of fin plate is 25 mm with variable thickness and spacing. The thickness of fin changes from 3 mm to 6 mm. In addition to this, considered spacing values are 2, 2.5, 3, 3.5, 4, 5 and 6 mm.

During the analyses, total mesh number is also simplified. All analyses are done with 278642 total mesh cells. This value is lower than the values in Chapter 3. Because 'What If' analysis solves the problem one by one, and then it compares the results. During this procedure, twenty-eight different analyses are considered in one setup. In other words, FloEFD has done 28 different analyses with consecutive calculations. In order to minimize the solution time, the number of total mesh cells is lowered. During the process, HP Z820 Workstation is used. This computer is configured with Intel Xeon Processor E5-2640 v2 2.0 GHz 8 cores CPU and installed memory (RAM) with 64 GB. Each run lasts approximately 100 minutes.

Finally, the average surface temperatures distributions on Heater 1.1 and Heater 1.2 is defined as constrain functions of the optimization steps. All calculations stop when these two constrains are achieved. During the calculation, approximately 420 iterations are done.

5.2.2 Results and Discussions of 'What If' Analyses

After all calculation is done, Table 5.1 is gathered. This table includes the change in geometrical dimensions of fin and the results of all calculations. As it is mentioned before, thickness of fin ranges from 3 mm to 6 mm. Besides, considered spacing values are 2, 2.5, 3, 3.5, 4, 5 and 6 mm. Performance trends of fins are given in Appendix C.

When table below is considered, the best values are the point with 3 mm thickness and 2.5 mm spacing between two fins, which is labelled in blue at Table 5.1. This result is also better than the pin fin configuration which is studied at experimental procedure. As it is seen in Table 5.1 and figures in Appendix C, the performance of fin decreases with increased spacing after a certain point. The reduction does not show linear trend, hence results cannot be linearized.

On the other hand, these numbers are results of the computational numbers. Apart from the performance of heat sink, another limitation is manufacturing. For example, in manufacturing plate fin by CNC milling machine, there is a rule of thumb, which suggest that the ratio between fin length to fin thickness should be between 5 and 6. Hence, 4, 5 and 6 mm thickness values provide the suggested ratio. When Table 5.1 is considered from this point of view, 4 mm thickness with 3.5 mm spacing and 5 mm thickness with 3 mm spacing have acceptable performance. These results are close to pin fin heat sink configuration, validated in the experiment. The results of the point with 5 mm thickness and 3 mm spacing will be covered in detail.

Table 5.1 Change in the average surface temperature distribution on the surface of heaters 1.1 and 1.2 with changed geometrical design variables

Thickness (mm)	*Spacing (mm)*	*Average Surface Temperature Distribution on the Surface of Heater 1.1 (°C)*	*Average Surface Temperature Distribution on the Surface of Heater 1.2 (°C)*
3	2	76.24	77.94
3	2.5	**72.72**	**74.29**
3	3	74.69	76.24
3	3.5	76.79	78.36
3	4	79.30	80.78
3	5	83.81	85.36
3	6	87.89	89.52
-	-	-	-
4	2	81.08	82.91
4	2.5	76.34	77.97
4	3	76.98	77.54
4	3.5	**79.09**	**80.66**
4	4	81.08	82.62
4	5	85.36	86.96
4	6	88.51	90.12
-	-	-	-
5	2	84.51	86.14
5	2.5	80.86	82.48
5	3	**78.79**	**80.30**
5	3.5	81.60	83.15
5	4	83.05	84.57
5	5	86.18	88.73
5	6	89.39	91.04
-	-	-	-
6	2	92.57	94.34
6	2.5	81.74	84.36
6	3	81.94	83.46
6	3.5	82.41	83.97
6	4	84.06	85.67
6	5	87.34	89.01
6	6	89.52	91.91

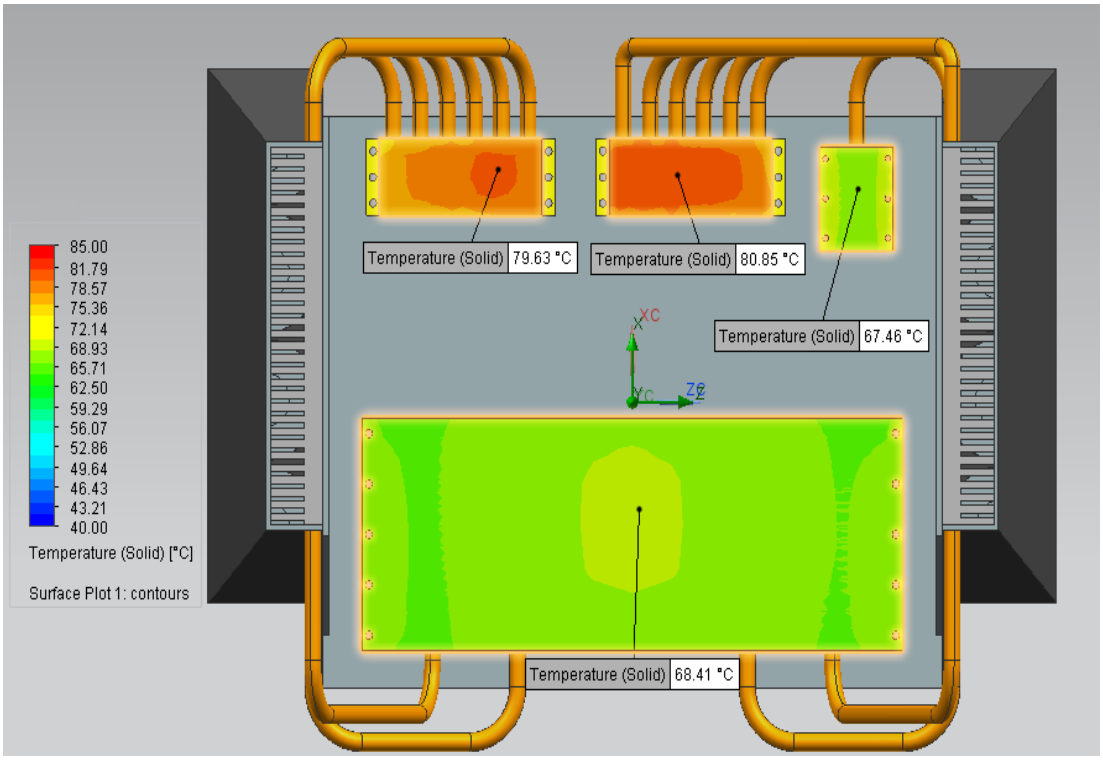

Figure 5.6 Average Surface Temperature Distributions of Heaters (Rectangular Plate Fin with Duct Structured with 5 mm Thickness and 3 mm Spacing)

The average surface temperatures on heaters are given in Figure 5.6.Heater 1.1 and Heater 1.2 have average nearly 80 ^{o}C temperature distribution. Other heaters surface temperatures are also easily seen in figure above. When the values are considered, these values are very close to the values at pin fin configuration.

In addition to temperature distributions on the heater surfaces, the temperature distributions on plate fin heat sinks are considered. As it is mentioned before, the major aim is to create nearly isothermal distributions on heat sinks. The average temperature distributions on the surfaces of heat sinks are very close to 57 ^{o}C (see Figure 5.7 and Figure 5.8). When these figures are examined, the first connecting points of heat pipes and heat sinks are observable. These points have higher temperatures than other surfaces.

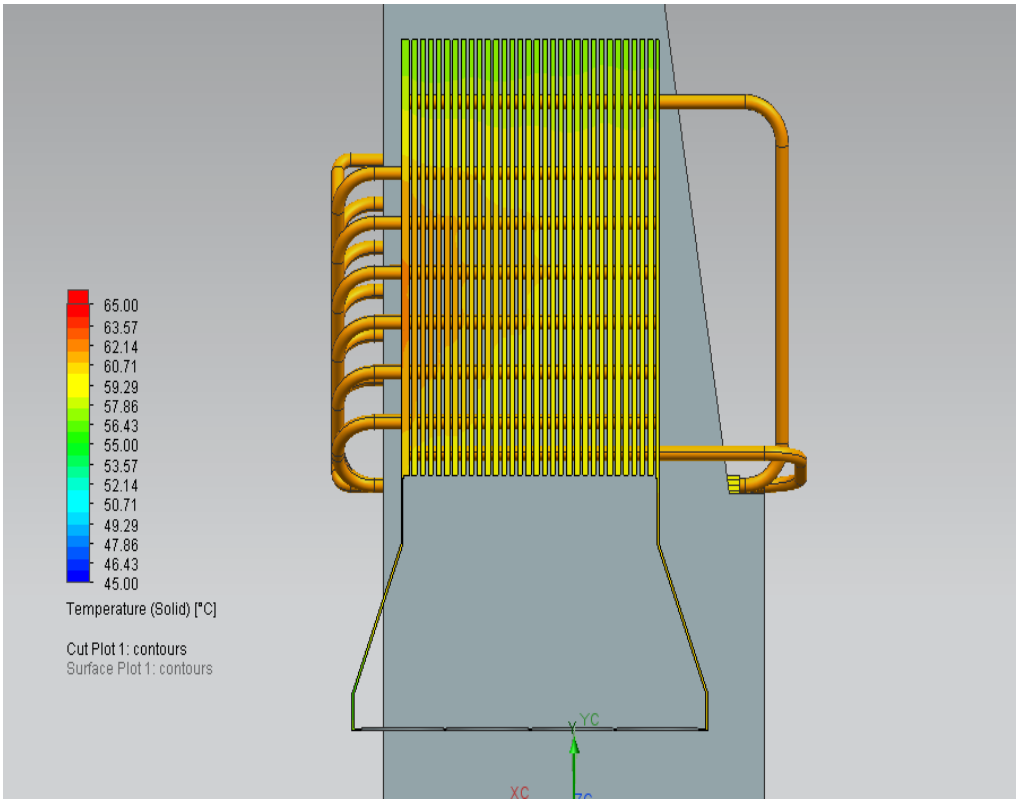

Figure 5.7 Average Surface Temperature Distribution on Right Fin (8 heat pipes are connected)

To conclude, design is upgraded by optimization. The performance of plate fin heat sink is enhanced according to initial design at preliminary part. During the 'what if' analyses, some of contact resistances and resistance due to interface materials are ignored. Because these materials are known for this design and these identifications extend the calculation time. However, when these materials are identified to numerical analyses, the results will slightly increase.

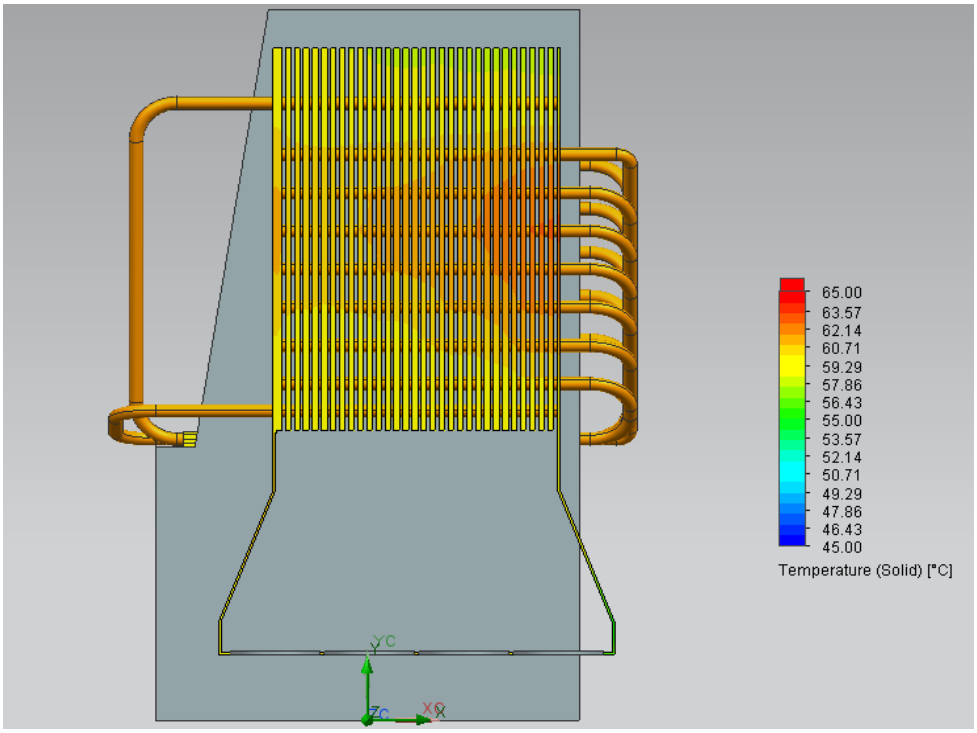

Figure 5.8 Average Surface Temperature Distribution on Right Fin (8 heat pipes are connected)

At first calculations in Chapter 3, the analyses show that the pin fin heat sink configuration has better performance than the rectangular plate fin heat sink with duct structure. After the optimization step, the performance of the rectangular heat sink with duct structure is improved by proper design. The optimization by numerical design only shows the numerical values and engineers choose the best point from the analyses. However, in real life application, manufacturing is another limitation. Engineers should also evaluate the results of optimization by considering economic concerns, manufacturability and usage purposes.

CHAPTER 6

RESULTS AND DISCUSSION

This part summarizes all the results and discussions in the study. This study has been created after 2 years of study about heat pipes. This study is supported by ASELSAN and Republic of Turkey Ministry of Science, Industry and Technology.

The first step of study started with preliminary conceptual design. By evaluating the operational conditions of military rotary platforms, two different configurations were designed. One of them is pin fin heat sink configuration and another one is the rectangular plate fin heat sink with duct structure configuration. These models are illustrated in Figure 3.5 and Figure 3.6. Numerical runs are done at 25 ^{o}C and 50 ^{o}C environmental temperature with 1 atm constant pressure. For pin fin case; the critical component has average surface temperature with 78 ^{o}C at 25 ^{o}C environment and it is 105 ^{o}C at 50 ^{o}C environment. For the rectangular plate fin heat sink configuration, these values are respectively 93 ^{o}C and 121 ^{o}C. However, pin fin heat sink configuration has 8 fan for every 8 pin fins and rectangular plate fin heat sink configuration has 6 fan for 2 ducts. Each duct includes 3 fans.

In the experimental setup, the heat dissipating components are connected to the pin fin heat sinks with 17 heat pipes of 12 mm diameter, which is shown in Figure 4.6. During the experiment, whole system reaches steady-state conditions approximately in 2000 seconds. However, the experimental procedure is completed in 2 hours. During the experiment, no dangerous conditions, such as fire, component malfunction have been observed. Therefore, experiment is successfully completed. Experiment are done at 25 ^{o}C conditioned environment temperature. The figures from 4.12 to 4.16 show the average temperature distributions on the surfaces of heaters. With respectively, Heater 1.1, Heater 1.2, Heater 2 and Heater 3 have average surface temperature with. 82.75 ^{o}C, 92.5 ^{o}C, 45.8 ^{o}C and 46.75 ^{o}C. Some of these values are different from the results

obtained in preliminary stages. In order to find the percentage relative temperature difference in the results of numerical study and the experimental study, Equation 6.1 below is used.

$$\%\ Relative\ Temperature\ Difference = \left|\frac{\Delta T}{\Delta T_{max}}\right| x100 \qquad \textbf{(6.1)}$$

where;

$$\Delta T = T_{measured} - T_{amb} \qquad \textbf{(6.2)}$$

$$\Delta T_{max} = T_{critical} - T_{amb} \qquad \textbf{(6.3)}$$

where $T_{critical}$ is the thermal shot-down point for TWT and PA modules. It is mentioned before as 120 ^{o}C. In order to provide consistent validation, the difference between percent relative temperature difference for numerical value and percent relative temperature difference for experimental value should be as small as obtained. The percent relative temperature difference values are given in Table 6.1.

Table 6.1 Comparison between numerical % relative temperature difference and experimental % relative temperature difference

Heaters	***% Relative Temperature Difference for Numerical Value***	***% Relative Temperature Difference for Experimental Value***
Heater 1.1	57.06	60.79
Heater 1.2	59.32	71.05
Heater 2	34.73	21.89
Heater 3	38.94	22.89

If Table 6.1 is considered, it can be easily seen that there is a quite large difference for heaters 1.2, 2 and 3. These values are evaluated after the preliminary run is obtained by experimental results. The most critical point is the difference between Heater 1.1 and Heater 1.2, because it is not normal. These two sources are identically same and the numerical values for these two sources are also close to each other. This results in manufacturing defect. In the first run of experiment, some of the mounting tolerances

are ignored, so at the contact points thermal resistances are too high. Another reason is also limitations in modelling heat pipes at numerical runs. They are modelled as super conductive rod with high axial conductivity. Solver ignores the phenomena behind two phase cooling mechanism and effects of operating conditions. These values are also recalculated after the new production of pin fins, which is explained below.

If the first run of experiment is considered, there is a difference between average surface temperature on heater 1.1 and 1.2 even though both two sources are identical. This result can be explained with manufacturing and mounting processes. The tolerance between a heat pipe and its connections is very important as it is mentioned before. The pin fins which are attached to Heater 1.2 has quite large mounting holes and these holes are filled up with thermal grease. Due to the high thermal resistance on the contact point, temperature difference between Heater 1.1 and 1.2 is observed. Then, the pin fins which are connected to Heater 1.2 are manufactured again by transition fit. As it is mentioned above the average surface temperature distribution on heater 1.2 is 92.5 ^{o}C, then by the corrected manufacturing this value reduces up to nearly 85 ^{o}C (see Figure 6.1). Results prove the importance of manufacturing and mounting step. Before the improvement, temperature difference between Heater 1.1 and 1.2 is close to 10 ^{o}C. After the new installation, this difference becomes less than 6 ^{o}C. However, it should not be forgotten that this difference also exists in numerical runs as close to 3 ^{o}C. Appendix D covers the results of all heaters' surface temperature distributions.

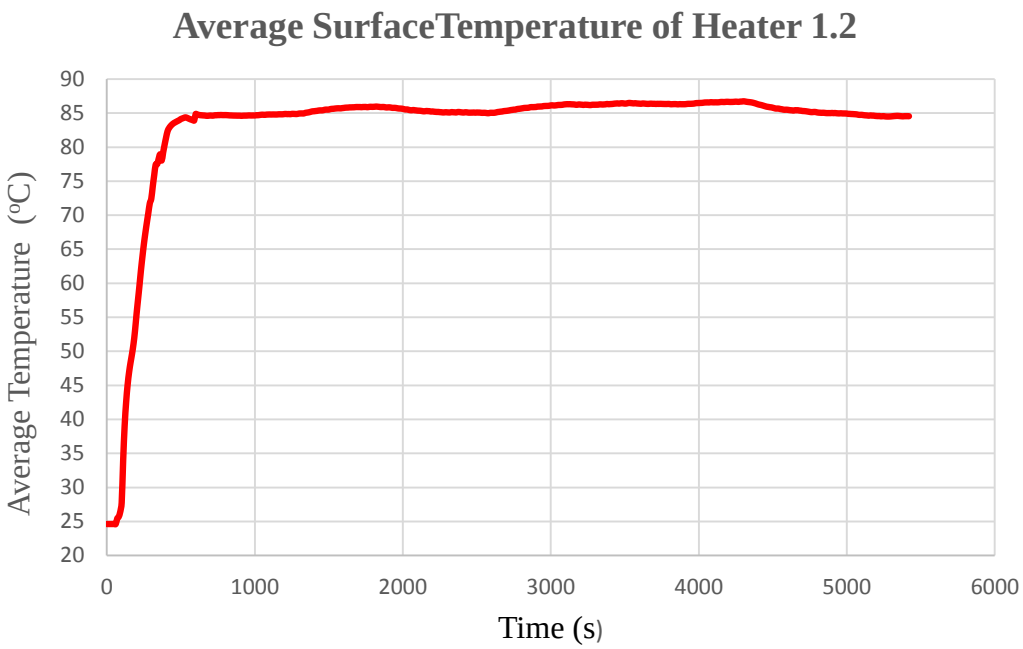

Figure 6.1 Average surface temperature of Heater 1.2 after manufacturing improvement

The assumption of adiabatic section and dry-out are investigated. According to Figure 6.2, the temperature wall surface difference between end of the evaporator and top of the condenser is close to 3 °C. This proves the adiabatic section assumptions and the performance of heat pipe. Besides, it also proves that there is no dry-out. If dry-out happens, the temperature difference between these two regions becomes large. Because the heat pipe loses its super conductivity and it transfers to heat on copper shell. This result is measured on the longest heat pipe, because length affects the performance of the heat pipe.

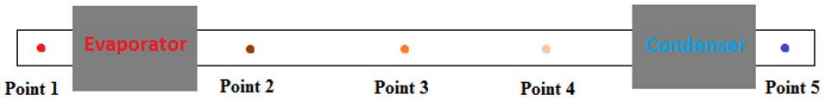

Illustration of Thermocouple couples' place on heat pipe

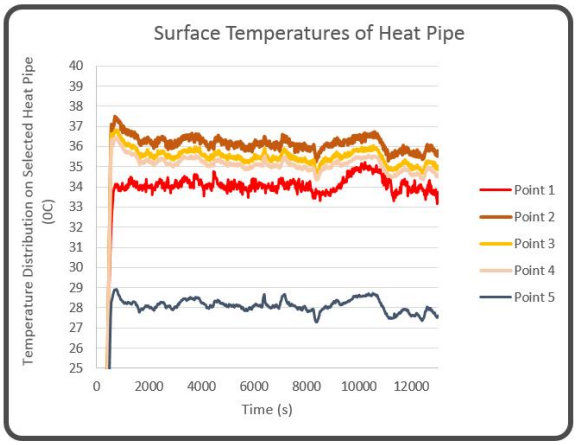

Temperature Distributions on Shell of Longest Heat Pipe

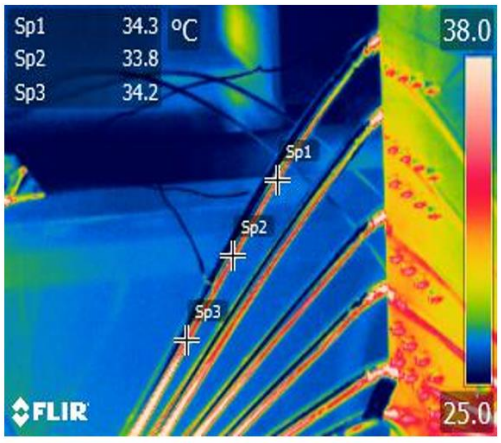

Axial temperature distribution on selected heat pipe

Figure 6.2 Observation for dry-out phenomena

The third step is generating corrected model for pin fin configurations. The creation procedures are explained in 5.1. The estimated effective thermal resistances of heat pipes at preliminary stage are corrected with the results of experiment. At the beginning of analyses, they are defined as 0.25 ^{o}C/W or 0.25 K/W. This value is updated to 0.084 ^{o}C/W or K/W for heat pipes connected to Heater 1.1 (600 W) and Heater 1.2 (600 W), 0.015 ^{o}C/W or K/W for heat pipes connected to Heater 2 (350 W) and 0.002 ^{o}C/W or K/W for heat pipes connected to Heater 3 (70 W). Another updated value is material contact resistance. As it is mentioned in the experiment, thermal grease is used between pipe and its mounting hole, and thermal pad is used to eliminate gap between heaters and surfaces of evaporators. Thermal grease 'Artic Silver 5' is defined according to its speciation in user guide. Thermal pad 'Tflex 640' is also defined in the same way. (see Appendix A). To conclude, the average surface temperatures of heaters with respectively Heater 1.1, Heater 2 and Heater 3 are 79.5 ^{o}C, 63.75 ^{o}C and 64.5 ^{o}C. They become closer to result of experiment. However the differences between results of corrected numerical run and experiment for Heater 2 and 3 increase slightly. Probably, this increase comes from the limitation in numerical modelling. A heat pipe cannot be modelled by real work situation. It is identified as

super conductive rod. Hence, FloEFD gives the results with super conductive constrain. However, as it is explained in Chapter 3, pipe diameter is selected as large as 12 mm in order to prevent dry-out or other limitation. From the data taken from manufacturer, a heat pipe with 12 mm, which is used in experiment, has heat carrying capacity with 120 Watt. Hence, the heat pipes, connected to Heater 2 and Heater 3, have very large safety margin. These results in unpredicted increase in performance. This parameters cannot be modelled with commercial CFD programs.

After the corrected experiment and corrected numerical run, the percent relative temperature difference for experiment and numerical run are recalculated. New values are tabulated in Table 6.2. If values are observed, all numerical result values get closer to the new experiment values. The difference for heater 1.2 decreases. Results demonstrate that tolerances in manufacturing and mounting are very important. However, for heater 2 and 3, reason is different. These values are better than the numerical ones. This is because, numerical solver cannot model the advantages and disadvantages of orientation and heat pipe geometry such as effects of diameter, effective length, operating position according to gravity, operating limits etc.

Table 6.2 Comparison between corrected numerical % relative temperature difference and corrected experimental % relative temperature difference after re-production of fins

Heaters	***% Relative Temperature Difference for Corrected Numerical Value***	***% Relative Temperature Difference for Corrected Experimental Value***
Heater 1.1	57.86	56.34
Heater 1.2	60.43	63.62
Heater 2	40.73	22.04
Heater 3	40.71	29.82

By optimization, the performance of the rectangular plate fin heat sink configuration is increased. The maximum performance is achieved the point that has 25 mm fin length, 3mm thickness and 2.5 mm spacing between two fins. The results of the optimization also shows that the performance of rectangular plate fin with 5 mm

thickness, 3 mm spacing and 4 mm thickness, 3.5 mm spacing is nearly equal to the tested pin fin configuration. All optimization trends are given in Appendix C.

The last comparison is the total heat transfer area for both configurations. A pin fin heat sink has 163980.43 mm^2 heat transfer surface area. 8pin fins are used, hence total heat transfer area on the surface of pin fin heat sinks is 1311843.4 mm^2 (~1.32 x 10^{-6} m^2).On the other hand, a plate fin heat sink has 583800 mm^2 heat transfer surface area. There are 2 plate fin heat sinks attached both left and right side of platform, hence total heat transfer area is 1167600 mm^2 (~1.17 x 10^{-6} m^2). To conclude, instead of using plate pin, using pin fin has an advantage of total heat transfer area with ease of getting good tolerances for small pieces in manufacturing process.

As a result of several simulations with various heat pipe arrangements and two different heat sink types and experiment of pin fin configuration, the following observations are made:

- The thermal management solution with pin fin heat sinks is more effective and easier than the solution with plate fins. If the pin fins are also optimized, the results will be better than plated fin.
- To dissipate high heat loads with heat pipes, heat pipes with large diameters are needed. The heat sink bases should be thicker to accommodate theses thicker heat pipes. In this case, small pin fin heat sinks are better than long parallel plate finned heat sinks. By small pieces, tolerances in manufacturing process can easily be obtained.
- In case of large plate fin heat sinks, smaller number of heat sinks may be enough but arrangement of heat pipes becomes more important.
- The connection between the ends of heat pipes and sources / sinks is very important. The gap or thermal interfaces material creates thermal resistance. Hence the performance of cooling system decreases with increasing thermal resistance.
- The operational position of a heat pipe is important. The suggested position is gravity added orientation.

- Bending is another design limitation. Bending diameter should be 3 times larger than diameter of a heat pipe. If it is less than suggested value, there might be cracks and shrinkage on the heat pipe's wall material.

In addition to these conclusions, it is observed that the optimization of customized heat sinks can be done with the aforementioned criteria, in the optimization, not only lengths of the heat pipes but also where they are connected to both heat distribution plates of the heat generating components and to the heat sinks.

CHAPTER 7

CONCLUSION

Electronics cooling with heat pipes which is the major topic of this study can be used instead of liquid cooling. Heat pipes are used as heat transfer enhancement products. The results of the present study show increase in reliability, and reduction in the cost of design and manufacturing by eliminating leakage problems of liquid cooling. In addition to the application investigated in this study, there are many other examples of the use of heat pipes in various areas. Heat pipe use is convenient and easy especially in military applications, and especially for cooling of electronic devices sensitive to operating environment.

In the present study, numerical analyses, experiments and optimizations show which points are critical in application of heat pipes for electronics cooling. From the results of this study and the conducted literature survey, it is deduced that the following points should be taken into consideration:

- Materials and types of heat pipes
- Heat pipe dimensions and geometrical features (diameter, length, angle of bends)
- The orientation and location of a heat pipe in the system
- The connection interfaces of the heat pipe at both ends: the heat sink at the condenser section and the cooling plate at the evaporator section.
- The tolerances in the production of condenser and evaporator section parts, interfaces and connectors.

To conclude, this study covers the alternative method of cooling to liquid cooling for military rotary platforms. The sample dummy rotary platforms are generated in CAD. There are two types of configurations: the one with pin fin heat sinks and the other one

with two rectangular plate fin heat sinks. These two configurations are designed according to where they will be used e.g. in land systems at deserts or on vehicles and in naval systems. The best average temperature values on critical components are nearly 79 ^{o}C with the pin fin heat sink configuration at 25 ^{o}C environment. This result is also verified with an experiment. By the optimization of the rectangular plate fin heat sink design, the performance of the cooling system is improved. The best performance is obtained with the fins having 3 mm thickness and 2.5 mm spacing. The average temperature value for this configuration is very close to 73 ^{o}C in a 25 ^{o}C environment.

In the following studies in the future, the performance of heat pipes should be investigated while the platform is rotating. As a result of this, the effects of rotation and Coriolis force on the heat pipe performance may be investigated. Moreover, this study only deals with a single pin fin configuration. The next study may cover the optimization of pin fin heat sinks.

REFERENCES

[1] When was the first computer invented? (n.d.). Retrieved June 14, 2015, from http://www.computerhope.com/issues/ch000984.htm

[2] Don't hold your breath for a Retina MacBook Air this week. (n.d.). Retrieved June 15,2015, from http://www.slashgear.comretina-macbook-air-tipped-for-2014-26322258

[3] Moore, G.E. (1965). Cramming more components onto integrated circuits. Electronics, 38

[4] Ellison, G.N. (2011). Thermal Computations for Electronics. CRC Press

[5] Lasance, C., & Simons, R. (2005, November 1). Advances In High-Performance Cooling For Electronics. Retrieved July 5, 2015, from http://www.electronics-cooling.com/2005/11/advances-in-high-performance-cooling-for-electronics/

[6] Laird Technologies. Thermoelectric - Structure and Function, 2010.

[7] Thermacore Inc. (2013). k-Core [Brochure]. Lancaster, USA.

[8] Streacom's FC10 and Nano150: Building a Fanless Ivy Bridge HTPC. (n.d.). Retrieved June 24, 2015, from http://www.anandtech.com/show/6523/streacoms-fc10-and-nano150-building-a-fanless-ivy-bridge-htpc/2

[9] Wits., W.W. (2008). Integrated Cooling Concepts for Printed Circuit Boards. PhD thesis, University of Twente.

[10] Açikalin, T., Wait, S., Garimella, S., & Raman, A. (2004). Experimental Investigation of the Thermal Performance of Piezoelectric Fans. *Heat Transfer Engineering, 25*, pp. 4-14.

[11] Mudawar, I. (2001). Assessment of high-heat-flux thermal management schemes. *IEEE Transactions on Components and Packaging Technologies, 24*, pp. 122-141.

[12] Liquid cooling technique uses microfluidic channels integrated onto the backs of chips. (2005, June 21). Retrieved July 5, 2015, from http://www.gtresearchnews.gatech.edu/newsrelease/cooling.htm

[13] Aselsan AS. (2013). DK-0000-0100 Isıl Tasarım Rehberi. Ankara, Türkiye.

[14] Balıkçı, Ç. (2013). Experimental study of spray cooling of electronics over high heat fluxed surface. MSc thesis, Middle East Technical University

[15] Öksüz, S. (2014). Characterization of spray cooling for electronics device. MSc thesis, Middle East Technical University

[16] Delta logo fan and thermal management. (n.d.). Retrieved June 19, 2015, from http://www.delta-fan.com/subcategory.aspx?id=116

[17] Noie, S. (2005). Heat transfer characteristics of a two-phase closed thermosyphon. *Applied Thermal Engineering, 25*, pp. 495-506.

[18] Thyrum, G., (2006). Critical Aspects of Modeling Heat Pipe Assisted Heat Sinks. *Thermacore Inc.*

[19] Yan, Z., Zhao, R., Duan, F., Wong, T.N., Toh, K.C., Choo, K.F., Chan, P.K., & Chua, Y.S. (2011). Spray Cooling, Two Phase Flow, Phase Change and Numerical Modeling. *Dr. Amimul Ahsan (Ed.), ISBN: 978-953- 307-584-6. InTech*. Available from: http://www.intechopen.com/books/twophase-flow-phase-change-andnumerical-modeling/spray-cooling

[20] Glassman, B.S. (2015). Spay cooling for land, sea, air and space based applications, a fluid management system for multiple nozzle spray cooing and a guide to high heat flux heater design. MSc thesis, University of Central Florida.

[21] Azar, K. (2002). Advanced cooling concepts and their challenges.

[22] Anderson, T.M., & Mudawar, I. (1989). Microelectronic cooling by enhanced pool boiling of a dielectric fluorocarbon liquid. *Journal of Heat Transfer*, 111, pp. 752- 759, 1989.

[23] Zuo, Z.J., North, M.T., & Wert K.L. (2001). High heat flux heat pipe mechanism for cooling of electronics. *IEEE transactions on Components and Packaging Technologies, 24*, pp. 220–225.

[24] Tuckerman, D.B., & Pease, R.F.W. (1981). High-performance heat sink for vlsi. *IEEE Electron Device Letters, 2, pp.*126–129.

[25] Riffat, S.B., & Ma X. (2004). Improving the coefficient of performance of thermoelectric cooling systems: a review. *International Journal of Energy Research, 28*, pp. 753–768.

[26] Rainey, K.N., You, S.M., & Lee, S. (2003). Effect of pressure, subcooling, and dissolved gas on pool boiling heat transfer from microporous square pin-finned surfaces in fc-72. *International Journal of Heat Transfer, 46,* pp. 23–25.

[27] Sturgis, J.C., & Mudawar, I. (1999). Critical heat flux in a long, rectangular channel subjected to one sided heating - ii. Analysis of critical heat flux data. *International Journal of Heat Mass and Transfer, 42*, pp. 1849–1862.

[28] Faulkner, D., Khotan, M., & Shekarriz, R. (2003). Practical design of a 1000 w/cm^2 cooling system. *19th IEEE SEMI-THERM Symposium*, pp. 223–230.

[29] Pais, M.R., Chow, L.C., & Mahefkey, E.T. (1992). Surface roughness and its effect on the heat transfer mechanism in spray cooling. *Journal of Heat Transfer, 114*, pp. 211–219.

[30] Overholt, M.R., McCandless, A., Kelly, K.W., Becnel, C.J., & Motakef, S. (2005). Micro-jet arrays for cooling of electronic equipment. *3rd International Conference on Microchannels and Minichannels*

[31] ASELSAN Naval Platform Radar ESM System. (n.d.). Retrieved June 26, 2015, from http://www.aselsan.com.tr/en-us/capabilities/electronic-warfare-systems/electronik- support-and-electronic-attack-systems/aselsan-naval-platform-radar-esm-system

[32] 25 mm STOP Uzaktan Komutalı Stabilize Top Sistemi. (n.d.). Retrieved June 26, 2015, from http://www.aselsan.com.tr/tr-tr/cozumlerimiz/silah-sistemleri/uzaktan-komutali-atis-sistemleri/25-mm-stop-uzaktan-komutali-stabilize -top-sistemi

[33] Peterson, G. (1994). Introduction. In An Introduction to Heat Pipe Modeling, Testing, and Applications. pp. 2-4. *A Wiley-Interscience Publication*.

[34] Gaugler, R.S., (1944). Heat Transfer Device. U.S. Patent 2350348 A

[35] Grover, G.M., Cotter, T.P., & Erikson, G.F. (1964). Structures of Very High Thermal Conductivity. *Journal of Applied Physics*, Vol. 35, pp. 1190-1191.

[36] Deverall,J.E., & Kemme, (1970). J.E. Satellite heat pipe. USAEC Report LA-3278, Contract W-7405-eng-36. Los Alamos Scientific Laboratory, University of California

[37] Anand, D.K. (1968). Heat pipe application to a gravity gradient satellite. *Proc.of ASME Annual Aviation and Space Conf.*, pp.634-658.

[38] Leefer, B.I. (1966). Nuclear Thermionic energy converter. *20th Annual Power Source Conf.*, pp. 172-175.

[39] Judge, J.F. (1969). RCA test thermal energy pipe. *Missiles and Rockets.*, 18, pp. 36-38.

[40] Dunn, P., & Reay, D. (1976). Historical Development. In Heat pipes: P. Dunn and D.A. Reay. 1st ed. Oxford: *Pergamon Press*., pp. 10

[41] Bainton, K.F. (1965). Experimental heat pipes. AERE-M1610, Harwell, Berks. *Atomic Energy Research Establishment.* Appl. Physics Div.

[42] Nozu,S. et al. (1969). Studies related to the heat pipe. Trans. Soc. Mech. Engrs., Japan, 35 (2), pp. 392-401.

[43] Savage, C.J. (1969). Heat pipes and vapor chambers for satellite thermal balance. RAE TR-63125, *Royal Aircraft Establishment*

[44] Calimbas, A.T., & Hulett, R.H. (1969). An avionic heat pipe. ASME Paper 69-HT-16 New York, *American Society of Mechanical Engineers*

[45] Kumar, V., Gangacharyulu, D., & Tathgir, R. (n.d.). Heat Transfer Studies of a Heat Pipe. *Heat Transfer Engineering*, pp. 954-965.

[46] Dunn, P., & Reay, D. (1976). Applications of the Heat Pipe. In *Heat Pipes* (1 st ed., pp. 232-233). *Pergamon Press.*

[47] Dunn, P., & Reay, D. (1976). 'Fig.7.1 Satellite Isothermalisation', Applications of the Heat Pipe. In *Heat Pipes* (1 st ed., pp. 233). *Pergamon Press.*

[48] Firouzfer, E., Soltanieh, M., Noie, S., & Saidi, M. (2011). Application of heat pipe heat exchangers in heating, ventilation and air conditioning (HVAC) systems. *Scientific Research and Essays, 6*(9), pp. 1900-1908.

[49] Dunn, P., & Reay, D. (1976). Applications of the Heat Pipe. In *Heat Pipes* (1 st ed., pp. 256-258). *Pergamon Press.*

[50] Korn, F. (2008). Heat pipes and its application. *2008 MVK 160 Heat and Mass Transport, Project Report.*

[51] Heat pipes in vertical supports maintain a frozen bulb around portions of the Trans-Alaska Pipeline that are at risk of thawing. (n.d.).

[52] The best design. For the best performance. (n.d.). Retrieved August 5, 2015, from http://www.apple.com/macbook-pro/design-retina/

[53] Scott, D., & Garner, P. (1996, September 1). Heat Pipes for Electronics Cooling Applications. Retrieved March 11, 2014, from http://www.electronics-cooling.com/1996/09/heat-pipes-for-electronics-cooling-applications/

[54] Heat Pipes. (n.d.). Retrieved August 9, 2015, from http://www.thermopedia.com/content/835/

[55] Peterson, G. (1994). 'Chapter 4' Other Operating Limits. In *An Introduction to Heat Pipe Modeling, Testing, and Applications.* p. 77. A Wiley-Interscience Publication.

[56] Peterson, G. (1994). 'Chapter 4' Other Operating Limits. In *An Introduction to Heat Pipe Modeling, Testing, and Applications.* p. 78. A Wiley-Interscience Publication.

[57] DeHoff, R., & Grubb, K. (n.d.). Heat pipe application guidelines. *Thermacore, Inc.*

[58] Peterson, G. (1994). 'Chapter 3' Capillary Limitation in Heat Pipes and Thermosyphons. In *An Introduction to Heat Pipe Modeling, Testing, and Aplications.* pp. 44-74. A Wiley-Interscience Publication.

[59] Peterson, G. (1994). 'Chapter 4' Other Operating Limits. In *An Introduction to Heat Pipe Modeling, Testing, and Applications.* pp. 97-99. A Wiley-Interscience Publication.

[60] Dunn, P., & Reay, D. (1976). 'Chapter 4' Theory of the Heat Pipe. In *HEAT PIPES* (1 st ed., pp. 52-54). Pergamon Press.

[61] Dorsey, G. (2005). High-Speed Data Transmission and Rotary Platforms: Slip Rings, Fiber Optic Rotary Joints, and Multiplexers. *MOOG Component Group,* (24).

[62] SPINNER High-Frequency Rotary Joints. (n.d.). Retrieved April 16, 2015, from http://www.militarysystems-tech.com/military-gallery/spinner-gmbh/spinner-high-frequency-rotary-joints

[63] FloEFD for Creo. (n.d.). Retrieved April 15, 2014, from http://www.mentor.com/products/mechanical/floefd/floefd-creo/

[64] Versteeg H.K., Malalasekera W., *An Introduction to Computational Fluid Dynamics, The Finite Volume Method,* Pearson Education Limited, 1995.

[65] K-epsilon models. (n.d.). Retrieved September 6, 2015, from http://www.cfd-online.com/Wiki/K-epsilon_models

[66] Wilcox, David C. (1998). Turbulence Modeling for CFD. Second edition. Anaheim: DCW Industries, pp. 174.

[67] Celik, I. (1999). *Introductory Turbulence Modeling - Lecture Notes*. West Virginia University Mechanical & Aerospace Engineering Dept.

[68] Enertron Inc. (2001). Heat pipe selection guide. *Enertron Inc.*

[69] FloEFD User Manual for V.14.0, Mentor Graphics Corporation

[70] FloEFD for Creo 13.0 Technical Reference, Mentor Graphics Corporation, 2013-12-07.

[71] FloEFD Electronic Cooling Module Data sheet. (n.d.). Retrieved May 19, 2015, from http://s3.mentor.com/public_documents/datasheet/products/mechanical/products/floefd-electronics-cooling-module.pdf

APPENDIX A

Design Items

ALPHA Novatech S20100 Series

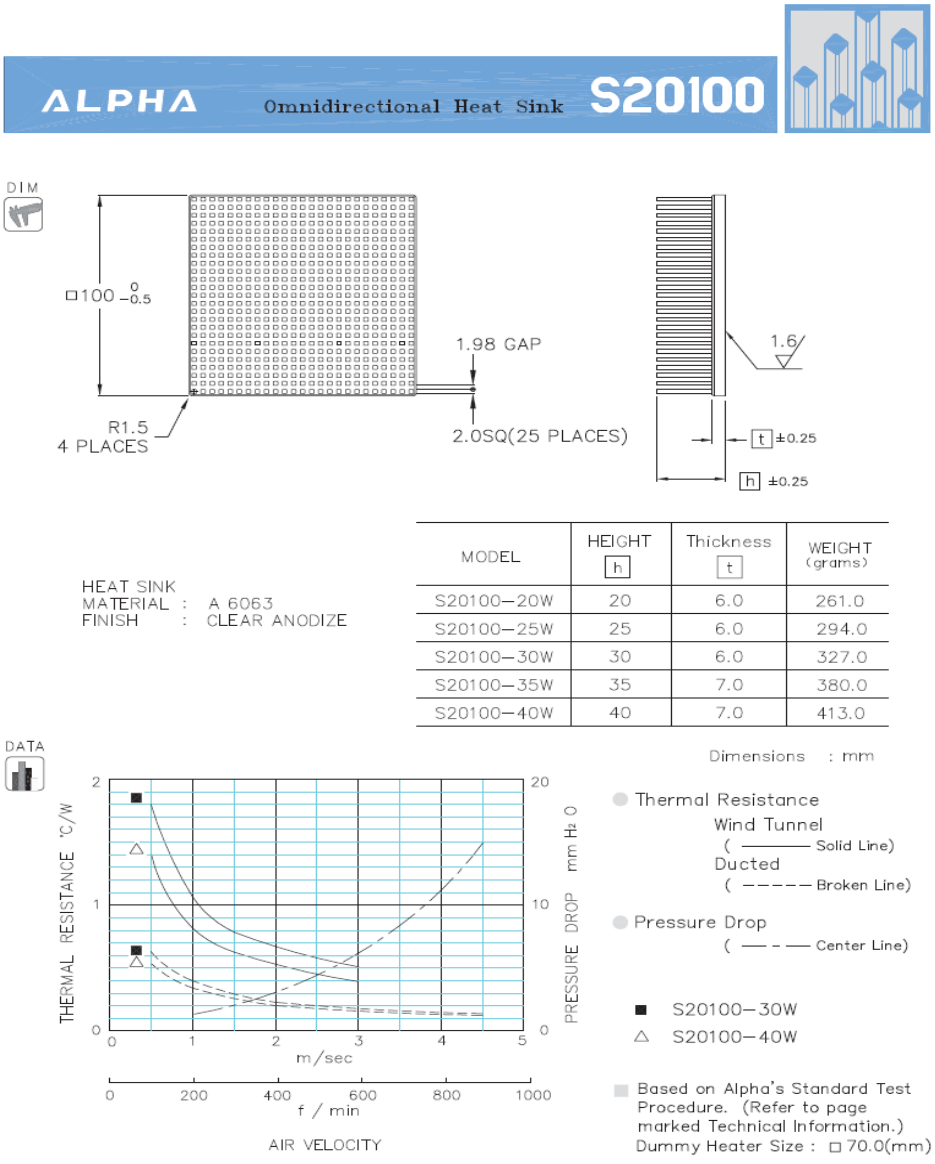

Figure A.1 Specification and dimensions Alpha Novatech S20100 series

ARTIC SILVER® 5 (99.9% Silver)

Table A.1 Product ingredient information of Artic Silver 5

Product Ingredient Information
Silver (Metallic)
Boron Nitride
Zinc Oxide
Aluminum Oxide
Ester Oil Blend

Figure A.2 Artic Silver 5

SPECIFICATIONS

Average Particle Size: <0.49 micron <0.000020 inch

Extended Temperature Limits: Peak: –50°C to >180°C
Long-Term: –50°C to 130°C

Performance:

3 to 12 degrees centigrade lower CPU full load core temperatures than standard thermal compounds or thermal pads when measured with a calibrated thermal diode imbedded in the CPU core.

Coverage Area:

A 3.5 gram syringe contains enough compound to cover at least 15 to 25 small CPU cores, or 6 to 10 large CPU cores, or 2 to 5 heat plates. At a layer 0.003" thick, the 3.5 gram syringe will cover approximately 16 square inches.

EBM Papst 8214 JH3 - DC Axial Fan

Nominal Data

Type	8214 JH3	
Nominal voltage	VDC	24
Nominal voltage range	VDC	12 .. 27.6
Speed	min-1	12000
Power input	W	26
Min. ambient temperature	°C	-20
Max. ambient temperature	°C	70
Air flow	m3/h	190
Sound power level	B	7.3
Sound pressure level	dB(A)	66

Figure A.3 View of EBM Papst 8214 JH3 and its nominal data

Fan Curve

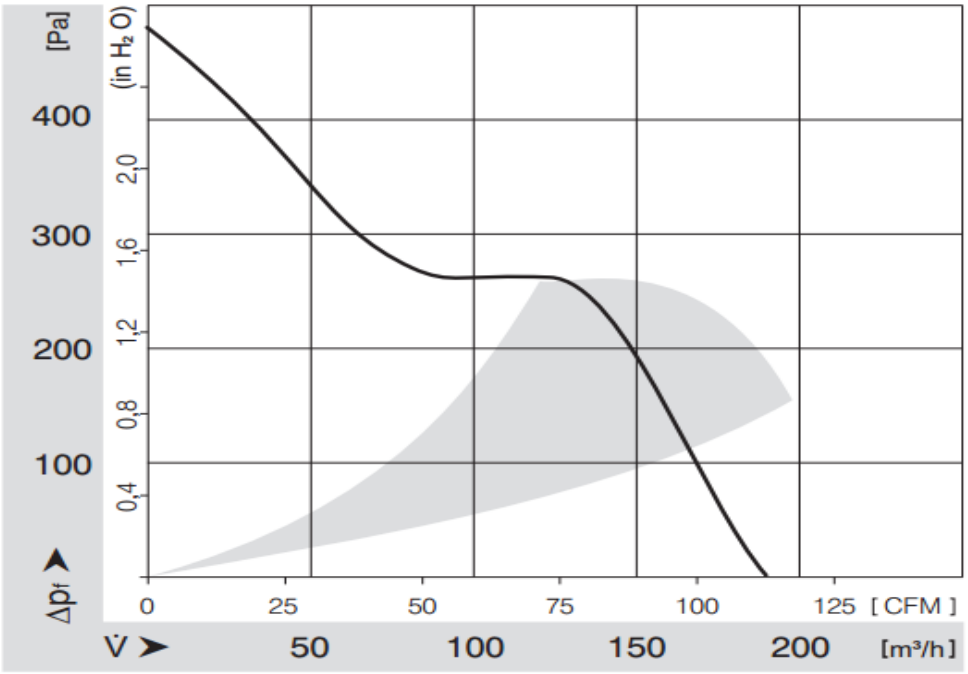

Figure A.4 Fan curve of EBM Papst 8214 JH3

Technical Features

Table A.2 Technical features of EBM Papst 8214 JH3

General description	Free air power consumption, these values may be considerably higher at the operating point
Housing material	Fiberglass-reinforced plastic (PBT)
Impeller material	Fiberglass-reinforced plastic (PA)
Mass	0.200 kg
Dimensions	80 x 80 x 38 mm
Direction of air flow	Air exhaust over bars
Direction of rotation	Left, looking at rotor
Bearing	Ball bearings
Connection line	Single strands AWG 22, TR 64, bared and tin-plated
Motor protection	Protected against reverse polarity and locking
Option	Speed signal

Laird T-flex 640

Tflex™ 600 is an exceptionally soft, highly compliant gap filling interface pad with a thermal conductivity of 3 W/mK. These outstanding properties are the result of a proprietary boron nitride filler in the composition. The high conductivity, in combination with extreme softness produces incredibly low thermal resistances. Tflex™ 600 is naturally tacky and requires no additional adhesive coating that can inhibit thermal performance. Tflex™ 600 is electrically insulating, stable from 45°C to 200°C and meets UL 94 V0 rating.

Table A.3 Technical data for Laird T-flex 640

	Tflex™ 600	TEST METHOD
Construction & Composition	Boron nitride filled silicone elastomer	
Color	Blue-Violet	Visual
Thickness Range	0.020" (0.50mm) - 0.200" (5.08mm)	
Thickness Tolerance	± 10%	
Density (g/cc)	1.34	Helium Pycnometer
Hardness (Shore 00)	51; 3 seconds 48; 30 seconds	ASTM D2240
Tensile Strength	15 psi	ASTM D412
% Elongation	75	ASTM D412
Outgassing Conditions	Post cured	
Outgassing TML (weight %)	0.13%	ASTM E595
Outgassing CVCM (weight %)	0.05%	ASTM E595
UL Flammability Rating	94 V0	UL FILE E180840
Temperature Range	-45°C to 200°C	
Thermal Conductivity	3.0 W/mK	Hot Disk
Thermal Impedance @ 40 mils, 10 psi @ 1 mm, 69kPa	 0.62°C–in²/W 4.00°C–cm²/W	 ASTM D5470 (modified)
Thermal Expansion	430 ppm/°C	IPC-TM-650 2.4.24
Volume Resistivity	2 x 10^{13} ohm-cm	ASTM D257
Dielectric Constant @ 1MHz	331%	ASTM D150

APPENDIX B

Equipments of Experiment

Data Logger

Technical Features

Table B.1 Properties of Agilent HP 34970A data logger

Description	:	AGILENT HP 34970A Data Logger
Manufacturer	:	Agilent Technologies
Scan Count	:	1 to 50,000 or continuous
Scan Interval	:	0-99 hours; 1ms step size
Power Supply	:	100V/ 120V/ 220V/ 240V ±10%
Power Consumption	:	12 W
Operating Environment	:	Full accuracy for 0 °C to 55 °C Full accuracy to 80% RH at 40 °C
Storage Environment	:	-40 °C to 70 °C
Weight	:	3.6 kg

Figure B.1 Agilent HP 34970A data logger

Power Supplies

Agilent 6032A System Power Supply 0-60V /0-50A, 1000W

Figure B.2 Agilent 6032A system power supply 0-60V /0-50A, 1000W

Technical Features

Output ratings

- Voltage: 0 to 60 V
- Current: 0 to 50 A

Programming accuracy at 25°C ±5°C

- Voltage: 0.035%, +40 mV
- Current: 0.2%, +85 mA

Ripple & noise 20 Hz to 20 MHz

- Voltage rms: 8 mV
- Voltage Peak-to-Peak: 40 mV
- Current rms: 25 mA

Read-back accuracy at 25°C ±5°C

- Voltage: 0.08%, +20 mV
- Current: 0.36%, +35 mA

Agilent 6692A DC Power Supply 0-60V /0-110A

Figure B.3 Agilent 6692A DC power supply 0-60V /0-110A

Technical Features

Output Ratings

- Voltage: 0 to 60 V
- Output current : 0 to 110 A

Programming Accuracy (at 25 ±5°C)

- Voltage: 0.04% + 60 mV
- Current: 0. 1% + 65 mA

Ripple & Noise (20 Hz to 20 MHz)

- Voltage: rms: 2.5 mV
- Voltage: Peak-to-peak: 25 mV

HP 6573A System DC Power Supply 0-35V /0-60A

Figure B.4 HP 6573A System DC Power Supply 0-35V /0-60A

Technical Features

Output Ratings at 40°C

- Output voltage: 0 to 35 V
- Output current: 0 to 60 A

Programming Accuracy at 25°C ±5°C

- Voltage: 0.04% + 35 mV
- Current: 0.1% + 40 mA

Ripple & Noise (20 Hz to 20 MHz)

- Voltage rms: 800 µV
- Peak-to-Peak: 9 mV
- Current rms: 40 mA

Agilent E3634A DC Power Supply 0-25V, 7A / 0-50V, 4A

Figure B.5 Agilent E3634A DC Power Supply 0-25V, 7A / 0-50V, 4A

Technical Features

Output ratings

- Range 1: 0 to 25 V, 7 A
- Range 2: 0 to 50 V, 4 A

Programming accuracy at 25°C ±5°C

- Voltage: 0.05% + 10 mV
- Current: 0.2% +10 mA

Ripple & noise (20 Hz to 20 MHz)

- Normal-mode voltage: <500 µVrms/3 mVp-p
- Normal-mode current: <2 mA rms
- Common-mode current: <1.5 µA rms

Readback accuracy at 25°C ±5°C

- Voltage: 0.05% + 5 mV
- Current: 0.15% + 5 mA

Table B.2 FLIR E60 infrared camera specifications

FLIR E60 Infrared Camera Specifications

Model Number	FLIR E60
Imaging	
Resolution	320 × 240 pixels
Total Pixels	76,800
Thermal Sensitivity	< 0.05° C
Accuracy	±2°C or ±2% of reading
Temperature Range	-4°F to 1,202°F (-20°C to 650°C)
Video Camera w/Lamp	3.1 MP
Lens Options	Standard: 25°; Optional: 15° Tele, 45° Wide
Zoom	4x Continuous Digital
Focus	Manual
Uncooled Microbolometer	x
Color LCD Touch Screen	3.5" (320 x 240)
Picture-in-Picture	Scalable
Fusion	x
Laser Spot	x
Video Out	Composite
Frame Rate	60 Hz
Analysis	
Moveable Spots‡	3
Box Areas	3
Delta T‡	x
Annotation	
Voice	x
Text	x
File Storage	
Radiometric JPG to SD Card	x
MPEG4 Video Recording	x
Other	
Wi-Fi to Apple and Andriod Mobile Devices	x
MeterLink	x
InstantReport	x
FLIR Tools	x
Battery Type / Op Time	Li Ion, 4 hours operating time
Dual-bay Charger and Spare Battery	Included
Weight	0.825 kg (1.82 lbs)
Optional Accessories	15° and 45° lenses, sunshield, tripod adapter, cigarette lighter adapter kit, Bluetooth headset, and more

APPENDIX C

Optimization Graphs

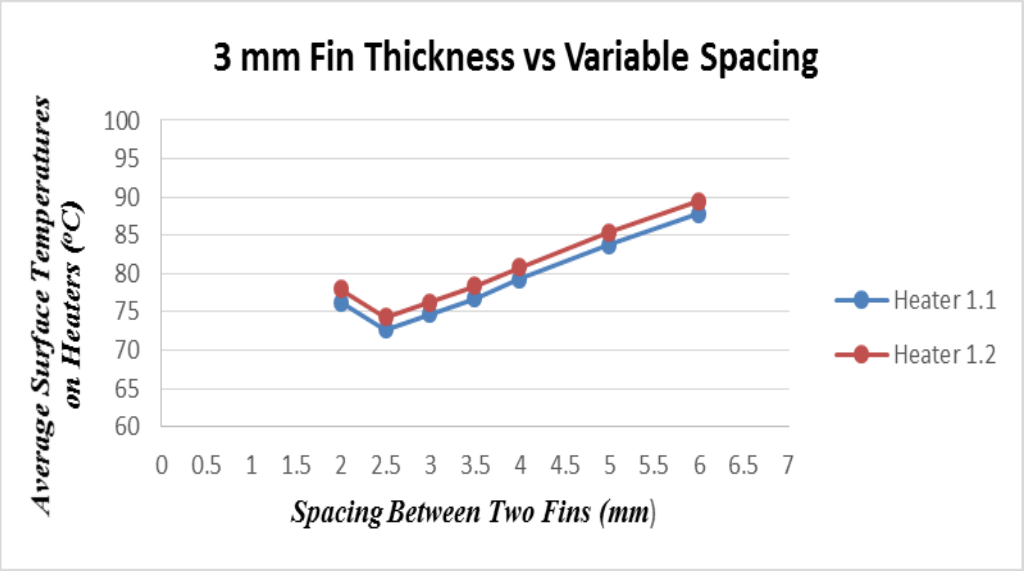

Figure C.1 Result of optimization for 3 mm fin thickness vs variable spacing

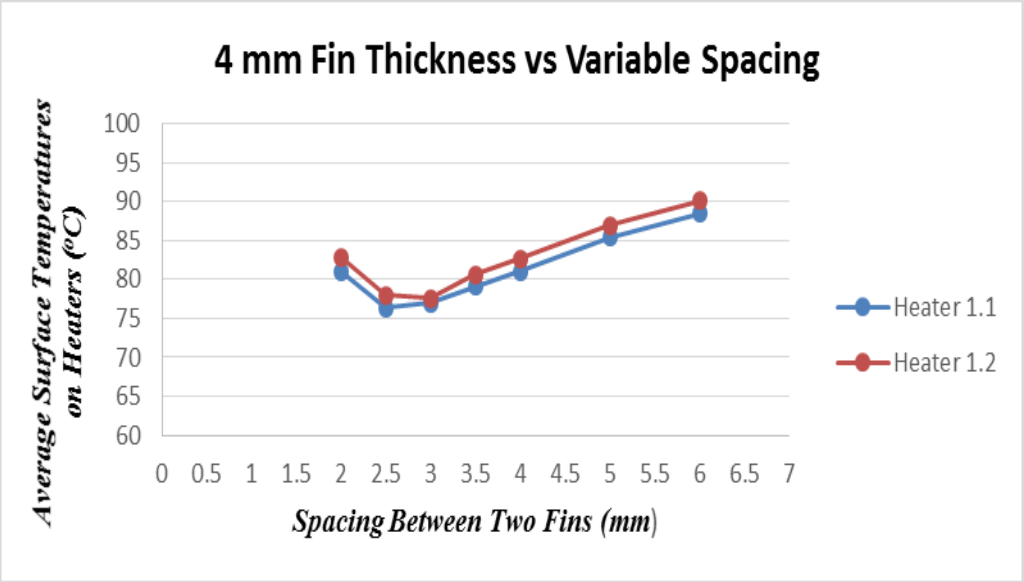

Figure C.2 Result of optimization for 4 mm fin thickness vs variable spacing

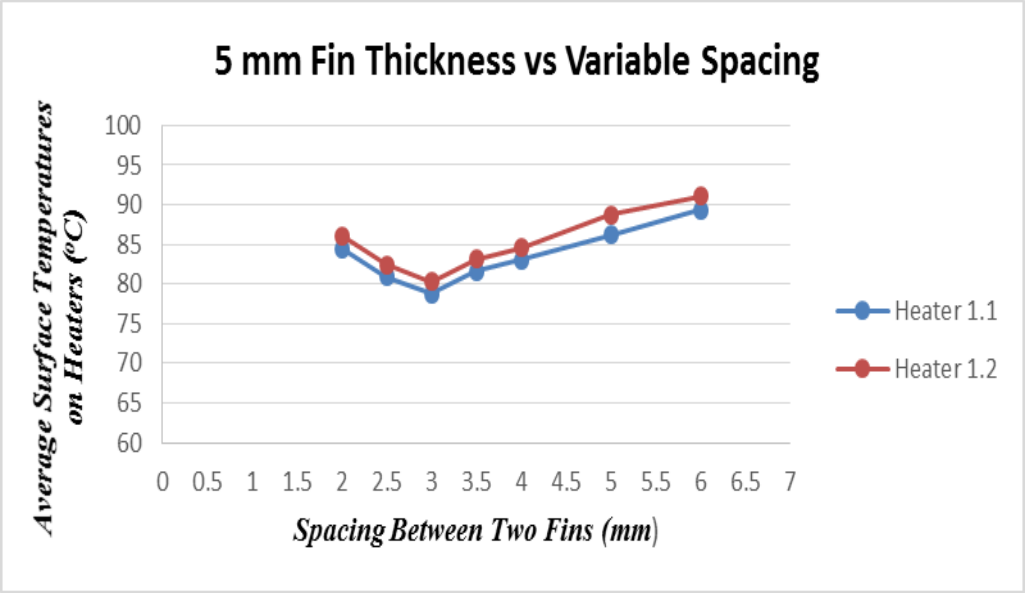

Figure C.3 Result of optimization for 5 mm fin thickness vs variable spacing

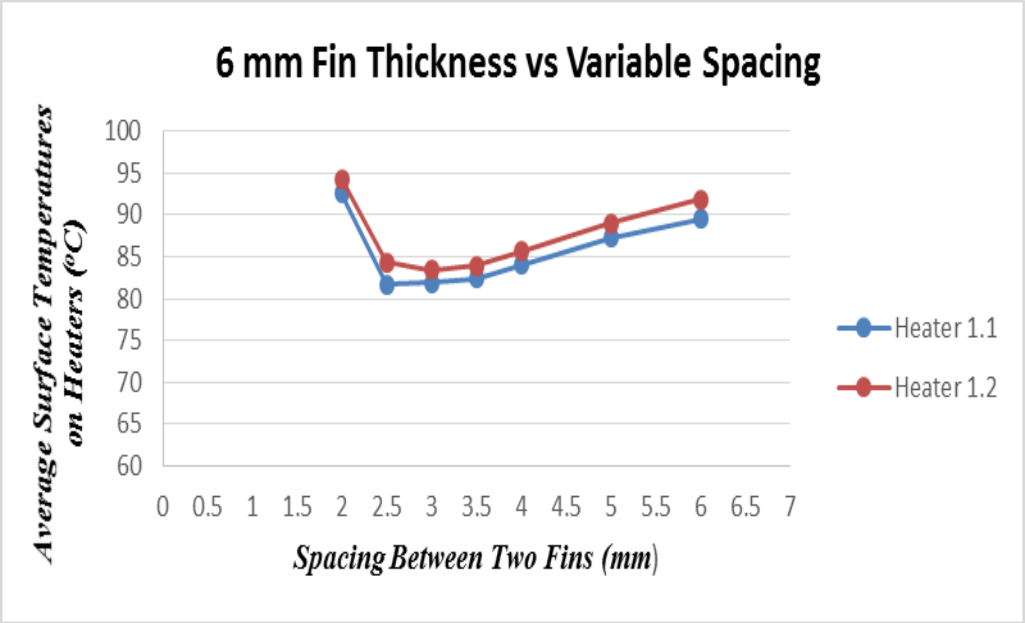

Figure C.4 Result of optimization for 6 mm fin thickness vs variable spacing

APPENDIX D

Results of Corrected Experiment

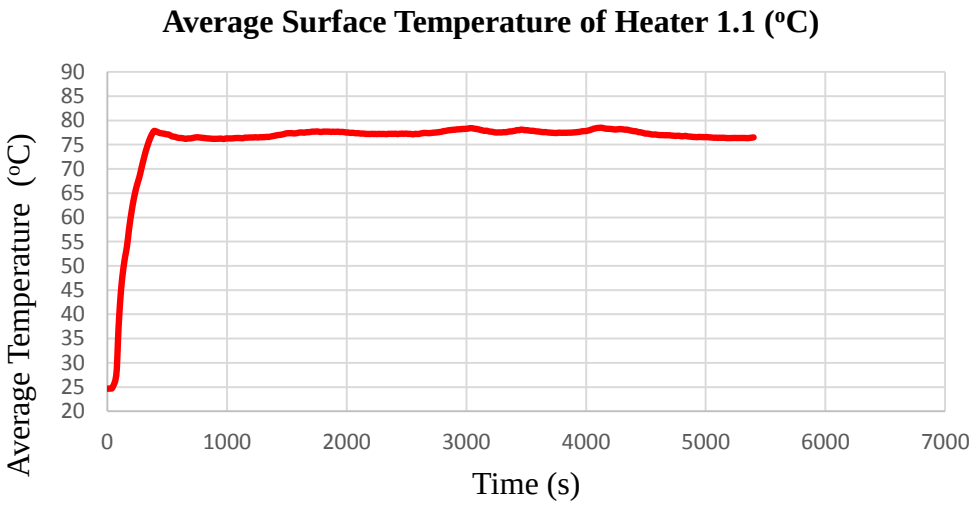

Figure D.1 Result of corrected experiment for heater 1.1

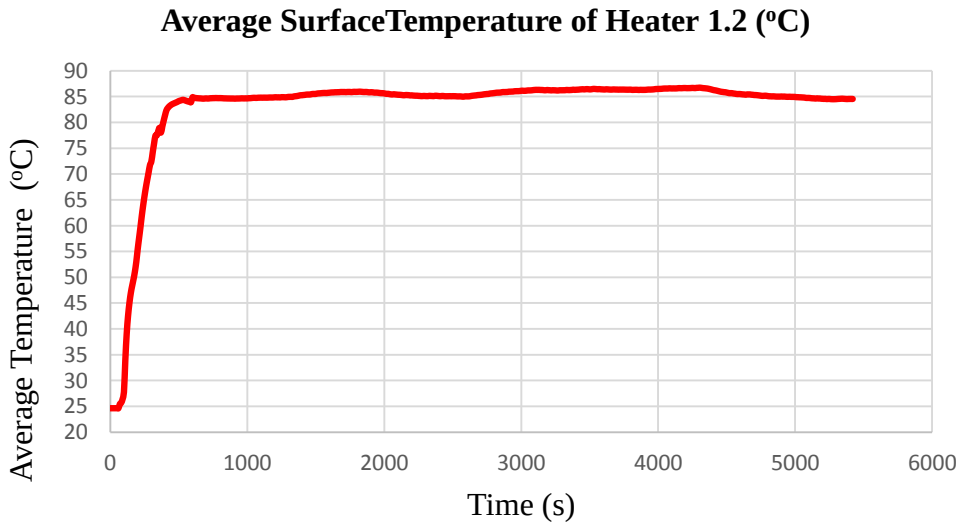

Figure D.2 Result of corrected experiment for heater 1.2

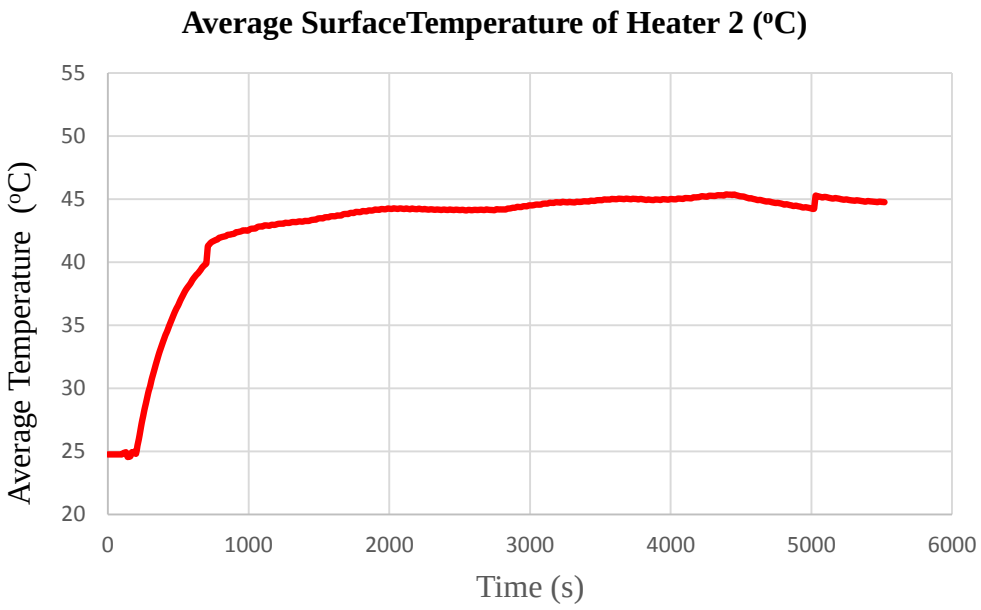

Figure D.3 Result of corrected experiment for heater 2

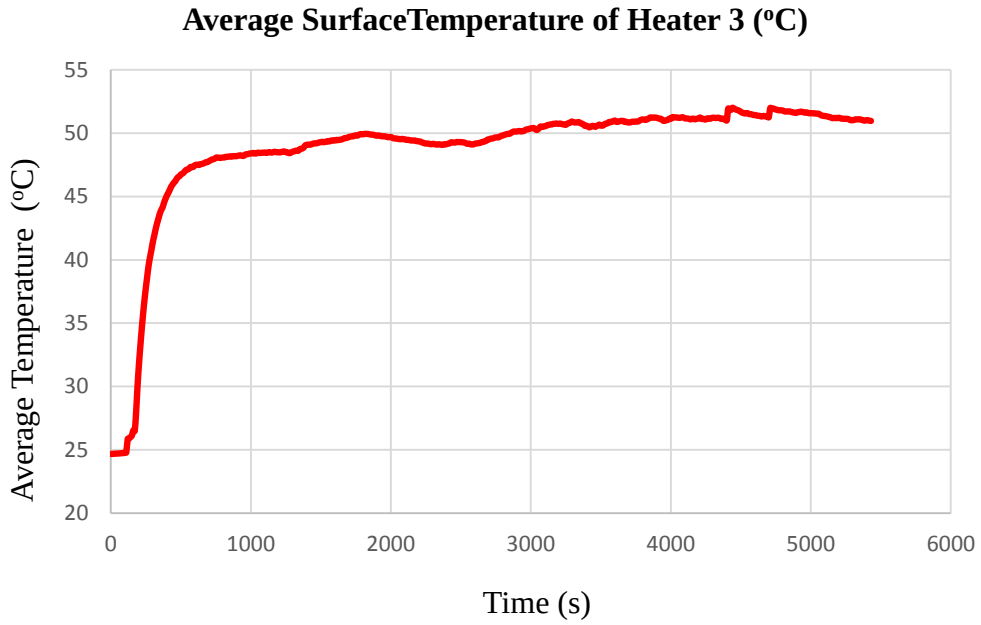

Figure D.4 Result of corrected experiment for heater 3